

## Distribution Agreement

In presenting this thesis or dissertation as a partial fulfillment of the requirements for an advanced degree from Emory University, I hereby grant to Emory University and its agents the non-exclusive license to archive, make accessible, and display my thesis or dissertation in whole or in part in all forms of media, now or hereafter known, including display on the world wide web. I understand that I may select some access restrictions as part of the online submission of this thesis or dissertation. I retain all ownership rights to the copyright of the thesis or dissertation. I also retain the right to use in future works (such as articles or books) all or part of this thesis or dissertation.

Signature:

---

Courtney Jane Matheny

---

Date

THE CHAPERONE UNC-45 HAS A CRUCIAL ROLE IN MAINTAINING THE  
STRUCTURE AND FUNCTION OF THE MUSCLE CONTRACTILE APPARATUS  
DURING AGING

By

Courtney Jane Matheny

B.S. Microbiology, University of Georgia, 2015

Graduate Division of Biological and Biomedical Science  
Biochemistry, Cell, and Developmental Biology

---

Guy M. Benian, MD  
Advisor

---

Hyojung Choo, PhD  
Committee Member

---

Michael Koval, PhD

---

Jennifer Kwong, PhD  
Committee Member

---

Shoichiro Ono, PhD  
Committee Member

Accepted:

---

Kimberly Jacob Arriola, Ph.D, MPH

Dean of the James T. Laney School of Graduate Studies

---

Date:

THE CHAPERONE UNC-45 HAS A CRUCIAL ROLE IN MAINTAINING THE  
STRUCTURE AND FUNCTION OF THE MUSCLE CONTRACTILE  
APPARATUS DURING AGING

By

Courtney Jane Matheny

B.S. Microbiology, University of Georgia, 2015

Advisor: Guy M. Benian, MD

An abstract of a dissertation submitted to the Faculty of the James T. Laney  
School of Graduate Studies of Emory University in partial fulfillment of the  
requirements for the degree of

Doctor of Philosophy

In

Graduate Division of Biological and Biomedical Science

Biochemistry, Cell, and Developmental Biology

2022

## Abstract

# THE CHAPERONE UNC-45 HAS A CRUCIAL ROLE IN MAINTAINING THE STRUCTURE AND FUNCTION OF THE MUSCLE CONTRACTILE APPARATUS DURING AGING

By Courtney Jane Matheny

As longevity increases, age-related diseases will become a greater public health concern. Sarcopenia is the age-related decline in muscle mass and function without any underlying disease. The molecular mechanisms responsible for this pathology remain unknown. Muscle function is dependent on having properly organized and functioning thick filaments, which are primarily composed of myosin. UNC-45 is required for the folding of the myosin head initially after translation and likely re-folds the myosin head to regain functionality after thermal or chemical stress causes unfolding. UNC-45 was first discovered using *C. elegans*, which is an excellent model organism for studying muscle biology and aging. We observe an early onset of sarcopenia when UNC-45 is perturbed during adulthood. We observe that during adult aging, there is a sequential decline of HSP-90, UNC-45, and then myosin. Myosin and UNC-45 protein decline are independent of steady state mRNA levels. Loss of UNC-45 is correlated with an increase in phosphorylation of the protein. By mass spectrometry S111 has been identified as being phosphorylated and this modification may affect binding to HSP-90. A longevity mutant with delayed onset of sarcopenia also shows a delay in the loss of HSP-90, UNC-45, and myosin. We also see a decrease in UNC-45 protein, but not transcript, in an *hsp-90* loss of function mutant, suggesting a role for HSP-90 in stabilizing UNC-45. These results lead us to propose the model that during aging, a loss of HSP-90 leads to UNC-45 being post translationally modified, such as phosphorylation, and degraded, which then leads to a loss of myosin, and thus reduction in muscle mass and function. A better understanding of how myosin and its chaperone proteins are regulated and affected by aging will lead to better preventative care and treatment of sarcopenia and, possibly, the age-related decline of heart muscle function.

THE CHAPERONE UNC-45 HAS A CRUCIAL ROLE IN MAINTAINING THE  
STRUCTURE AND FUNCTION OF THE MUSCLE CONTRACTILE  
APPARATUS DURING AGING

By

Courtney Jane Matheny

B.S. Microbiology, University of Georgia, 2015

Advisor: Guy M. Benian, MD

A dissertation submitted to the Faculty of the James T. Laney School of  
Graduate Studies of Emory University in partial fulfillment of the requirements for  
the degree of

Doctor of Philosophy

In

Graduate Division of Biological and Biomedical Science

Biochemistry, Cell, and Developmental Biology

2022

## Table of Contents

<b>Chapter 1: Introduction .....</b>	<b>1</b>
<b>Muscle Anatomy.....</b>	<b>1</b>
Overview .....	1
Myosin structure and mechanism.....	3
<b>The myosin head chaperone UNC-45.....</b>	<b>5</b>
Discovery and importance .....	5
Structure and mechanism .....	7
Interacting proteins .....	9
<b>Sarcopenia .....</b>	<b>11</b>
Overview .....	11
Molecular discoveries made in models other than <i>C. elegans</i> .....	12
Therapeutic discoveries made in models other than <i>C. elegans</i> .....	15
<i>Caenorhabditis elegans</i> as a model organism to study muscle assembly, maintenance, and aging .....	17
Overview of <i>C. elegans</i> as a model to study muscle .....	17
Muscle aging discoveries made using <i>C. elegans</i> .....	19
<b>Scope of Dissertation .....</b>	<b>25</b>
<b>Figures .....</b>	<b>28</b>
Figure 1.1.....	28
Figure 1.2.....	29
Figure 1.3.....	30
Figure 1.4.....	31
Figure 1.5.....	32
Figure 1.6.....	33
<b>Literature cited.....</b>	<b>35</b>
<b>Chapter 2: In vivo mutational analysis of conserved residues of UNC-45 using <i>C. elegans</i></b>	

<b>Introduction .....</b>	<b>44</b>
<b>Results.....</b>	<b>49</b>
Dominant-negative inhibition of thick filament assembly by expression of mutant UCS proteins in <i>C. elegans</i> .....	49
Effects on <i>unc-45</i> temperature sensitive mutants on sarcomere organization, MHC B and UNC-45 protein levels.....	51
<b>Discussion .....</b>	<b>53</b>
<b>Materials and methods .....</b>	<b>60</b>
<b>Figures and Tables.....</b>	<b>63</b>
Figure 2.1.....	63
Figure 2.2.....	64
Figure 2.3.....	65
Figure 2.4.....	66
Figure 2.5.....	67
Figure 2.6.....	68
Figure 2.7.....	69
Table 2.1.....	70
Table 2.2.....	70
<b>Acknowledgements .....</b>	<b>70</b>
<b>Literature cited .....</b>	<b>71</b>
<b>Chapter 3: UNC-45 has a crucial role in maintaining muscle sarcomeres during aging in <i>C. elegans</i></b>	
<b>Introduction .....</b>	<b>75</b>
<b>Results.....</b>	<b>77</b>
<i>C. elegans</i> develop sarcopenia and show decreased numbers of assembled thick filaments during aging.....	77
UNC-45 has a role in maintaining assembled thick filaments and nematode motility during adulthood.....	78

UNC-45 degradation may be increased in aging muscles.....	79
UNC-45 phosphorylation increases with aging.....	80
A delayed onset of Sarcopenia is associated with increased UNC-45 and HSP-90.....	82
HSP-90 may play a pivotal role in UNC-45 protein regulation.....	83
<b>Discussion.....</b>	<b>84</b>
<b>Materials and Methods.....</b>	<b>88</b>
<b>Figures.....</b>	<b>94</b>
Figure 3.1.....	94
Figure 3.2.....	95
Figure 3.3.....	96
Figure 3.4.....	96
Figure 3.5.....	97
Figure 3.6.....	98
Figure 3.7.....	99
Figure 3.8.....	100
Figure 3.9.....	101
<b>Supplemental Figures and Tables.....</b>	<b>102</b>
Table S3.1.....	102
Figure S3.2.....	103
Figure S3.3.....	103
Figure S3.4.....	104
Figure S3.5.....	105
Figure S3.6.....	106
Figure S3.7.....	106
Graphical Abstract.....	107
<b>Acknowledgments.....</b>	<b>107</b>
<b>Literature cited.....</b>	<b>108</b>
<b>Chapter 4: Indole improves aging muscle mass and function and increases Myosin in aged nematodes in an AHR-1/HSP-90/UNC-45 dependent manner</b>	
<b>Introduction .....</b>	<b>113</b>

<b>Results</b> .....	<b>115</b>
Indole protects against loss of muscle mass and function with age.....	115
Indole increases myosin MHC B and its chaperone UNC-45.....	116
Indole’s protective qualities are AHR-1, HSP-90, and UNC-45 dependent.....	118
Indole causes more HSP-90 to bind to UNC-45.....	119
<b>Discussion</b> .....	<b>120</b>
<b>Materials and Methods</b> .....	<b>122</b>
<b>Figures</b> .....	<b>126</b>
Figure 4.1.....	126
Figure 4.2.....	127
Figure 4.3.....	128
Figure 4.4.....	129
<b>Supplemental Figures</b> .....	<b>130</b>
Figure S4.1.....	130
Figure S4.2.....	131
Figure S4.3.....	132
<b>Acknowledgments</b> .....	<b>133</b>
<b>Literature cited</b> .....	<b>134</b>
<b>Chapter 5: Conclusions and future directions</b>	
<b>Overview of findings and significance</b> .....	<b>137</b>
Conserved regions of the UCS domain of UNC-45 are essential for thick filament assembly and organization.....	137
UNC-45 has a crucial role in maintaining muscle sarcomeres during aging in <i>C. elegans</i> .....	138
Indole improves aging muscle mass and function and increases Myosin in aged nematodes in an AHR-1/HSP-90/UNC-45 dependent manner.....	141
Additional data – UNC-45 is increased during stress .....	142
<b>Pitfalls and technical difficulties</b> .....	<b>143</b>
<b>Future directions</b> .....	<b>144</b>
Identification of new clients of UNC-45, as well as new PTMs of UNC-45.....	144
Increasing UNC-45 in older animals to alleviate sarcopenia.....	145

Knocking down HSP-90 or UNC-45 in young adults.....	146
Analysis of TPR domain <i>unc-45</i> mutants from the million-mutation project.....	146
High throughput drug screening.....	147
Analysis of UNC-45 Phosphorylation.....	150
<b>Figures .....</b>	<b>151</b>
Figure 5.1.....	151
Figure 5.2.....	152
Figure 5.3.....	153
Figure 5.4.....	153
Figure 5.5.....	154
<b>Acknowledgments.....</b>	<b>155</b>
<b>Literature Cited .....</b>	<b>155</b>
<b>Abbreviations.....</b>	<b>157</b>

## Chapter 1: Introduction

### Muscle anatomy

#### Overview:

Skeletal muscle is the largest tissue in the animal body, accounting for 40-50% of mass(1). Muscle cells, otherwise known as muscle fibers or myocytes, are multinucleated cells ranging from 10 to 120  $\mu\text{m}$  in diameter and up to 35cm in length(2). Muscle cells are surrounded by a plasma membrane known as the sarcolemma, which is important for proper synaptic transmission, action potential propagation, and excitation-contraction coupling(3). Muscle cells are grouped together and compartmentalized by sheaths of connective tissue. Each cell is surrounded by a thin layer of connective tissue, called the endomysium. Several muscle cells are then grouped together in a more robust layer of connective tissue, called the perimysium, to form a bundle of muscle fibers known as the fasciculus. Fasciculi are then bound and wrapped together in an even stronger layer of connective tissue, called the epimysium, to form the complete muscle (2, 3). The epimysium is continuous with the tendon, which attaches the muscle to the bone.

One unique feature of skeletal muscles is their ability to regenerate from a population of mononucleated quiescent stem cells, called satellite cells, located between the sarcolemma and the basement membrane of the terminally differentiated muscle cells(4). These satellite cells are considerably active during postnatal development, proliferating and fusing with each other to form new myofibers or fusing to existing muscle fibers to grow the muscles during growth(3). Even after maturity has been reached, satellite cells are able to be activated by muscle injury to repair/replace the damaged muscle fibers. Resistance training works by causing muscle injury and inducing this repair and growth mechanism. Resistance training also results in more myofibrils (the contractile

apparatus) being added to existing muscle cells. When satellite cells are activated, they can proliferate to give rise to new satellite cells before differentiating(5). However, there is evidence that the population of satellite cells is heterogenous because not all the satellite cells proliferate before differentiating. These non-proliferating precursor cells are thought to be more committed to the muscle cell fate(6). Despite their ability to self-renew, the number of satellite cells is highest postnatally and declines with age(3, 7, 8).

Each muscle cell is tightly packed with thousands of myofibrils, which are composed of a series of sarcomere subunits. The sarcomere, which is the smallest unit of contraction, is a highly ordered structure consisting of Z-lines (or discs), thin filaments, thick filaments, M-lines, and connectin/titin (Figure 1.1A). The sarcomere is the area between two Z-lines, which serves as a connection between thin filaments of opposite orientation. The thin filament mostly consists of a long double helix of actin monomers, but also contains tropomyosin and troponin in between the two actin chains(2). Titin, also known as connectin, is the largest known protein at ~3-4MDa and the third most abundant muscle protein, after actin and myosin. A single titin polypeptide spans the distance between the Z-line and the M-line, which sits at the center of the sarcomere and the A-band. Titin filaments with opposite polarity overlap at the Z-lines and M-lines. The N-terminus of titin (~80kDa) spans the entire Z-line region. Between 0.8 and 1.5 MDa (depending on the isoform) of titin is located within the I band and is composed of tandemly arranged Immunoglobulin (Ig) domains and a number of intrinsically disordered regions that together form an elastic 'spring'. The ~2MDa A-band region of titin is made of Ig-like and fibronectin type III domains and is tightly associated with the thick filament and accessory proteins, like myosin binding protein C. The final ~200 kDa of the C-

terminus cover the M-line region and contains a pseudo kinase domain and binding sites for obscurin, obscurin-like 1, and MURF-1 (muscle specific ring finger protein-1)(9, 10). The thick filament, or A-band, is primarily composed of myosin, which is the most abundant myofibrillar protein. Thick filaments self-assemble from the rod portion of myosin and are bipolar, with the head domain of myosin projecting from their surface, except in the middle bare zone. Parallel thick filaments assemble into an A-band, held together by the M-line. EM views of this portion through the M-line reveal that in this region of the sarcomere, thick filaments are crosslinked together. Muscle contraction occurs through a “sliding filament” mechanism, by which thin filaments of opposite polarity are pulled inwards by the cyclical attachment, pulling, and release of myosin heads on the surface of the actin thin filament. This is the region of the sarcomere that this dissertation is primarily concerned with.

#### Myosin structure and mechanism:

There is a superfamily of myosins composed of at least 30 classes of myosins(11). Muscle myosin belongs to the class II of myosins, which form bipolar filaments and are considered conventional. A single muscle myosin molecule consists of two myosin heavy chains (MYHs), which interact with two pairs of myosin regulatory light chains and myosin essential light chains to form a hexamer(2, 12). The head domain, or subfragment 1 (S1) is located at the N-terminus and is the motor domain that generates force by ATP hydrolysis when myosin interacts with actin thin filaments. The “neck”, or subfragment 2 (S2), is an  $\alpha$ -coiled-coil structure linking S1 and the “tail”, or light meromyosin (LMM). The “tail”, or LMM, at the C-terminus mediates the dimerization of myosin heavy chains (Figure 1.1B and 1.1C). Myosin forms into highly organized bipolar thick filaments

facilitated by the distribution of charge along the LMM, as well as chaperones that are necessary for the initial folding of myosin head(13, 14). The head is a complex structure that converts the energy of ATP hydrolysis to the mechanical work of binding and moving along F-actin tracks(11). The myosin of the thick filament is an actin-based motor powered by ATP hydrolysis. The pulling of actin filaments by myosin heads protruding from the thick filaments produces the force necessary to move the muscle, and thus the animal. The contraction cycle may continue if ATP is available and calcium in the sarcoplasm, the cytoplasm of striated muscle cells, is high. The myosin in striated muscle is always active and available, unless the myosin binding sites on the actin filament are covered by a coiled-coil dimer protein called tropomyosin. When calcium is readily available, it binds to troponin, which binds to and moves tropomyosin out of the way(2, 11, 15).

Sliding filament assays can be used to test the functionality of myosin heads by binding purified S1 (head domain) or heavy meromyosin (HMM), which consists of part of the rod and two heads, on a glass slide or nitrocellulose film and observing if fluorescently labeled actin filaments are able to slide along the myosin heads(16). When expressed as recombinant protein in bacteria, myosin light chains are able to bind to myosin heavy chains(17), and the rod portions of myosin are able to self-assemble into thick filament like structures(18). However, when expressed in bacteria, myosin heads are not active in sliding filament assays(19, 20). Myosin heads derived from cardiac and skeletal muscle are only active in the presence of muscle extract, suggesting that the heads do not fold spontaneously and require other factors, like chaperones(21, 22).

## The Myosin head chaperone UNC-45

### Discovery and Importance:

UNC-45, the first, and only, myosin head chaperone conserved across all eukaryotes, was discovered in *Caenorhabditis elegans*, and named for the uncoordinated (impaired movement) phenotype observed in mutant animals(23). UNC-45 is essential for proper formation of myofibrils in skeletal muscle, as well as the myocardium. UNC-45 has 2 mammalian homologs: Unc-45a – expressed ubiquitously – and Unc-45b – expressed mainly in cardiac and skeletal muscle(24). Through antisense RNA experiments, Unc-45a has been shown to be important for cell proliferation and fusion, whereas Unc-45b is essential for myoblast fusion and myofibril development(24). Mis-regulation of Unc-45a and Unc-45b is associated with several diseases including myopathies(25-27), cardiomyopathies(27, 28), cataracts(29), cancer metastasis(30), and other less defined syndromes(31).

In *C. elegans*, *unc-45* null mutants are embryonic lethal (Pat – paralyzed and arrested at the two-fold embryonic stage) (26). When grown at the restrictive temperature, *unc-45* temperature sensitive mutants develop into adults that are paralyzed with myofibril disorganization, reduced numbers of thick filaments, reduced accumulation of myosins, and randomization of the two body wall muscle myosin isoforms, MHC A and MHC B, localization in thick filaments (23, 32, 33). *Drosophila* with a null *unc-45* allele were embryonic lethal with a dramatic reduction in myosin heavy chain and a near absence of any thick filaments(34). RNAi knockdown of *unc-45* in later stage fly embryos (blastoderm) resulted in normal muscle fiber patterning with no contractility, further

supporting UNC-45's importance in the function of the thick filament(35). The UAS-Gal4 inducible RNAi knockdown of *unc-45* in *Drosophila* cardiac cells at different stages of fly development demonstrated that UNC-45 is essential during all stages of heart development(28). In the vertebrate *Xenopus tropicalis* (western clawed frog), mutation of *unc-45b* (*dicky ticker*) results in disrupted skeletal muscle myofibrillogenesis, paralysis, and lack of a heartbeat(36). This *dicky ticker* phenotype is also seen when UNC-45b is depleted using an antisense morpholino oligonucleotide. In zebrafish, morpholino oligonucleotide mediated knockdown of *unc-45b* resulted in embryonic paralysis, cardiac dysfunction, and embryonic lethality(27). In mice, recessive loss of function mutations in *unc-45b* resulted in cardiac developmental arrest and embryonic lethality, despite the presence of *Unc-45a*(37). Intriguingly, it was first shown in *C. elegans*, and later confirmed in zebrafish, that significant overexpression of UNC-45 also results in paralysis and disorganized myofibrils(25, 38). Since too little or too much results in a diseased state, UNC-45 protein levels must be tightly regulated to maintain healthy sarcomeres.

Using a classical chaperone assay, nematode UNC-45 has been shown to prevent the thermal aggregation of myosin S1 (39). Thus, UNC-45 is thought to be required to fold the myosin head initially after translation and, likely, to re-fold the myosin head after stress results in unfolding (40, 41). UNC-45 may be crucial in mature muscle because of the physical, thermal, and oxidative stress muscle cells undergo throughout life and the relatively slow turnover rate of myosin in established thick filaments(42). In *C. elegans*, UNC-45 has been shown to localize stably with MHC B in the A-band and more diffusely with the I-band, however these results were obtained with transgenically expressed fluorescent UNC-45 and may not be reflective of how the endogenous protein behaves

(43, 44). In zebrafish, it has been shown that UNC-45 localizes to the Z-discs and can be recruited to the thick filaments after stress has occurred (cold, heat, chemical, and physical stress)(40). Through CRISPR, we have added an mNeonGreen tag to the C-terminus of endogenous UNC-45 and observe strong levels of UNC-45 localized in striated patterns in the adult body wall, pharyngeal, and vulva muscles (Figure 1.2).

### Structure and Mechanism:

UNC-45 belongs to a family of proteins containing a UCS (UNC-45/Cro1/She4p) domain that interacts with myosins. *C. elegans* UNC-45 was the first UCS protein identified, followed by the fungal proteins She4p and Cro1, which share high sequence similarity to each other and UNC-45. In 1996, She4p was identified from two independent *S. cerevisiae* screens. Deletion of *SHE4* resulted in decreased growth and endocytosis, altered cell morphology, and loss of actin cytoskeleton polarity(45, 46). In 1998, CRO1 was identified from a *P. anserina* screen for defects in sexual sporulation. The null *cro1* mutant displayed abortive meiosis, leading to polyploidy, an inability to form septa between the daughter nuclei, and decreased filamentous growth. The authors speculate that in the absence of CRO1, myosins that interact with and organize the actin cytoskeleton may not be functional and as a result, actin assembly and microtubule disassembly is disrupted(47). Around the same time, Rng3p was identified in an *S. pombe* screen for defective actomyosin ring assembly and cytokinesis(48). When *RNG3* missense mutants were crossed with *myo2* mutants, synthetic lethality resulted, suggesting a functional interaction between the two proteins(49). Thus, all three of the fungal UCS proteins and UNC-45 are linked by sequence similarity in their C-terminal

domains and by their association with processes related to or requiring conventional and unconventional myosins.

The UCS domain is sufficient to rescue both lethal null *unc-45* and temperature sensitive loss-of-function mutants(50). In addition to the UCS domain at the C-terminal, UNC-45 is comprised of an N-terminal tetratricopeptide repeat (TPR) domain that interacts with the heat shock co-chaperone protein HSP-90(39), and a central domain that acts as an inhibitor of the myosin power stroke(51). In fact, Ni et al. found that the UCS domain alone has more activity in vivo than full length UNC-45(44). This is thought to be because of the inhibitory nature of the TPR domain - HSP-90 interaction. In sliding filament assays, Unc-45b alone inhibits the myosin power stroke, but not the myosin head ATPase activity. This inhibition is alleviated by adding HSP-90. The rescue of the power stroke by HSP-90 is only observed when the TPR domain of Unc-45b is present(52). Bujalowski et al. hypothesize that under normal conditions the UCS domain of UNC-45 is bound to the myosin head and the TPR domain is bound to HSP-90. Under stress conditions, HSP-90 detaches from the TPR domain, causing a conformational change in UNC-45 that allows the Central domain to bind to the myosin neck resulting in inhibition of the myosin power stroke while the UCS domain protects/re-folds the myosin head. After refolding of the myosin head, by some unknown mechanism, HSP-90 can then rebind the TPR domain, causing the Central domain to release the myosin neck, restoring movement of the myosin motor(51) (Figure 1.3).

The crystal structure of *C. elegans* UNC-45 shows that the overall shape is of an “L” with the UCS domain forming one leg, and the central and TPR forming the other

leg(53) (Figure 1.4). In addition, all of the central region and UCS domain consists of 17 armadillo (ARM) repeats, each consisting of 2-3  $\alpha$ -helices. Most significantly, UNC-45 forms linear multimers in which the length of the repeating unit (17 nm) is similar to the absolutely conserved distance between pairs of myosin heads along the surface of thick filaments (closest distance between adjacent double heads is 14.3 nm). Thus, these UNC-45 multimers may help stabilize this arrangement during thick filament and sarcomere assembly. Also, this architecture provides additional evidence that UNC-45 may be able to refold myosin heads that are damaged by heat or oxidation as the muscle is used and ages.

#### Interacting proteins:

UNC-45's major client is conventional myosin. A direct association with the major *C. elegans* body wall muscle myosin heavy chain isoform MHC B is supported by immunofluorescence co-localization of the two proteins(43). *unc-45* temperature sensitive loss-of-function mutants have reduced levels of MHC A, B, C, and D and display highly disorganized A-bands when immunostained with antibodies to either MHC A or B(38, 54). We also observe high levels of endogenous UNC-45::mNeonGreen in the adult pharynx muscle, which is composed of MHC C and D (Figure 1.2). This all supports the idea that UNC-45 chaperones all the different muscle myosin heavy chain isoforms. It also chaperones a non-muscle myosin II, NMY-2, and interacts (likely chaperones) with the non-conventional class V myosin HUM-2(55, 56). In early embryos UNC-45 co-localizes with NMY-2 at cell boundaries and facilitates embryonic polarity establishment, cytokinesis, and germline establishment(56).

As described above, the TPR domain of UNC-45 has a strong binding affinity for HSP-90 at a conserved MEEVD region(39). This interaction is likely to prevent UNC-45 from aberrantly, and continuously, binding myosin and inhibiting the myosin power stroke(51). We speculate that during cellular stress, HSP-90 unbinds UNC-45 so that it can re-fold other proteins within the cytoplasm while UNC-45 re-folds the myosin head. HSP-90 is quite a promiscuous protein, with several hundred binding partners/clients(57). UNC-45 has also been shown to interact with HSP-70, though not as strongly as with HSP-90(53). Multiple groups have found evidence that UNC-45, HSP-70, and HSP-90 form a chaperone complex to properly fold Myosin(53, 58, 59)

UNC-45 has also been shown to bind to and possibly act as a chaperone for Apobec2, GATA4, and the progesterone receptor (directly or indirectly). Apobec2, a cytidine deaminase responsible for editing apolipoprotein mRNA, interacts with both the central and UCS domains on Unc-45b (but not Unc-45a) in a yeast two hybrid screen and co-localized with Unc-45b in zebrafish at the myoseptal boundary (connective tissue between bundles of muscle fibers) and Z-disks(60). The localization of Apobec2 was dependent on Unc-45b, but Unc-45b localization was not dependent on Apobec2. The authors hypothesize that Apobec2 functions in cytoplasmic RNA editing or repair, modifying or maintaining the large mRNAs of the proteins the form the dystrophin-glycoprotein complex. In mice, expression of mutant Unc-45b resulted in a transcript independent reduction in the cardiogenic transcription factor GATA4(37). Unc-45b was able to bind to GATA4 and may act as a chaperone its proper folding. UNC-45 is able to protect citrate synthase from forming aggregates *in vitro*, but this does not necessarily correlate physiologically(39). Unc-45a is able to bind progesterone receptors *in vivo* and

appears to stimulate their enhancement of transcription(61). It is likely that there are more unknown clients and/or binding partners to discover. In my concluding chapter, I outline a genetic screen to identify more potential clients of UNC-45.

UNC-45 is a substrate of an E3/E4-multiubiquitination complex containing CHN-1, a homolog to human CHIP, and UFD-2(62). UNC-45 is regulated and degraded through ubiquitination by CHN-1 and UFD-2 working in tandem as an E3/E4 (ubiquitin ligase/conjugation factor) complex. The egg laying (Bag phenotype) and movement defect of two *unc-45* temperature sensitive mutants (*e286* and *m94*) were suppressed when crossed with a *chn-1(by155)* loss of function mutant. This is most likely due to the increased stabilization of the corresponding mutant UNC-45 proteins. Excess UNC-45 transgenically expressed in *chn-1(by155)* animals displayed disrupted sarcomere structures and a severe motility defect.

## **Sarcopenia**

### Overview:

Sarcopenia, the decline in skeletal muscle mass and function without any underlying disease, is a major contributor to physical disability, poor quality of life, and death among the elderly(63). 40-50% of individuals over 80 years of age suffer from this loss of muscle mass and function(64, 65). The molecular mechanisms responsible for this age-related condition remain unknown(66). Improved diet and exercise have a modest effect on improving and maintaining muscle mass and function, but the best diet and resistance training regimen for maintaining muscle health into late adulthood has yet to be determined(67, 68). Increasing essential amino acids, milk-based proteins, creatine monohydrate, essential fatty acids, and even vitamin D have been shown to be beneficial

to building and maintaining muscle mass in older adults who are also exercising their muscle(69). There is a direct association between poor hand grip strength, reduced physical function and a higher risk of falling(70). Intriguingly, even in middle age (40-69), there is a correlation between reduced grip strength and all-cause mortality and incidence of and mortality from cardiovascular disease, respiratory disease, and cancer(71). A GWAS study of over 200,000 individuals identified 64 genes associated with grip strength, and many of these genes are known to have roles in neural development or brain function(72). Interestingly, one hypothesis about sarcopenia is that it is caused by motor neuron decline with age(73). Elderly individuals at a higher risk of falling are thus at a higher risk of vertebral and non-vertebral fractures(70) – leading to surgeries, hospitalization, and increased medical complications and risks. Additionally, the increased risk of respiratory illness in individuals over 65 years of age may be partially explained by the ageing-related weakening of the diaphragm muscle resulting in non-productive coughs and more severe respiratory illnesses(74). With the ever-increasing population of elderly and the predicted strain on the healthcare system(75-77), it is crucial we understand the molecular mechanisms responsible for age-related diseases like sarcopenia so that we can develop more effective therapies and prevention methods.

#### Molecular discoveries in models other than *C. elegans*:

In 2010 Altun et al. investigated the activity of the ubiquitin proteasome pathway in aged muscles of Sprague Dawley rats (71). They found 2–3-fold higher levels of 26S proteasomes than those of young adult controls. 26S proteasomes purified from muscles of aged and young adult rats showed a similar capacity to degrade peptides, proteins, and an ubiquitylated substrate, but differed in levels of proteasome-associated proteins

(26S proteasome subunits, ubiquitin ligases, and deubiquitylating enzymes were all increased in aged rats). The aged muscles contained higher levels of the ubiquitin ligase CHIP, involved in eliminating misfolded proteins, and MuRF1, which ubiquitylates myofibrillar proteins. Nevertheless, their content of polyubiquitylated proteins was higher than in young adult animals – suggesting that the increase in proteasome associated proteins could be due to impaired degradation of these proteins, causing an increase in non-functional polyubiquitylated proteins that are neither properly degraded nor functional (78). This group also tested the effects of dietary restriction (70% of what the control group was fed – not enough to cause starvation) on ubiquitination and the proteasome pathway in aged rat muscle. They found that reducing the caloric intake of these rats resulted in decreased or complete prevention of the age-associated increases in ubiquitin proteasome system components. The dietary restriction rats experienced significantly less muscle atrophy compared to the control rats at 30 months, however the authors did not comment on muscle function or show any results from motility tests(78).

Tribbles Homolog 3 (TRB3) is a pseudokinase that acts as a modulator of substrate ubiquitination and as a molecular scaffold for the assembly and regulation of signaling modules(79). TRB3 was previously reported to exhibit an age-related increase in expression(80) and play a vital role in cell proliferation, differentiation, and fibrosis. It has been demonstrated that overexpression of TRB3 caused muscle fiber atrophy and a decrease in muscle function by negatively modulating protein turnover in the condition of food deprivation(81, 82) and could inhibit the myogenic differentiation of C2C12 (mouse myoblast) tissue culture cells(83). Shang et al. acquired TRB3 knockout mice and found that sarcopenia was attenuated in these mice compared to aged controls via the

alleviation of atrophy and fibrosis of skeletal muscles(84). The TRB3 knockout mice had reduced atrophy and a greater exercise capacity compared to the wild type mice at the same age. The authors did not reveal if the TRB3 knockout mice lived longer or at what age they may have developed sarcopenia.

Like what has been found in rats, analysis of gene expression changes in *Drosophila* muscles during aging has shown increased expression of 26S proteasome components as well as increased expression of antioxidant stress response elements(85). Another group found that overexpression of FOXO (Forkhead Box O), an important transcription factor associated with longevity regulation (86), reduced the age-related accumulation of p62–poly-ubiquitin protein aggregates in fly muscles and preserved muscle function(87). P62 is an autophagy receptor that also binds to poly-ubiquitinated proteins, enabling ubiquitinated proteins to aggregate and connecting the ubiquitin proteasome system to the autophagy-lysosome system(88). FOXO is the near terminal output of the insulin / insulin growth factor signaling pathway and is inhibited by Akt (protein kinase B) phosphorylation via this pathway(89). Antagonizing insulin signaling via transcriptional induction of the *Drosophila* ortholog of insulin-like growth factor binding protein 7 caused lifespan extension and prevented age-related muscle deterioration(90).

An age-related reduction in available calcium, which is necessary for muscle contraction, is a possible contributor to sarcopenia pathology. Lorenzo et al. found that in *Drosophila* there is a decrease in sarcoplasmic reticulum (SR) calcium with age that correlates with the decline in muscle function (84). They hypothesized that this decline was due to increased leakiness of the ryanodine receptor calcium channel

allowing more calcium to leave the SR (91). As mentioned earlier, calcium is necessary for the contraction cycle to take place and the SR contains stores of calcium for this purpose. Without the proper balance of calcium between the SR and the cytoplasm, muscle function would become impaired.

#### Therapeutic discoveries in models other than *C. elegans*:

The major contribution rodent studies have made to sarcopenia research has been discovering therapeutics, drugs and lifestyle changes, that can attenuate the symptoms of sarcopenia. Ryu et al. found that urolithin A, a natural dietary compound found in some nuts and fruit, was able to improve muscle function in aged mice via inducing mitophagy (mitochondrial autophagy)(92). Another group of naturally occurring compounds that may extend the muscle health of mice are indoles, which come from commensal microbiota(93). While mice treated with indoles retain greater motility as they age (presumably because muscle function is maintained) as compared to the age-matched controls, they do not experience an extension of lifespan(93). Myostatin, a TGF family member, is a myokine secreted by skeletal muscle cells that acts to limit muscle cell growth. It does so by binding to an activin type II receptor and inhibiting the differentiation of myoblasts during development, or satellite cells in mature muscle (94). While crucial for proper development, myostatin might be detrimental for aging muscles. Multiple groups have found that inhibiting myostatin via antibodies in aged mice improves muscle mass and strength, as well as insulin sensitivity(95-97). Ferraro et al. found that trimetazidine (a metabolic modulator that improves the efficiency of glycolysis) administration to ageing mice increased muscle strength, expression of slow myosin heavy chain isoform in gastrocnemius muscle, and the number of small-sized myofibers

in tibialis anterior muscle(98). Potech et al. found that the small molecule espidolol significantly increased lean body mass with reduced fat mass in ageing rats(99). Espindolol treatment leads to a reduction of catabolic/atrophic signaling by blocking the chronic activation of the  $\beta$ -1 adrenergic receptor, while inducing anabolic signaling by the intrinsic sympathomimetic activity effect on the  $\beta$ -2 adrenergic receptor(99). Another group found that long-term moderate exercise combined with metformin treatment induced a hormetic response in Wistar rats that prevented age-associated loss of muscle strength and muscle mass(100). Metformin is known to inhibit hepatic gluconeogenesis thereby decreasing glucose plasma levels and is often prescribed to treat type II diabetes(101, 102). It has also been found that metformin inhibits mitochondrial respiratory chain complex I and generates low levels of reactive oxygen species, which induce the antioxidant response producing a hormetic effect – a favorable biological response to a light stressor. At the same time, reduced ATP levels activate AMPK (AMP activated protein kinase), which activates diverse protective pathways.

In line with what has been found in rats, Katewa et al. have shown that dietary restriction alleviates flight defects in aged flies(103). The authors show that this is likely due to increasing mitochondrial function and fatty acid oxidation in the predominately aerobic flight muscles(103). However, dietary restriction in flies does not prevent the senescence of the primarily glycolytic muscles used for walking and climbing(104). These and previous findings suggest that dietary restriction is useful for extending lifespan and preserving some, but not all, types of muscle cells. Sonowal et al. demonstrated positive effects of indole on motility (again, presumably reflecting improved muscle function) of elderly *Drosophila*. While they saw no difference in climbing motility in young flies, aged

flies (20 days old) treated with indole or indole producing bacteria were approximately two-fold more motile compared to age matched controls(93). They found that the benefits gained by indole treatment were dependent on the aryl hydrocarbon receptor (AHR), a conserved receptor for xenobiotic small molecules, and known to bind to indoles (93). See Figure 1.5 for a summary of the therapeutic and mechanistic discoveries made in model organisms.

***Caenorhabditis elegans* as a model organism to study muscle assembly, maintenance, and aging**

*C. elegans* muscle:

The development, regulation, and maintenance of the most basic unit of muscle contraction - the sarcomere - is highly conserved from worms to humans. For nearly fifty years, the model system *Caenorhabditis elegans* has been crucial to uncovering the molecular mechanisms that govern sarcomere biology(105). Since Sydney Brenner first established *C. elegans* as an excellent model organism, there have been at least 200 proteins identified as crucial for sarcomere assembly and organization(106). Like us, *C. elegans* have both striated and non-striated muscles. This body of work, however, is primarily concerned with the 95 diamond-shaped striated body wall muscles that run from head to tail of the animal. These muscle cells are comparable to vertebrate skeletal muscles (Figure 1.6). While vertebrates exhibit cross-striated muscles, striation in *C. elegans* muscles appears slightly oblique with respect to the longitudinal axis of the muscle cell with which it forms an angle of  $5.9^\circ$ (107). As in mammalian muscle, each sarcomere is composed of a bundle of thick filaments primarily composed of myosin, called the A-band, organized around an M-line and thin filaments primarily composed of

actin, which are associated with dense bodies, the nematode analog of Z-disks. The A-band of body wall muscle contains two myosin isoforms: Myosin Heavy Chain A/ MHC A (*myo-3*) and Myosin Heavy Chain B/ MHC B (*unc-54*), each encoded by different genes. MHC A is located in the middle of the A-band with MHC B on either side. This differentiated localization of the two MHC isoforms extends to the individual thick filaments, with MHC A located in the middle and MHC B located in the polar regions(108). This makes MHC B the more abundant myosin isoform in body wall muscle, making up about 70% of the total myosin in the adult. MHC A makes up about 20% of the total myosin heavy chain, while the other 10% is comprised of isoforms C and D, which are located primarily in the pharynx muscle.

Unlike vertebrates, *C. elegans* muscles lack satellite cells (muscle stem cells) and thus, the ability to regenerate muscle cells. The muscle cells present after development are all the worm has, making the study of complex processes, such as muscle aging and degeneration, easier to accomplish. Additionally, the body wall muscle cells in adult worms are completely post-mitotic, do not fuse, and remain mononucleated. This makes nematode body wall muscle a much simpler system of study compared to mammalian muscle, which, through myogenesis, does fuse to form multinucleated skeletal muscle cells called syncytia.

Muscle function is easy to monitor in worms since they require functioning body wall muscles for locomotion. Because worms are transparent, muscle structure can easily be assessed by polarized light microscopy, electron microscopy, fluorescently tagged proteins, and immunofluorescent staining. The optical transparency of *C. elegans* can also be exploited for mutant and drug screens (e.g., based on fluorescently tagged

proteins expressed at endogenous levels via CRISPR)(109). *C. elegans* mutants can be easily studied by traditional genetic screens after chemical mutagenesis, RNAi, which can be provided as dsRNA through their bacterial food, transgenic arrays, and CRISPR generated mutants. The million-mutation project (MMP) used EMS (ethyl methanesulfonate) and ENU (N-ethyl-N-nitrosourea) to mutagenize wild type worms to create 2,000 independent homozygous mutant adult viable strains(110). The genome of all 2,000 strains have been sequenced and the data is available on Wormbase. The strains are available individually or as the complete strain set from the Caenorhabditis Genetic Center. These methods make it relatively easy to determine if a gene of interest has any significant function in muscle biology and to perform large scale screens for new genes important for sarcomere development, function, and regulation.

The study of *C. elegans* has led to a number of discoveries relevant to muscle biology, in general. Here are a few of the most note-worthy ones: (1) The cloning, sequencing, and analysis of the first complete myosin heavy chain, *unc-54*(23, 111). Analysis of this sequence led to the first model for the parallel assembly of myosin rods into the thick filament. (2) The discovery that integrin and associated proteins are critical for sarcomere assembly(112-115). The first complete sequence of a giant titin-like protein called twitchin(116, 117). (4) The discovery that actin regulatory proteins are crucial for sarcomere assembly (118-120).

#### *C. elegans* muscle aging discoveries:

In order to better tease out the molecular “players” responsible for muscle maintenance and determine how they change with age we need to look more towards

model organisms for insight. Model organisms provide the benefit of shorter lifespans, larger sample sizes, genetic manipulation, and controlled environmental conditions. Currently the sarcopenia research field has utilized rodents, *Drosophila*, and *C. elegans* as models for aging muscle. The *C. elegans* model provides the shortest lifespan and largest possible sample size among these models. Their short lifespan (average 18-21 days) makes them particularly convenient for aging studies. Muscle function is easy to monitor in worms since they require functioning body wall muscles for locomotion. The optical transparency of *C. elegans* can be exploited for mutant and drug screens (e.g., based on fluorescently tagged proteins expressed at endogenous levels via CRISPR). Additionally, like *Drosophila*, nematode muscle does not contain stem cells and thus provides an opportunity to investigate how the assembled muscle contractile apparatus is maintained and functions during aging in the absence of regeneration. Monica Driscoll's lab was the first to report that *C. elegans* undergo an age-dependent decline in whole animal locomotion and deterioration of the muscle myofilament lattice and thus *C. elegans* is a good model for sarcopenia (121). They found variability among same-age animals, even of advanced age, in the time of onset and severity of reduced locomotion. Because these animals have the same genomes (i.e., they are isogenic), this indicated that like humans, a major factor in nematode aging is stochastic.

Through genetic analysis, it has been discovered that many genes that when mutated, result in lifespan extension in *C. elegans* (122, 123). A major pathway that affects longevity is the insulin receptor pathway: Loss of function mutations in the single insulin receptor, DAF-2, or in the downstream PI(3)kinase, AGE-1, result in lifespans that are 2-2.5X longer, respectively, compared with wild type animals. Herndon et al. reported

that in an *age-1* mutant there was significant delay in the onset of the dysmorphology of muscle nuclei compared with wild type(121). This same *age-1* mutant also delays loss of locomotion in aging worms(124). A DAF-2 (insulin receptor) mutant was found to have a transcription dependent increase in muscle mass and abundance of key sarcomere proteins, like myosin(125). Loss of function of *daf-2* results in an induction of mitophagy in body wall muscle, including an increase in level of the mRNA for DCT-1, the nematode ortholog for mammalian BNIP3, the mitophagy receptor (126). Thus, induction of mitophagy, a quality control mechanism for mitochondria, might partly account for the preserved muscle function in older *daf-2* mutant animals.

*C. elegans* microarray analysis has revealed 27 genes encoding evolutionarily conserved muscle sarcomere proteins that undergo a 2-fold decrease in mRNA expression between day 0 and day 7 adults (127). This decline occurs as early as day 1 of adulthood, which is perhaps not surprising since sarcomere assembly is completed by day 0 of adulthood(109) and sarcomeres are quite stable structures(42). To understand the mechanism by which there is an early decline in sarcomeric protein transcripts, Lamarche et al. examined the transcript levels during aging of two myogenic transcription factors, UNC-120 (serum response factor/SRF) and HLH-1 (MyoD) that are known to be required for embryonic muscle differentiation but are also expressed in adult muscle. They found that between day 0 adults and day 7 adults, there was a 40% decrease in the level of *unc-120* mRNA, but a weak increase in the level of *hlh-1* mRNA. They found that changes in *unc-120* expression did not affect lifespan, however, reducing *unc-120* expression via RNAi accelerated muscle aging and, conversely, overexpression of *unc-120* delayed muscle aging (127). Interestingly, markers of muscle aging included an age-

dependent increase in mitochondrial fragmentation (usually associated with decreased function) and an increase in autophagic vesicles. Lamarche et al. also saw a 2-8-fold increase in sarcomere transcripts at day 5 of adulthood in a *daf-2* mutant. This mutant also showed a 2-fold increase in *unc-120* transcripts from day 1 through day 5. They found via RNAi of *unc-120* that the beneficial effects of the *daf-2* mutation on muscle aging are dependent on *unc-120*. This suggests that the downstream DAF-16 (FOXO) transcription factor may regulate the *unc-120* promoter.

Several studies have shown that mitochondrial organization and function decline in body wall muscle of nematodes as they age. Yasuda et al. showed that by EM, there is a progressive enlargement and swelling of mitochondria in body wall muscle(128), similar to what has been shown in mouse muscle(129). In a carefully performed study, Gaffney et al. showed that by assessing mitochondrial network structure and A-band organization using fluorescence microscopy, there is a progressive loss of mitochondrial and A-band organization from adult day 0 through adult day 16 (130). Interestingly, the authors show that mitochondrial fragmentation is evident at day 4, whereas A-band disorganization is evident at day 6, and that the extent of the mitochondrial defect is better correlated with the decline in whole animal locomotion than is the extent of the A-band defect. Intriguingly, the authors demonstrated that a loss of mitochondrial function precedes, and thus may result in loss of mitochondrial structure: they observed a decline in maximal mitochondrial ATP production rate from day 0 to day 2 of adulthood, and a loss of mitochondrial membrane potential from day 0 to day 4 of adulthood. One weakness of their study, however, is that they performed these mitochondrial function experiments on mitochondria purified from whole nematodes. It will be important to

determine if the same results can be obtained using mitochondria isolated from body wall muscle, using a recently developed method (131). Nevertheless, this leads to an intriguing possibility that the decline in mitochondrial function may explain the onset and progression of loss of muscle function before there is a decline in sarcomere organization.

Like rodents, flies, and most other species(132), dietary restriction leads to increased longevity of *C. elegans* through multiple pathways(133). Depuydt et al. found that dietary restriction causes an increase in muscle mass and abundance of integral sarcomere proteins, like the different myosin isoforms(125). They found that this increase in sarcomere proteins is transcription independent and theorize that it is caused by selective inhibition of structural muscle protein degradation or an increase in muscle-specific protein synthesis. Like in mammals, exercise has been shown to have a modest, yet significant, positive effect on the lifespan and muscle function of *C. elegans* (134, 135). The report from Hartman et al. is particularly intriguing. Starting from adult day 2, they forced the worms to undertake swimming as exercise twice a day (90 min each) for 6 consecutive days and then assessed mitochondrial health on day 12. Exercise clearly led to less fragmentation of body wall muscle mitochondria, and less whole animal lethality from the mitotoxicants rotenone and arsenic, as compared to animals that had not exercised, but it did not increase the mitochondrial DNA copy number, or reduce the extent of mitochondrial DNA lesions, or increase basal respiration.

The naturally occurring compounds uralithin A and indole also improve the muscle function in aged *C. elegans* (92, 93). Urolithin A extended the worms' lifespan and prolonged normal activity – crawling mobility and pharyngeal pumping – via inducing

mitophagy and improving the mitochondrial health of body wall muscle mitochondria(92). Sonowal et al. found that treating with indole or indole producing bacteria also improved whole animal locomotion and pharyngeal pumping of older adults (presumably due to improved muscle function) but did not increase the lifespan of *C. elegans*. They found that, like in *Drosophila*, the effects of indole are dependent on the aryl hydrocarbon receptor, AHR-1(93).

There are multiple conserved cellular pathways and mechanisms that appear to be involved in sarcopenia pathogenesis across multiple model organisms. In *C. elegans*, *Drosophila*, and mice there is evidence that the insulin/IGF1 and Akt signaling pathways appear to play a role in both ageing and the age-related decline in muscle health through the FOXO transcription factor. Data from these three models provide evidence for identifying compounds that increase FOXO nuclear translocation as a possible therapeutic for sarcopenia patients. The quality of the skeletal muscle mitochondria is another conserved factor to consider when searching for sarcopenia therapeutics. Mitochondria quality is reduced in both *C. elegans* and rodent aged muscle, and there is evidence that this precedes the decline in muscle function with age. Additionally, the loss of muscle mass may, at least in part, be explained by the increase in protein degradation via the proteasome system. In both *Drosophila* and rats, components of the 26S proteasome were elevated in aged animals.

Currently, the NIH clinical trials database ([clinicaltrials.gov](http://clinicaltrials.gov)) shows over 400 studies related to sarcopenia with 23 active and 177 completed interventional studies. Sarcopenia research would greatly benefit from the use of *Drosophila* and *C. elegans* to identify more therapeutic strategies and the use of rodents to then test those therapies

further. Such an evolutionary pipeline approach was reported recently to identify small molecules that might be useful for treating RYR1-related myopathies (Benian & Choo, 2020; Volpatti et al., 2020). Currently, research in rodents has been focused on muscle regeneration instead of muscle maintenance despite the known depletion of muscle satellite cells during aging (7, 8). Without the normal population of muscle satellite cells or a way to replenish the satellite cells with age, research may need to shift focus to how existing muscle cells (fibers) can be better maintained. Both *Drosophila* and *C. elegans* are well suited models for muscle maintenance since they do not have any muscle satellite cells. High throughput screenings to identify drugs, small molecules, or conditions that improve muscle maintenance with aging can be done easily with both flies and worms. Candidate therapies for sarcopenia can be identified in this way. Any treatments that alleviate muscle aging in these models will be independent of regeneration through satellite cells and, thus, possibly more suitable for aged individuals who have lost much of their satellite cell population. These types of treatments may also be beneficial for the maintenance of cardiac muscle, which does not possess stem cells and the ability to regenerate.

**Scope of dissertation:**

In this dissertation I will describe the work I have done to further investigate the role of the myosin head chaperone UNC-45 during adulthood and its importance during the aging process. Previously, UNC-45's role during development has been well characterized but its role during adulthood has not been sufficiently studied.

I have further characterized six temperature sensitive loss-of-function *unc-45* mutants, two of which were newly identified using the million-mutation project(136). I have

also created and analyzed novel *unc-45* mutations using transgenic animals to determine the roles and importance of multiple conserved regions within the protein structure(54).

I characterized the onset of sarcopenia within wildtype nematodes and the correlated changes in HSP-90, UNC-45, and Myosin steady state protein and transcript levels. HSP-90 protein declines at day 3 of adulthood right after the transcript declines at day 2. UNC-45 and Myosin transcripts declined at the young adult stage, immediately following development, days before the decline in protein. UNC-45 protein declined at day 4, right after HSP-90 decline, and MHC B (the main myosin client of UNC-45) declined at day 8 of adulthood. Using a temperature sensitive *unc-45* mutant, I found that a loss of functional UNC-45 starting at young adulthood is sufficient to cause early onset of sarcopenia. This provides evidence that UNC-45 is not only crucial to muscle structure and function during development, but also during adulthood. Using an *hsp-90* m I found that a longevity mutant with a delayed onset of sarcopenia also has a delayed loss of HSP-90, UNC-45, and Myosin. Using an *hsp-90* temperature sensitive mutant, I identified a role for HSP-90 in the stabilization and regulation of UNC-45 protein. Thus, loss of HSP-90 with age could be a part of the potential mechanism for the loss of UNC-45 and the subsequent loss of Myosin during aging. When I run aged samples on a 4-15% or 4-20% gradient SDS-PAGE and immunoblot for UNC-45, I see a modified species of UNC-45 increase as the UNC-45 species at the predicted molecular weight of the unmodified protein decreases. To further investigate this mysterious post-translational modification, I ran aged samples on a gel designed to separate proteins based on phosphorylation status (SuperSep™Phostag™) and found that during aging, phosphorylated UNC-45 increases. Through mass spectrometry analysis, we have identified one phosphorylation

site on UNC-45 at serine 111, which is in the TPR domain and would likely inhibit the interaction between UNC-45 and HSP-90. This phosphorylation site is also close to the interface of UNC-45 oligomers and may prevent UNC-45 oligomerization and stable association with the thick filament. Thus, phosphorylation at serine 111 could cause UNC-45 to be left in a state that is more susceptible to ubiquitination and degradation.

I demonstrated that supplemental indole improves muscle health in older animals and began to tease out the mechanism by which indole can alleviate sarcopenia. Older worms treated with indole in their bacteria diet and supplemented into their agar growth media exhibited improved crawling motility, increased A-band number, and increased steady state levels of UNC-45 and Myosin protein in a transcript independent manner. The positive effects of indole were dependent on HSP-90, AHR-1, and UNC-45. Though indole did not increase the protein levels of HSP-90, it did cause more HSP-90 to be associated with UNC-45, which we postulate improved UNC-45 stabilization. We hypothesize that indole is binding to AHR-1, releasing HSP-90 from the complex so that more HSP-90 is freely available to bind to and stabilize UNC-45. This leads to improved maintenance of the thick filament during aging, thus improving the muscle health span.

Altogether, this body of work supports the hypothesis that during aging a decline in HSP-90 leads to the increased phosphorylation and degradation of UNC-45, which leaves Myosin heads susceptible to unfolding, aggregation, and degradation. Loss of Myosin leads to a reduction in the number of assembled thick filaments, a loss of muscle mass, and an ultimate decline in mobility. One path to better treating and preventing sarcopenia is to maintain the existing assembled sarcomeres.

## Figures:

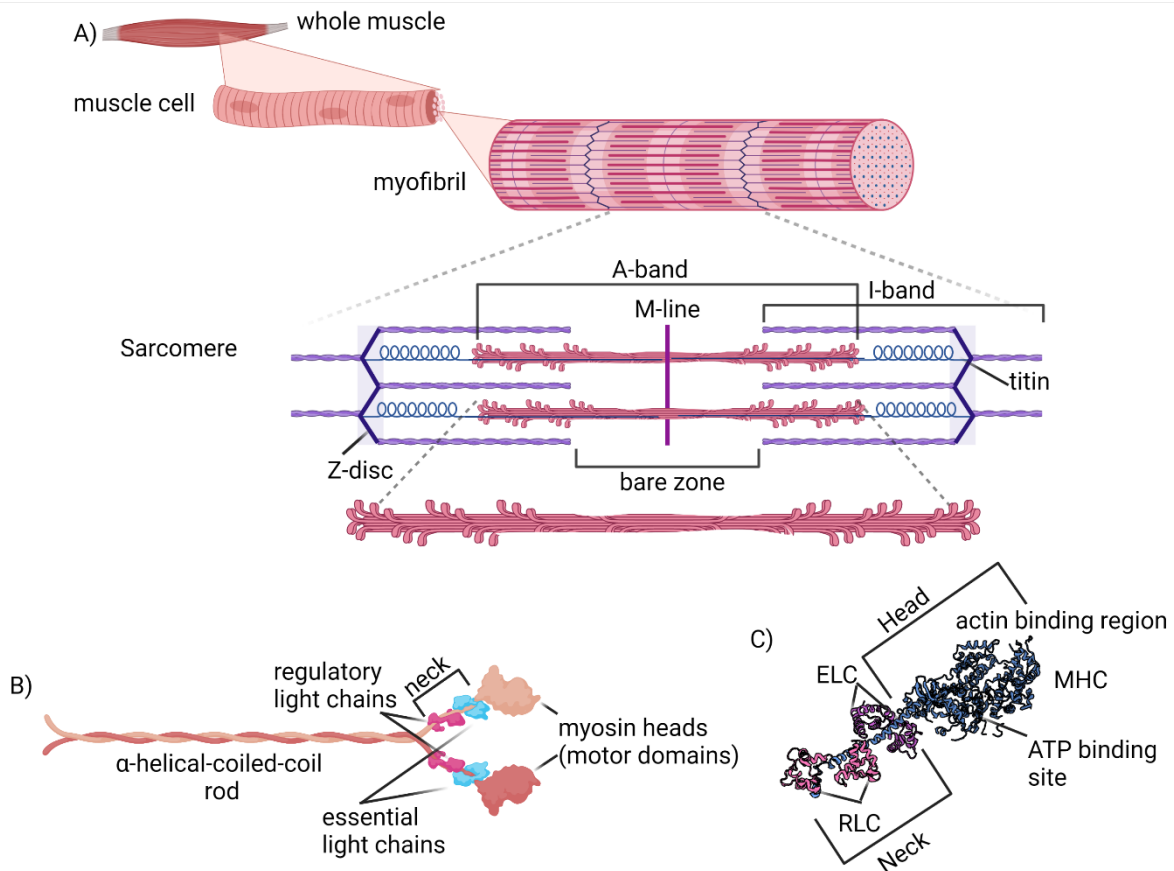


**Figure 1.1 Muscle anatomy.** A) Depiction of the different layers of muscle, including the whole muscle, a muscle cell or fiber, a myofibril, a sarcomere, and finally a thick filament. B) Depiction of one myosin hexamer, consisting of two myosin heavy chains, and two copies each of regulatory and essential light chains. C) Depiction of the myosin head structure solved by X-Ray diffraction from Scallop, *Argopecten irradians*, myosin in the near rigor conformation PDB 1KK7(137). Created with Biorender.com

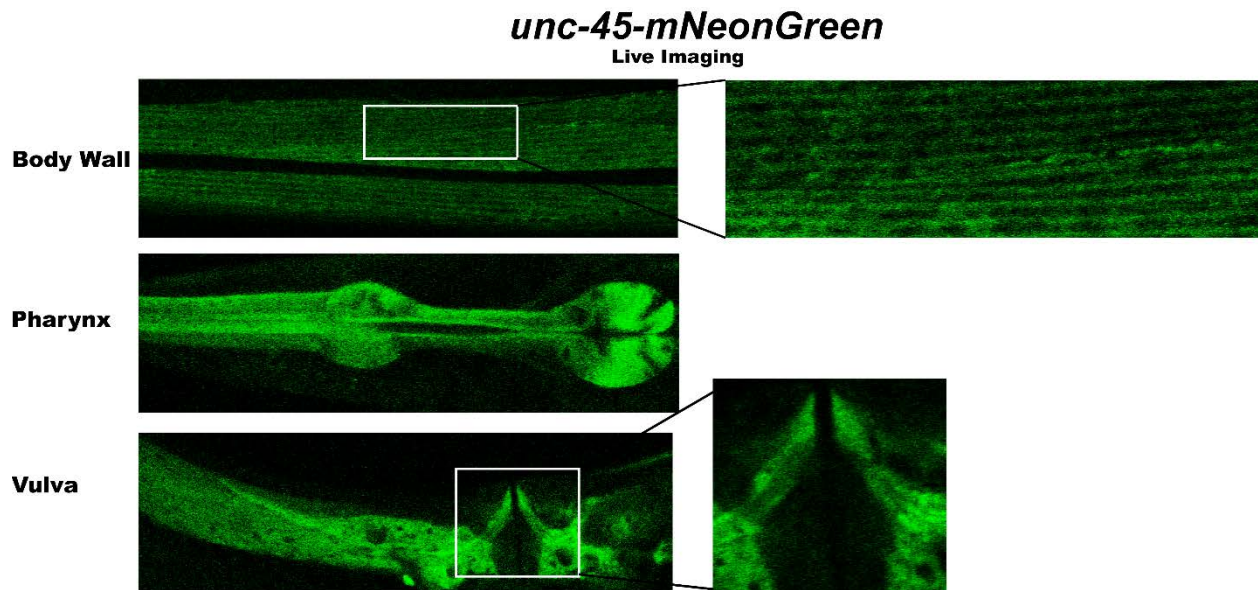


**Figure 1.2 Live imaging of *unc-45:mNeonGreen* animals.** Images of immobilized animals expressing mNeonGreen tagged UNC-45. Localization is shown in the muscle cells of the body wall, pharynx, and vulva. The zoomed-in view shown on top right indicates that UNC-45-mNeonGreen properly localizes in the sarcomere since the same pattern is seen with anti-UNC-45 antibody staining.

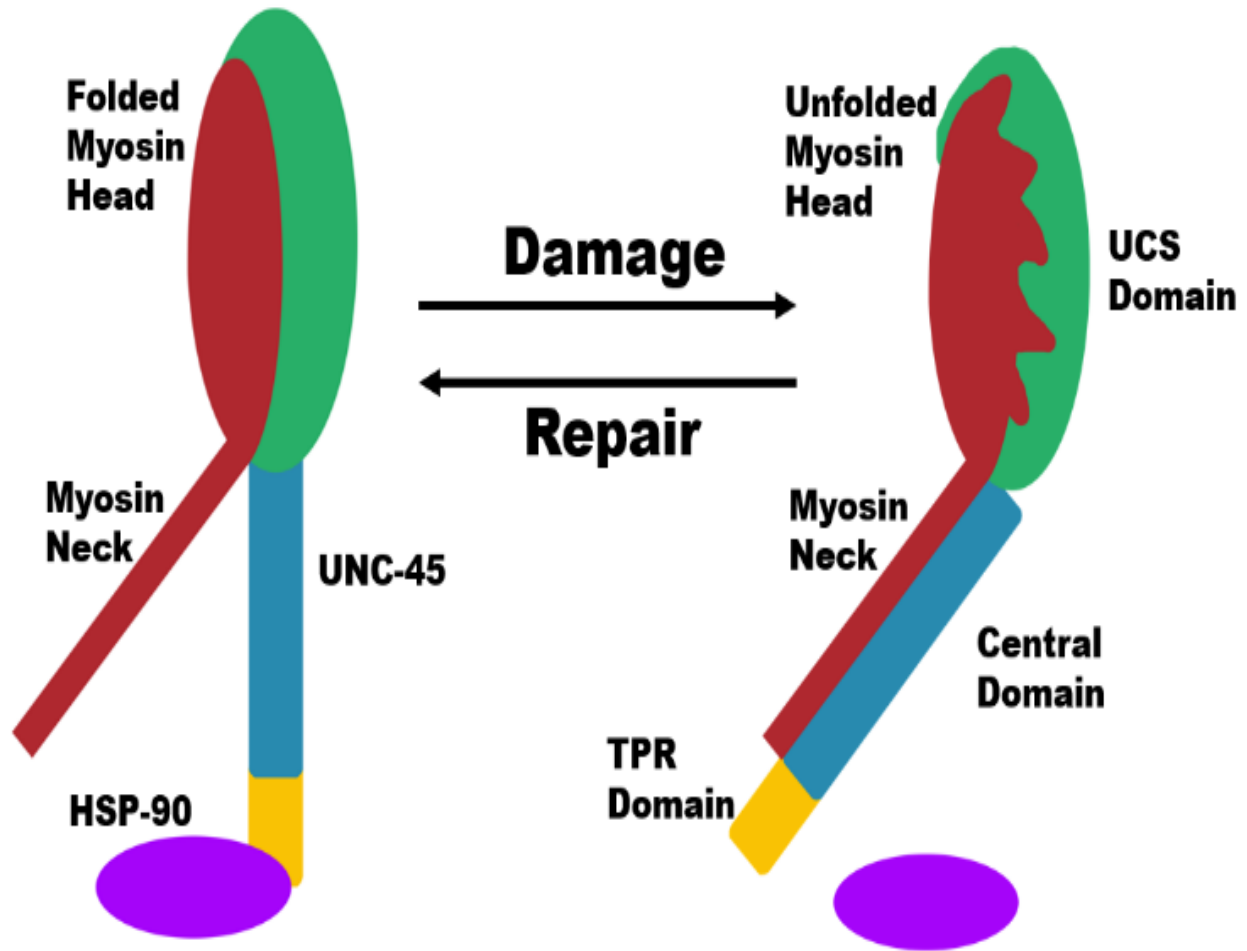


**Figure 1.3 Proposed Model for UNC-45 Function.** Under normal conditions the UCS domain of UNC-45 (shown in green) is bound to the myosin head (in red) and the TPR domain (in yellow) is bound to HSP-90 (in purple). Under stress conditions, HSP-90 detaches from the TPR domain, causing a conformational change in UNC-45 that allows the Central domain (in blue) to bind to the myosin neck (in red) resulting in inhibition of the myosin power stroke while the UCS domain protects/re-folds the myosin head. After refolding of the myosin head is completed, by some unknown mechanism, HSP-90 then rebinds the TPR domain, causing the Central domain to release the myosin neck, allowing resumption of the power stroke. Note that only the myosin head and neck are shown for simplicity of illustration. Figure modified from Bujalowski et al. (45).

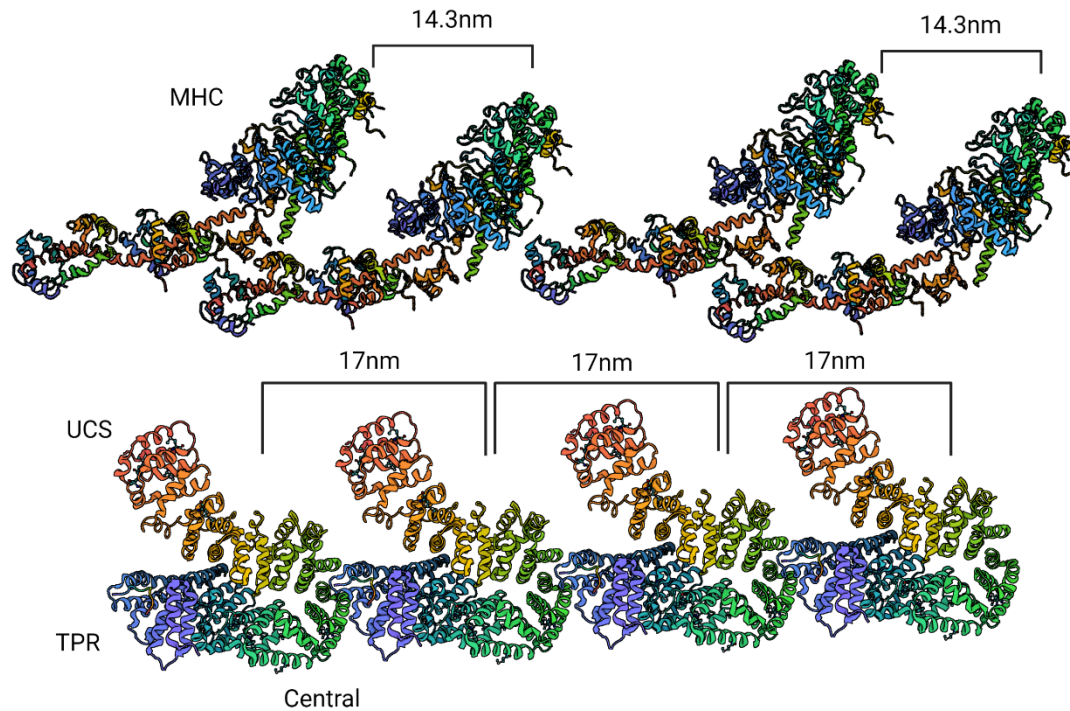


**Figure 1.4 Theoretical depiction of how UNC-45 oligomeric chains may associate with the thick filament.** The top of the figure shows two Myosin head dimers (heads and necks only for simplicity) with 14.3 nm between the adjacent myosin heads on the surface of a thick filament (PDB1KK7)(137). The bottom of the figure shows four UNC-45 molecules forming an oligomer with the oligomer interface at the TPR domain and the “neck” region above the Central domain and 17nm between each repeating unit (PDB4I2Z)(53).

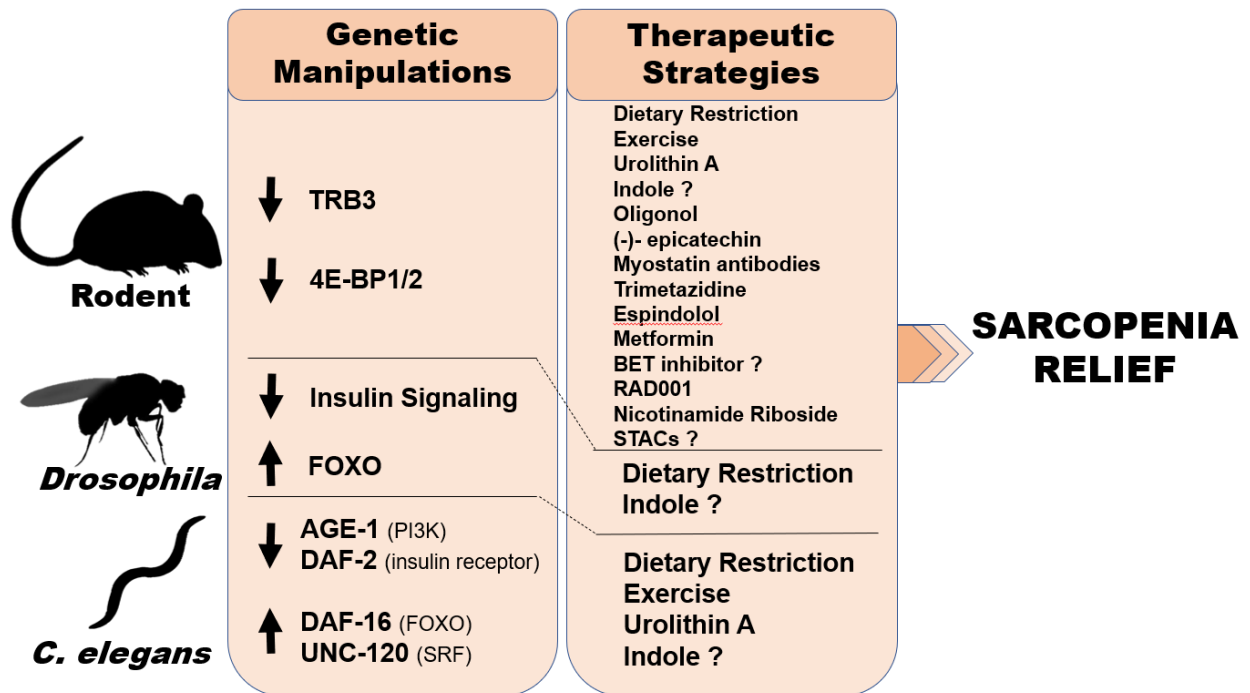


**Figure 1.5** Summary of genetic manipulations and therapeutic strategies that have been found to alleviate sarcopenia in rodents, *Drosophila*, and/or *C. elegans*(138).

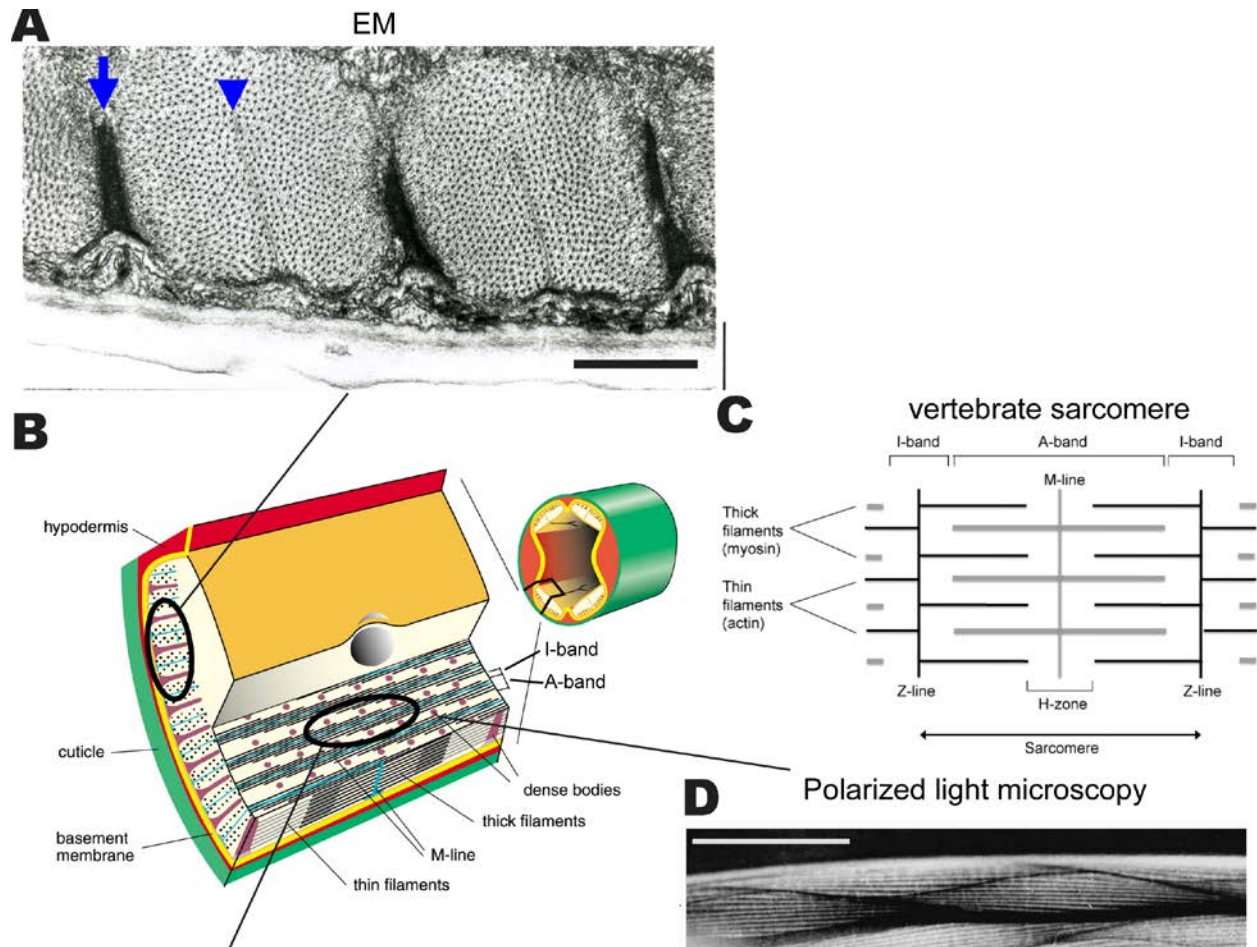


**Figure 1.6 The body wall muscle of *C. elegans*.** (A) Transmission electron microscopy (EM) of a cross-section of a body wall muscle cell showing two full sarcomeres. An arrow points to a dense body and arrowhead points to an M-line. The largest black dots are cross sections of thick filaments in the A-bands; the smallest dots are cross sections of thin filaments in the I-bands (surrounding the dense bodies). Note that all the dense bodies and the M-lines are anchored to the muscle cell membrane, which sits on top of a basement membrane, a thin hypodermis, and thick cuticle. Scale bar 1  $\mu\text{m}$ . (B) shows a cross-section through an adult worm emphasizing that the body wall muscle consists of four quadrants. Each quadrant consists of interlocking pairs of mononuclear spindle-shaped cells (23 or 24 per quadrant). In the enlargement, note that the myofilament lattice is limited to one side of the cell rather than filling the entire cross-sectional area as in a vertebrate striated muscle cell. Several planes of section are depicted, one of which emphasizes the muscle's striated organization with typical A-bands containing thick filaments organized around M-lines, and overlapping thin filaments probably attached to Z-disk-like structures called dense bodies. The sarcomere, which is defined as the repeating distance from one dense body to the next dense body is approximately 12  $\mu\text{m}$  in adult muscle. Note that the plane of section parallel to the page is the plane viewed

when an animal crawls on agar or is placed on a slide and examined by light microscopy. (C) A drawing of a typical sarcomere in vertebrate striated muscle. The sarcomere, which is defined as the repeating distance from one Z-line to the next Z-line is typically 2.2-2.5  $\mu\text{m}$ . (D) Polarized light microscopy on a live nematode of portions of two muscle quadrants, each containing interlocking pairs of spindle shaped cells. The parallel white lines are A-bands, which alternate with parallel dark lines that are I-bands. Scale bar 10  $\mu\text{m}$ . (modified from Gieseler et al. (109))

## Literature Cited

1. Lindberg MR & Lamps LW (2018) Skeletal Muscle. *Diagnostic Pathology: Normal Histology (Second Edition)*, eds Lindberg MR & Lamps LW (Elsevier), pp 76-81.
2. Exeter D & Connell DA (2010) Skeletal muscle: functional anatomy and pathophysiology. *Seminars in musculoskeletal radiology* 14(2):97-105.
3. Engel A. G. F-AC (1994) *Myology* (McGraw-Hill, New York) 2nd Ed.
4. Mauro A (1961) Satellite cell of skeletal muscle fibers. *The Journal of biophysical and biochemical cytology* 9(2):493-495.
5. Blaveri K, *et al.* (1999) Patterns of repair of dystrophic mouse muscle: studies on isolated fibers. *Developmental dynamics : an official publication of the American Association of Anatomists* 216(3):244-256.
6. Zammit P & Beauchamp J (2001) The skeletal muscle satellite cell: stem cell or son of stem cell? *Differentiation; research in biological diversity* 68(4-5):193-204.
7. Jones DL & Rando TA (2011) Emerging models and paradigms for stem cell ageing. *Nature cell biology* 13(5):506-512.
8. Garcia-Prat L, Sousa-Victor P, & Munoz-Canoves P (2013) Functional dysregulation of stem cells during aging: a focus on skeletal muscle stem cells. *The FEBS journal* 280(17):4051-4062.
9. Kellermayer D, Smith JE, 3rd, & Granzier H (2019) Titin mutations and muscle disease. *Pflugers Archiv : European journal of physiology* 471(5):673-682.
10. Ottenheijm CA & Granzier H (2010) Role of titin in skeletal muscle function and disease. *Advances in experimental medicine and biology* 682:105-122.
11. Squire JM, Paul DM, & Morris EP (2017) Myosin and Actin Filaments in Muscle: Structures and Interactions. *Sub-cellular biochemistry* 82:319-371.
12. Weeds AG & Lowey S (1971) Substructure of the myosin molecule. II. The light chains of myosin. *Journal of molecular biology* 61(3):701-725.
13. Atkinson SJ & Stewart M (1991) Molecular basis of myosin assembly: coiled-coil interactions and the role of charge periodicities. *Journal of cell science. Supplement* 14:7-10.
14. Vikstrom KL, *et al.* (1997) The vertebrate myosin heavy chain: genetics and assembly properties. *Cell structure and function* 22(1):123-129.
15. Squire JM (2016) Muscle contraction: Sliding filament history, sarcomere dynamics and the two Huxleys. *Global cardiology science & practice* 2016(2):e201611.
16. Toyoshima YY, *et al.* (1987) Myosin subfragment-1 is sufficient to move actin filaments in vitro. *Nature* 328(6130):536-539.
17. Saraswat LD & Lowey S (1991) Engineered cysteine mutants of myosin light chain 2. Fluorescent analogues for structural studies. *The Journal of biological chemistry* 266(29):19777-19785.
18. Sohn RL, *et al.* (1997) A 29 residue region of the sarcomeric myosin rod is necessary for filament formation. *Journal of molecular biology* 266(2):317-330.
19. Mitchell EJ, Jakes R, & Kendrick-Jones J (1986) Localisation of light chain and actin binding sites on myosin. *European journal of biochemistry* 161(1):25-35.

20. McNally EM, Goodwin EB, Spudich JA, & Leinwand LA (1988) Coexpression and assembly of myosin heavy chain and myosin light chain in *Escherichia coli*. *Proceedings of the National Academy of Sciences of the United States of America* 85(19):7270-7273.
21. Srikakulam R & Winkelmann DA (1999) Myosin II folding is mediated by a molecular chaperonin. *The Journal of biological chemistry* 274(38):27265-27273.
22. Chow D, Srikakulam R, Chen Y, & Winkelmann DA (2002) Folding of the Striated Muscle Myosin Motor Domain\*. *Journal of Biological Chemistry* 277(39):36799-36807.
23. Epstein HF & Thomson JN (1974) Temperature-sensitive mutation affecting myofilament assembly in *Caenorhabditis elegans*. *Nature* 250(467):579-580.
24. Price MG, Landsverk ML, Barral JM, & Epstein HF (2002) Two mammalian UNC-45 isoforms are related to distinct cytoskeletal and muscle-specific functions. *Journal of cell science* 115(Pt 21):4013-4023.
25. Bernick EP, Zhang PJ, & Du S (2010) Knockdown and overexpression of Unc-45b result in defective myofibril organization in skeletal muscles of zebrafish embryos. *BMC cell biology* 11:70.
26. Janiesch PC, *et al.* (2007) The ubiquitin-selective chaperone CDC-48/p97 links myosin assembly to human myopathy. *Nature cell biology* 9(4):379-390.
27. Wohlgemuth SL, Crawford BD, & Pilgrim DB (2007) The myosin co-chaperone UNC-45 is required for skeletal and cardiac muscle function in zebrafish. *Developmental biology* 303(2):483-492.
28. Melkani GC, Bodmer R, Ocorr K, & Bernstein SI (2011) The UNC-45 chaperone is critical for establishing myosin-based myofibrillar organization and cardiac contractility in the *Drosophila* heart model. *PloS one* 6(7):e22579.
29. Hansen L, *et al.* (2014) The myosin chaperone UNC45B is involved in lens development and autosomal dominant juvenile cataract. *European journal of human genetics : EJHG* 22(11):1290-1297.
30. Bazzaro M, *et al.* (2007) Myosin II co-chaperone general cell UNC-45 overexpression is associated with ovarian cancer, rapid proliferation, and motility. *The American journal of pathology* 171(5):1640-1649.
31. Esteve C, *et al.* (2018) Loss-of-Function Mutations in UNC45A Cause a Syndrome Associating Cholestasis, Diarrhea, Impaired Hearing, and Bone Fragility. *American journal of human genetics* 102(3):364-374.
32. Venolia L & Waterston RH (1990) The unc-45 gene of *Caenorhabditis elegans* is an essential muscle-affecting gene with maternal expression. *Genetics* 126(2):345-353.
33. Barral JM, Bauer CC, Ortiz I, & Epstein HF (1998) Unc-45 mutations in *Caenorhabditis elegans* implicate a CRO1/She4p-like domain in myosin assembly. *The Journal of cell biology* 143(5):1215-1225.
34. Lee CF, *et al.* (2011) *Drosophila* UNC-45 accumulates in embryonic blastoderm and in muscles, and is essential for muscle myosin stability. *Journal of cell science* 124(Pt 5):699-705.
35. Estrada B, *et al.* (2006) An integrated strategy for analyzing the unique developmental programs of different myoblast subtypes. *PLoS genetics* 2(2):e16.
36. Geach TJ & Zimmerman LB (2010) Paralysis and delayed Z-disc formation in the *Xenopus tropicalis* unc45b mutant dicky ticker. *BMC developmental biology* 10:75.

37. Chen D, *et al.* (2012) Dual function of the UNC-45b chaperone with myosin and GATA4 in cardiac development. *Journal of cell science* 125(Pt 16):3893-3903.
38. Landsverk ML, *et al.* (2007) The UNC-45 chaperone mediates sarcomere assembly through myosin degradation in *Caenorhabditis elegans*. *The Journal of cell biology* 177(2):205-210.
39. Barral JM, Hutagalung AH, Brinker A, Hartl FU, & Epstein HF (2002) Role of the myosin assembly protein UNC-45 as a molecular chaperone for myosin. *Science (New York, N.Y.)* 295(5555):669-671.
40. Etard C, Roostalu U, & Strahle U (2008) Shuttling of the chaperones Unc45b and Hsp90a between the A band and the Z line of the myofibril. *The Journal of cell biology* 180(6):1163-1175.
41. Kachur TM & Pilgrim DB (2008) Myosin assembly, maintenance and degradation in muscle: Role of the chaperone UNC-45 in myosin thick filament dynamics. *International journal of molecular sciences* 9(9):1863-1875.
42. Solomon V & Goldberg AL (1996) Importance of the ATP-ubiquitin-proteasome pathway in the degradation of soluble and myofibrillar proteins in rabbit muscle extracts. *The Journal of biological chemistry* 271(43):26690-26697.
43. Ao W & Pilgrim D (2000) *Caenorhabditis elegans* UNC-45 is a component of muscle thick filaments and colocalizes with myosin heavy chain B, but not myosin heavy chain A. *The Journal of cell biology* 148(2):375-384.
44. Gaiser AM, Kaiser CJ, Haslbeck V, & Richter K (2011) Downregulation of the Hsp90 system causes defects in muscle cells of *Caenorhabditis elegans*. *PloS one* 6(9):e25485.
45. Jansen RP, Dowzer C, Michaelis C, Galova M, & Nasmyth K (1996) Mother cell-specific HO expression in budding yeast depends on the unconventional myosin myo4p and other cytoplasmic proteins. *Cell* 84(5):687-697.
46. Wendland B, McCaffery JM, Xiao Q, & Emr SD (1996) A novel fluorescence-activated cell sorter-based screen for yeast endocytosis mutants identifies a yeast homologue of mammalian eps15. *The Journal of cell biology* 135(6 Pt 1):1485-1500.
47. Berteaux-Lecellier V, *et al.* (1998) A homologue of the yeast SHE4 gene is essential for the transition between the syncytial and cellular stages during sexual reproduction of the fungus *Podospora anserina*. *The EMBO journal* 17(5):1248-1258.
48. Balasubramanian MK, *et al.* (1998) Isolation and characterization of new fission yeast cytokinesis mutants. *Genetics* 149(3):1265-1275.
49. Wong KC, Naqvi NI, Iino Y, Yamamoto M, & Balasubramanian MK (2000) Fission yeast Rng3p: an UCS-domain protein that mediates myosin II assembly during cytokinesis. *Journal of cell science* 113 ( Pt 13):2421-2432.
50. Ni W, Hutagalung AH, Li S, & Epstein HF (2011) The myosin-binding UCS domain but not the Hsp90-binding TPR domain of the UNC-45 chaperone is essential for function in *Caenorhabditis elegans*. *Journal of cell science* 124(Pt 18):3164-3173.
51. Bujalowski PJ, Nicholls P, Garza E, & Oberhauser AF (2018) The central domain of UNC-45 chaperone inhibits the myosin power stroke. *FEBS open bio* 8(1):41-48.
52. Nicholls P, *et al.* (2014) Chaperone-mediated reversible inhibition of the sarcomeric myosin power stroke. *FEBS letters* 588(21):3977-3981.

53. Gazda L, *et al.* (2013) The myosin chaperone UNC-45 is organized in tandem modules to support myofilament formation in *C. elegans*. *Cell* 152(1-2):183-195.
54. Moncrief T, *et al.* (2021) Mutations in conserved residues of the myosin chaperone UNC-45 result in both reduced stability and chaperoning activity. *Protein science : a publication of the Protein Society* 30(11):2221-2232.
55. Kachur T, Ao W, Berger J, & Pilgrim D (2004) Maternal UNC-45 is involved in cytokinesis and colocalizes with non-muscle myosin in the early *Caenorhabditis elegans* embryo. *Journal of cell science* 117(Pt 22):5313-5321.
56. Kachur TM, Audhya A, & Pilgrim DB (2008) UNC-45 is required for NMY-2 contractile function in early embryonic polarity establishment and germline cellularization in *C. elegans*. *Developmental biology* 314(2):287-299.
57. Schopf FH, Biebl MM, & Buchner J (2017) The HSP90 chaperone machinery. *Nature reviews. Molecular cell biology* 18(6):345-360.
58. Srikakulam R & Winkelmann DA (2004) Chaperone-mediated folding and assembly of myosin in striated muscle. *Journal of cell science* 117(Pt 4):641-652.
59. Liu L, Srikakulam R, & Winkelmann DA (2008) Unc45 activates Hsp90-dependent folding of the myosin motor domain. *The Journal of biological chemistry* 283(19):13185-13193.
60. Etard C, Roostalu U, & Strähle U (2010) Lack of Apobec2-related proteins causes a dystrophic muscle phenotype in zebrafish embryos. *The Journal of cell biology* 189(3):527-539.
61. Chadli A, *et al.* (2006) GCUNC-45 is a novel regulator for the progesterone receptor/hsp90 chaperoning pathway. *Molecular and cellular biology* 26(5):1722-1730.
62. Hoppe T, *et al.* (2004) Regulation of the myosin-directed chaperone UNC-45 by a novel E3/E4-multiubiquitylation complex in *C. elegans*. *Cell* 118(3):337-349.
63. Cruz-Jentoft AJ, *et al.* (2014) Prevalence of and interventions for sarcopenia in ageing adults: a systematic review. Report of the International Sarcopenia Initiative (EWGSOP and IWGS). *Age and ageing* 43(6):748-759.
64. Iannuzzi-Sucich M, Prestwood KM, & Kenny AM (2002) Prevalence of sarcopenia and predictors of skeletal muscle mass in healthy, older men and women. *The journals of gerontology. Series A, Biological sciences and medical sciences* 57(12):M772-777.
65. Barbosa-Silva TG, Bielemann RM, Gonzalez MC, & Menezes AM (2016) Prevalence of sarcopenia among community-dwelling elderly of a medium-sized South American city: results of the COMO VAI? study. *Journal of cachexia, sarcopenia and muscle* 7(2):136-143.
66. Zembron-Lacny A, Dziubek W, Rogowski L, Skorupka E, & Dabrowska G (2014) Sarcopenia: monitoring, molecular mechanisms, and physical intervention. *Physiological research* 63(6):683-691.
67. Candow DG (2011) Sarcopenia: current theories and the potential beneficial effect of creatine application strategies. *Biogerontology* 12(4):273-281.
68. Forbes SC, Little JP, & Candow DG (2012) Exercise and nutritional interventions for improving aging muscle health. *Endocrine* 42(1):29-38.
69. Candow DG, *et al.* (2012) Effect of nutritional interventions and resistance exercise on aging muscle mass and strength. *Biogerontology* 13(4):345-358.

70. Szulc P, Feyt C, & Chapurlat R (2016) High risk of fall, poor physical function, and low grip strength in men with fracture-the STRAMBO study. *Journal of cachexia, sarcopenia and muscle* 7(3):299-311.
71. Celis-Morales CA, et al. (2018) Associations of grip strength with cardiovascular, respiratory, and cancer outcomes and all cause mortality: prospective cohort study of half a million UK Biobank participants. *BMJ (Clinical research ed.)* 361:k1651.
72. Tikkanen E, Gustafsson S, & Ingelsson E (2018) Associations of Fitness, Physical Activity, Strength, and Genetic Risk With Cardiovascular Disease: Longitudinal Analyses in the UK Biobank Study. *Circulation* 137(24):2583-2591.
73. Kwan P (2013) Sarcopenia, a neurogenic syndrome? *Journal of aging research* 2013:791679.
74. Gosselin LE, Johnson BD, & Sieck GC (1994) Age-related changes in diaphragm muscle contractile properties and myosin heavy chain isoforms. *American journal of respiratory and critical care medicine* 150(1):174-178.
75. Statistics FIFoA-R (2012) Older Americans 2012: Key Indicators of Well-Being. U.S. Government Printing Office; Washington, DC.
76. Kahn JH, Magauran BG, Jr., Olshaker JS, & Shankar KN (2016) Current Trends in Geriatric Emergency Medicine. *Emergency medicine clinics of North America* 34(3):435-452.
77. Meara E, White C, & Cutler DM (2004) Trends in medical spending by age, 1963-2000. *Health affairs (Project Hope)* 23(4):176-183.
78. Altun M, et al. (2010) Muscle wasting in aged, sarcopenic rats is associated with enhanced activity of the ubiquitin proteasome pathway. *The Journal of biological chemistry* 285(51):39597-39608.
79. Evers PA, Keeshan K, & Kannan N (2017) Tribbles in the 21st Century: The Evolving Roles of Tribbles Pseudokinases in Biology and Disease. *Trends in cell biology* 27(4):284-298.
80. Meyer GA, Schenk S, & Lieber RL (2013) Role of the cytoskeleton in muscle transcriptional responses to altered use. *Physiological genomics* 45(8):321-331.
81. Choi RH, et al. (2017) Tribbles 3 regulates protein turnover in mouse skeletal muscle. *Biochemical and biophysical research communications* 493(3):1236-1242.
82. Choi RH, et al. (2019) TRB3 regulates skeletal muscle mass in food deprivation-induced atrophy. *FASEB journal : official publication of the Federation of American Societies for Experimental Biology* 33(4):5654-5666.
83. Kato S & Du K (2007) TRB3 modulates C2C12 differentiation by interfering with Akt activation. *Biochemical and biophysical research communications* 353(4):933-938.
84. Shang GK, et al. (2020) Sarcopenia is attenuated by TRB3 knockout in aging mice via the alleviation of atrophy and fibrosis of skeletal muscles. *Journal of cachexia, sarcopenia and muscle*.
85. Wheeler JC, Bieschke ET, & Tower J (1995) Muscle-specific expression of Drosophila hsp70 in response to aging and oxidative stress. *Proceedings of the National Academy of Sciences of the United States of America* 92(22):10408-10412.
86. Murtaza G, et al. (2017) FOXO Transcriptional Factors and Long-Term Living. *Oxidative medicine and cellular longevity* 2017:3494289.
87. Demontis F & Perrimon N (2010) FOXO/4E-BP signaling in Drosophila muscles regulates organism-wide proteostasis during aging. *Cell* 143(5):813-825.

88. Liu WJ, *et al.* (2016) p62 links the autophagy pathway and the ubiquitin-proteasome system upon ubiquitinated protein degradation. *Cellular & molecular biology letters* 21:29.
89. Sasako T & Ueki K (2016) [Insulin/IGF-1 signaling and aging]. *Nihon rinsho. Japanese journal of clinical medicine* 74(9):1435-1440.
90. Owusu-Ansah E, Song W, & Perrimon N (2013) Muscle mitohormesis promotes longevity via systemic repression of insulin signaling. *Cell* 155(3):699-712.
91. Delrio-Lorenzo A, Rojo-Ruiz J, Alonso MT, & Garcia-Sancho J (2020) Sarcoplasmic reticulum Ca(2+) decreases with age and correlates with the decline in muscle function in *Drosophila*. *Journal of cell science* 133(6).
92. Ryu D, *et al.* (2016) Urolithin A induces mitophagy and prolongs lifespan in *C. elegans* and increases muscle function in rodents. *Nature medicine* 22(8):879-888.
93. Sonowal R, *et al.* (2017) Indoles from commensal bacteria extend healthspan. *Proceedings of the National Academy of Sciences of the United States of America* 114(36):E7506-e7515.
94. Lee SJ (2004) Regulation of muscle mass by myostatin. *Annual review of cell and developmental biology* 20:61-86.
95. Camporez JP, *et al.* (2016) Anti-myostatin antibody increases muscle mass and strength and improves insulin sensitivity in old mice. *Proceedings of the National Academy of Sciences of the United States of America* 113(8):2212-2217.
96. LeBrasseur NK, *et al.* (2009) Myostatin inhibition enhances the effects of exercise on performance and metabolic outcomes in aged mice. *The journals of gerontology. Series A, Biological sciences and medical sciences* 64(9):940-948.
97. Murphy KT, *et al.* (2011) Antibody-directed myostatin inhibition enhances muscle mass and function in tumor-bearing mice. *American journal of physiology. Regulatory, integrative and comparative physiology* 301(3):R716-726.
98. Ferraro E, *et al.* (2016) Improvement of skeletal muscle performance in ageing by the metabolic modulator Trimetazidine. *Journal of cachexia, sarcopenia and muscle* 7(4):449-457.
99. Potsch MS, *et al.* (2014) The anabolic catabolic transforming agent (ACTA) espidolol increases muscle mass and decreases fat mass in old rats. *Journal of cachexia, sarcopenia and muscle* 5(2):149-158.
100. Hernandez-Alvarez D, *et al.* (2019) Long-Term Moderate Exercise Combined with Metformin Treatment Induces an Hormetic Response That Prevents Strength and Muscle Mass Loss in Old Female Wistar Rats. *Oxidative medicine and cellular longevity* 2019:3428543.
101. Wessels B, Ciapaite J, van den Broek NM, Nicolay K, & Prompers JJ (2014) Metformin impairs mitochondrial function in skeletal muscle of both lean and diabetic rats in a dose-dependent manner. *PloS one* 9(6):e100525.
102. Hundal RS, *et al.* (2000) Mechanism by which metformin reduces glucose production in type 2 diabetes. *Diabetes* 49(12):2063-2069.
103. Katewa SD, *et al.* (2012) Intramyocellular fatty-acid metabolism plays a critical role in mediating responses to dietary restriction in *Drosophila melanogaster*. *Cell metabolism* 16(1):97-103.

104. Bhandari P, Jones MA, Martin I, & Grotewiel MS (2007) Dietary restriction alters demographic but not behavioral aging in *Drosophila*. *Aging cell* 6(5):631-637.
105. Brenner S (1974) The genetics of *Caenorhabditis elegans*. *Genetics* 77(1):71-94.
106. Benian GM & Epstein HF (2011) *Caenorhabditis elegans* muscle: a genetic and molecular model for protein interactions in the heart. *Circulation research* 109(9):1082-1095.
107. Mackenzie JM, Jr. & Epstein HF (1980) Paramyosin is necessary for determination of nematode thick filament length in vivo. *Cell* 22(3):747-755.
108. Miller DM, 3rd, Ortiz I, Berliner GC, & Epstein HF (1983) Differential localization of two myosins within nematode thick filaments. *Cell* 34(2):477-490.
109. Gieseler K, Qadota H, & Benian GM (2017) Development, structure, and maintenance of *C. elegans* body wall muscle. *WormBook : the online review of C. elegans biology 2017*:1-59.
110. Thompson O, *et al.* (2013) The million mutation project: a new approach to genetics in *Caenorhabditis elegans*. *Genome research* 23(10):1749-1762.
111. McLachlan AD & Karn J (1982) Periodic charge distributions in the myosin rod amino acid sequence match cross-bridge spacings in muscle. *Nature* 299(5880):226-231.
112. Barstead RJ & Waterston RH (1991) Vinculin is essential for muscle function in the nematode. *The Journal of cell biology* 114(4):715-724.
113. Rogalski TM, Williams BD, Mullen GP, & Moerman DG (1993) Products of the *unc-52* gene in *Caenorhabditis elegans* are homologous to the core protein of the mammalian basement membrane heparan sulfate proteoglycan. *Genes & development* 7(8):1471-1484.
114. Williams BD & Waterston RH (1994) Genes critical for muscle development and function in *Caenorhabditis elegans* identified through lethal mutations. *The Journal of cell biology* 124(4):475-490.
115. Rogalski TM, Mullen GP, Gilbert MM, Williams BD, & Moerman DG (2000) The *UNC-112* gene in *Caenorhabditis elegans* encodes a novel component of cell-matrix adhesion structures required for integrin localization in the muscle cell membrane. *The Journal of cell biology* 150(1):253-264.
116. Benian GM, Kiff JE, Neckelmann N, Moerman DG, & Waterston RH (1989) Sequence of an unusually large protein implicated in regulation of myosin activity in *C. elegans*. *Nature* 342(6245):45-50.
117. Benian GM, L'Hernault SW, & Morris ME (1993) Additional sequence complexity in the muscle gene, *unc-22*, and its encoded protein, twitchin, of *Caenorhabditis elegans*. *Genetics* 134(4):1097-1104.
118. McKim KS, Matheson C, Marra MA, Wakarchuk MF, & Baillie DL (1994) The *Caenorhabditis elegans unc-60* gene encodes proteins homologous to a family of actin-binding proteins. *Molecular & general genetics : MGG* 242(3):346-357.
119. Ono S, Baillie DL, & Benian GM (1999) *UNC-60B*, an ADF/cofilin family protein, is required for proper assembly of actin into myofibrils in *Caenorhabditis elegans* body wall muscle. *The Journal of cell biology* 145(3):491-502.
120. Ono S (2014) Regulation of structure and function of sarcomeric actin filaments in striated muscle of the nematode *Caenorhabditis elegans*. *Anatomical record (Hoboken, N.J. : 2007)* 297(9):1548-1559.

121. Herndon LA, *et al.* (2002) Stochastic and genetic factors influence tissue-specific decline in ageing *C. elegans*. *Nature* 419(6909):808-814.
122. Kenyon C, Chang J, Gensch E, Rudner A, & Tabtiang R (1993) A *C. elegans* mutant that lives twice as long as wild type. *Nature* 366(6454):461-464.
123. Kenyon CJ (2010) The genetics of ageing. *Nature* 464(7288):504-512.
124. Duhon SA & Johnson TE (1995) Movement as an index of vitality: comparing wild type and the age-1 mutant of *Caenorhabditis elegans*. *The journals of gerontology. Series A, Biological sciences and medical sciences* 50(5):B254-261.
125. Depuydt G, *et al.* (2013) Reduced insulin/insulin-like growth factor-1 signaling and dietary restriction inhibit translation but preserve muscle mass in *Caenorhabditis elegans*. *Molecular & cellular proteomics : MCP* 12(12):3624-3639.
126. Palikaras K, Lionaki E, & Tavernarakis N (2015) Coupling mitogenesis and mitophagy for longevity. *Autophagy* 11(8):1428-1430.
127. Mergoud Dit Lamarche A, *et al.* (2018) UNC-120/SRF independently controls muscle aging and lifespan in *Caenorhabditis elegans*. *Aging cell* 17(2).
128. Yasuda K, *et al.* (2006) Age-related changes of mitochondrial structure and function in *Caenorhabditis elegans*. *Mechanisms of ageing and development* 127(10):763-770.
129. Leduc-Gaudet JP, *et al.* (2015) Mitochondrial morphology is altered in atrophied skeletal muscle of aged mice. *Oncotarget* 6(20):17923-17937.
130. Gaffney CJ, *et al.* (2018) Greater loss of mitochondrial function with ageing is associated with earlier onset of sarcopenia in *C. elegans*. *Aging* 10(11):3382-3396.
131. Ahier A, *et al.* (2018) Affinity purification of cell-specific mitochondria from whole animals resolves patterns of genetic mosaicism. *Nature cell biology* 20(3):352-360.
132. Masoro EJ (2005) Overview of caloric restriction and ageing. *Mechanisms of ageing and development* 126(9):913-922.
133. Greer EL & Brunet A (2009) Different dietary restriction regimens extend lifespan by both independent and overlapping genetic pathways in *C. elegans*. *Aging cell* 8(2):113-127.
134. Chuang HS, Kuo WJ, Lee CL, Chu IH, & Chen CS (2016) Exercise in an electrotactic flow chamber ameliorates age-related degeneration in *Caenorhabditis elegans*. *Scientific reports* 6:28064.
135. Hartman JH, *et al.* (2018) Swimming Exercise and Transient Food Deprivation in *Caenorhabditis elegans* Promote Mitochondrial Maintenance and Protect Against Chemical-Induced Mitotoxicity. *Scientific reports* 8(1):8359.
136. Gaziova I, *et al.* (2020) Mutational Analysis of the Structure and Function of the Chaperoning Domain of UNC-45B. *Biophysical journal* 119(4):780-791.
137. Himmel DM, *et al.* (2002) Crystallographic findings on the internally uncoupled and near-rigor states of myosin: further insights into the mechanics of the motor. *Proceedings of the National Academy of Sciences of the United States of America* 99(20):12645-12650.
138. Christian CJ & Benian GM (2020) Animal models of sarcopenia. *Aging cell* 19(10):e13223.

## **Chapter 2: In vivo mutational analysis of conserved residues of UNC-45 using *C. elegans***

These data were included in the following publications:

Gaziova I, Moncrief T, Christian CJ, Villarreal M, Powell S, Lee H, Qadota H, White MA, Benian GM, Oberhauser AF. Mutational Analysis of the Structure and Function of the Chaperoning Domain of UNC-45B. *Biophys J*. 2020 Aug 18;119(4):780-791. doi: 10.1016/j.bpj.2020.07.012. Epub 2020 Jul 22. PMID: 32755562; PMCID: PMC7451893.

Moncrief T, Matheny CJ, Gaziova I, Miller JM, Qadota H, Benian GM, Oberhauser AF. Mutations in conserved residues of the myosin chaperone UNC-45 result in both reduced stability and chaperoning activity. *Protein Sci*. 2021 Nov;30(11):2221-2232. doi: 10.1002/pro.4180. Epub 2021 Sep 28. PMID: 34515376.

## 2.1 - Introduction:

The arrangement of not just the thick and thin filaments but also numerous other proteins into the exact structure of the semicrystalline lattice making up the sarcomere is essential for muscle contractile function. This process is partially autonomous, an intrinsic property of its component proteins. However, the assembly of a functional sarcomere requires molecular chaperones(1). The molecular mechanism(s) for the roles of chaperones in the assembly process or prevention of stress-induced aggregation states are presently unknown. Answering this question is a problem at the core of muscle development and function(2, 3). Unraveling these mechanisms may provide critical insights into the molecular nature of the pathogenesis of many muscle disorders such as skeletal myopathies, cardiomyopathies, and sarcopenia. Among the sarcomeric chaperone proteins known to be involved in the folding of the myosin head is UNC-45, which is required for the assembly of myosin into the thick filament(4-9). UNC-45 homologs are found in all metazoans (4). *Drosophila* and *C. elegans* have one UNC-45 gene expressed in all cells, whereas vertebrates have two UNC-45 genes, one expressed in striated muscle (UNC-45B), and one expressed in all cells (UNC-45A). The first clue to the existence of UNC-45 came from classical genetics experiments in *C. elegans*. The gene was identified by a temperature sensitive mutant, *unc-45(e286)*, that when grown at the restrictive temperature of 25°C shows striated muscle with disorganized sarcomeres and reduced numbers of thick filaments(10, 11). Identification of the gene at the molecular level showed that it encodes a protein of 961 amino acids and comprised of three regions: a 100 residue long TPR (tetratricopeptide repeat) region, a 400 residue central region, and a 430 residue UCS (UNC-45, CRO1, She4p) domain(11, 12). The UCS domain was defined by sequence similarity to two fungal proteins, CRO1 and

She4p, that also functionally interact with myosin. When grown at the restrictive temperature, *unc-45(e286)* animals show decreased accumulation of MHC B (myosin heavy chain B), the major myosin heavy chain of thick filaments in the body wall muscle of *C. elegans*(11). These thick filaments consist of MHC A in a small middle portion, and MHC B in the major outer portions(13). Interestingly, antibodies to UNC-45 co-localize with MHC B but not with MHC A in sarcomeric A-bands in already assembled sarcomeres of adult muscle(14, 15).

The regions or domains of UNC-45 are functionally distinct. The TPR region binds to heat shock protein 90 (Hsp90), the central region may bind to myosin to inhibit the power stroke, and the UCS domain binds to, and chaperones myosin heads(16). UNC-45 can inhibit the thermal aggregation of myosin heads in vitro, suggesting that indeed UNC-45 chaperones the myosin head(16). *unc-45* mutants can be rescued by full length UNC-45, UNC-45 in which the TPR has been deleted, and even the UCS domain itself(17). The crystal structure of *C. elegans* UNC-45 shows that the overall shape is of an “L” with the UCS domain forming one leg, and the central and TPR forming the other leg. In addition, all of the central region and UCS domain consists of 17 armadillo (ARM) repeats, each consisting of 2–3  $\alpha$ -helices. Most significantly, UNC-45 forms linear multimers in which the length of the repeating unit (17 nm) is similar to the repeating unit in the staggered display of pairs of myosin heads along the surface of thick filaments (closest distance between adjacent double heads is 14.3 nm)(15). Thus, these UNC-45 multimers may help stabilize this arrangement during thick filament and sarcomere assembly. Also, this architecture suggests the possibility that in the assembled thick filament in which UNC-45 seems to be associated, myosin heads that are damaged by

heat or oxidation as the muscle is used may be easily refolded. Based upon actin filament gliding assays of myosin heads with and without the presence of UNC-45 and/or HSP-90, the following model has been proposed: Under normal conditions the UCS domain of UNC 45 is bound to the myosin head and the TPR domain is bound to HSP 90, and yet the myosin head is active in pulling actin thin filaments. However, under stress conditions, HSP 90 detaches from the TPR domain, causing a conformational change in UNC-45 that allows the central domain to bind to the myosin neck resulting in inhibition of the myosin power stroke while the UCS domain refolds the myosin head. Then, when the refolding is complete, some sort of signal is received for HSP-90 to re-bind the TPR domain of UNC-45, causing the central domain to release the myosin neck, thus allowing the myosin power stroke to resume(18, 19).

Although no human UNC-45 structure is available, homology models have been created via in silico molecular modeling and simulations(20). Figure 2.1 A shows a homology model of the UCS domain of human UNC-45B depicting armadillo repeats 9–17 (armadillo repeats 1–8 reside in the central domain). These armadillo repeats consist of three  $\alpha$ -helices (a short H1 of roughly two helical turns followed by two longer H2 and H3 helices) with an average of 42 residues from diverse sequences but highly conserved structures (Fig. 1 B). These helices arrange in a superhelical structure defining a protein-binding groove that is conserved in many armadillo-repeat-containing proteins(15, 21-23). In the human homology model for UNC45B, this groove is comprised of highly conserved residues in the UCS domain, such as the NYE.LTNL and DRLK sequences in repeats 13 and 15, respectively (highlighted in green in Figure 2.1 B). When mapped onto the human model, these highly conserved amino acid residues in helix 13H3 form a large

surface patch in the groove (highlighted in red in Figure 2.2 A). Based on the marked similarity of the UCS domain to  $\beta$ -catenin, Gazda et al. predicted that this groove may serve as a myosin-binding surface and were able to identify key residues for myosin interaction(15). By mapping a  $\beta$ -catenin ligand onto the *C. elegans* UNC45 UCS domain, they predicted that N758 (N745 in human sequence) should be critical for tethering the main chain of the captured substrate, whereas the nearby Y750 (Y737 in human) should contribute to the hydrophobic character of the outer rim of the UCS groove (Figure 2.2). In vivo mutagenesis analysis revealed that in contrast to a Y750W mutant, which was still capable of restoring muscle function, an N758Y mutant failed to rescue a temperature-sensitive *unc-45* mutant (in worms carrying the ts allele *unc45(m94)*, mutation E781K) grown at the nonpermissive temperature (25°C causes UNC-45 to be nonfunctional). Further analysis of *C. elegans* mutations affecting the myosin binding groove by the same group confirmed that UNC-45 with the Y750W mutation was able to support production of soluble myosin motor domain when co-expressed in insect cells, even though to a lesser extent than wild-type (WT) UNC-45(24). N758Y unfortunately failed to express in insect cells efficiently, suggesting the structure-destabilizing nature of this mutation. Another potential myosin-interacting region of UCS proteins is a flexible loop with minimal electron density conserved in the UNC-45 structures of *C. elegans* and *Drosophila melanogaster* that has been shown to be susceptible to trypsin digestion in the *Drosophila* protein(24). This flexible loop is colored green in Figs. 1 B and 2 and, when deleted, should disrupt the substrate-binding cleft, and abrogate interaction with myosin. It was found that a D602–630 mutant (N584-D614 in human sequence) neither rescued the defect in sarcomere organization nor bound to myosin in immunoprecipitation

experiments(25). These data indicated that this loop was important for UNC-45 to interact with myosin in worms. Our collaborator, Dr. Andres Oberhauser (UTMB), used mutagenesis to test the following hypotheses: 1) that the putative “client-binding” groove in the UCS domain of human UNC-45B is functional, and 2) that the homology-modeled loop, N584-D614, in the UCS domain of human UNC-45B is essential for binding and holding myosin. Our collaborators used in vitro techniques (circular dichroism, small-angle x-ray scattering, and heat-inactivation protection assays) to test our hypotheses, while I used *C. elegans* to examine the in vivo importance of these UCS regions on sarcomere structure and organization. In vitro and in vivo effects are summarized in Table 2.1.

Two major phenotypic classes of mutants affect *C. elegans* sarcomere assembly and muscle activity: (1) A subclass of the “uncoordinated” (Unc) class which are viable adults that are either paralyzed or move more slowly or in a strange way compared with wild type; although most of the 129 Unc genes affect the nervous system, 40 are specific for muscle. (2) The “paralyzed arrested at two-fold” (Pat) embryonic lethal class of 20 genes(26). These genes encode proteins essential for embryonic sarcomere assembly, especially components of the integrin adhesion complex. For some genes, the null state is Pat, and the loss of function or hypomorphic state is Unc, and *unc-45* is an example of such a gene. For *unc-45*, the Pat embryonic lethal mutants have stop codons upstream of the UCS domain, whereas the Unc mutants, all of which are temperature sensitive (ts), are amino acid substitutions in the central and UCS domains(8, 11, 12, 24). We have expanded the number of known *C. elegans unc-45* Unc alleles by two, assessed the effect of all six known missense mutations on sarcomere organization, and measured the levels

of UNC-45 mutant proteins as compared to wild type UNC-45 protein. Our collaborators then created the same mutations in the comparable residues of human UNC-45B (see Figure 2.3), expressed and purified the proteins in *E. coli*, and characterized their thermal stability, and myosin chaperone activities. Through a combination of in vitro and in vivo data, we can conclude that the Unc (paralysis and disorganized thick filaments) phenotype is caused by both a decline in chaperoning activity and a decline in overall steady state UNC-45 and myosin protein levels. In vitro and in vivo effects of these mutations are summarized in Table 2.2.

## **Results:**

### Dominant-negative inhibition of thick filament assembly by expression of mutant UCS proteins in *C. elegans*:

Using the alignment of human and *C. elegans* UNC-45 UCS domains (Figure 2.2B), we identified residues in the nematode sequence that are comparable to the residues mutated in the human UNC-45B UCS domain that we are studying. We attempted to use CRISPR/Cas9 gene editing to generate several of these mutants in the *C. elegans* genome, without success; in several cases we could identify heterozygotes, but could not isolate homozygotes, probably because of embryonic lethality. Therefore, we undertook a different strategy in which we utilized transgenic worms to assess the dominant negative *in vivo* effects of four different UCS domain mutations – Groove (LTNL→ AAVQ), R805W, Pro (QFAKH→ PPGPP), and 2xW (Y750W, N758W). We generated nematodes carrying extrachromosomal arrays with either wildtype or mutated HA tagged *unc-45* under the control of the body wall muscle specific *myo-3* promoter and used *sur-5::GFP* as the transgenic marker. Three independently generated transgenic

lines were studied for each mutant protein. Animals were grown to adults, fixed, and immunostained with antibodies to myosin (MHC A; red in Figure 2.4), to GFP, and to UNC-95 (both green in Figure 2.4). Because such transgenic lines show somatic mosaicism, i.e. not every muscle cell receives the array and expresses the protein, we identified which muscle cells actually express the protein, by finding those that also expressed the transformation marker fused to GFP (cells with green nuclei in Figure 2.4). In addition, to locate the region of the muscle cell that normally contains the thick filaments, we immunostained with anti-UNC-95, which localizes to the base of integrin adhesion complexes in muscle (also green in Figure 2.4). All three lines expressing wt UNC-45 displayed normal thick filament assembly and organization with parallel A-bands, indicating that the extrachromosomal *unc-45* was not being overexpressed to the point of causing a phenotype. Two out of the three Groove and Pro mutation lines created displayed disorganized thick filaments. All three R805W and 2xW lines created displayed disorganized thick filaments in the muscle cells expressing the extrachromosomal array. The R805W mutation, which disrupts a salt bridge between helices 15H2 and 14H2, appeared to have the most drastic effect on the structure and organization of the worm sarcomeres. The mutant protein expressed in the two lines (Groove line 2 and Pro line 2) that showed relatively normal thick filament organization may not have been expressed at a high enough level to give a dominant phenotype or the mutant protein was so unstable that it was degraded quickly after translation. We used an antibody to the HA tag, along with antibodies to Myosin A and GFP, to verify expression and localization of the HA-tagged UNC-45 protein in the different strains (Figure 2.5). Wherever the thick filament structure and organization remained intact, the HA antibody can be seen

localizing as striations to either side of Myosin A, which is normal UNC-45 localization. However, in the mutants wherever the thick filaments were disrupted, the HA-UNC-45 failed to localize properly and appeared to either be aggregating or reduced compared to the intact portions of the muscle cell. This result suggests that the mutant UNC-45 proteins act as dominant negative poisons. Perhaps this occurs by binding to the normal endogenous UNC-45 and reducing the overall concentration of functional UNC-45, so that myosin heads are not properly folded, and thick filament assembly and organization are affected. This would be consistent with the fact that in crystal structures, UNC-45 has been found to exist as oligomeric structures(15, 20, 25). These results provide evidence for the biological importance of specific residues and sequences within the UCS domain of the UNC-45 chaperone.

Effects on *unc-45* temperature sensitive mutants on sarcomere organization, MHC B and UNC-45 protein levels:

There are four well known temperature-sensitive (ts) mutations in *C. elegans* UNC-45: one found in the central domain (G427E) and three found in the UCS domain (L559S, E781K, L822F). To obtain additional ts mutants in the UNC-45 UCS domain, we used WormBase to look for missense mutations in conserved residues of the UCS domain amongst the Million Mutation Project mutant strain collection(27). Six strains (see Figure 2.3A) conforming to these criteria were obtained from the Caenorhabditis Genetics Center and were grown at the permissive temperature of 15°C, and the restrictive temperature of 25°C, and immunostained with antibodies to myosin heavy chain A in order to assess the organization of assembled thick filaments (A-bands) in adult muscle. From this

analysis, we identified two new *ts* mutants that showed normal or nearly normal thick filament organization at 15°C, but disorganized thick filaments at 25°C, and these are G703R and F724S. These mutant strains retained the same phenotype after outcrossing 5 times to wild type to remove most of the background mutations (data not shown). Figure 2.6A shows thick filament organization for the now new total of 6 *ts* missense mutations in the UCS domain of UNC-45.

One interpretation of the reduced thick filament assembly in these mutants is that at the restrictive temperature their UCS domains display reduced myosin chaperone activity. However, an additional contribution to the phenotype might be that these missense mutations result in reduced levels of mutant UNC-45 proteins due to instability and degradation. To explore this possibility, we wished to determine the steady state levels of these mutant UNC-45 proteins in comparison with the steady state level of wild type UNC-45 protein. Although antibodies to UNC-45 have been described by several labs we wanted to generate our own antibodies for this and future studies(14, 15). As shown in Figure 6B, we used a 120 residue segment of the UCS domain as the antigen to generate rabbit polyclonal antibodies. After affinity purification, these antibodies reacted to a protein of expected size (~100 kDa) from wild type and a larger fusion protein from a CRISPR strain in which mNeonGreen was fused to the C-terminus of UNC-45. We then compared the levels of UNC-45 protein from wild type and the 6 *ts* mutant alleles at 15°C and 25°C (Figure 6C). As indicated in Figure 2.6D, all of the mutants except for F724S, showed a significant decrease in the level of UNC-45 protein when the temperature was changed from 15°C to 25°C degrees. This result indicates that some of

the defect in thick filament assembly is due to reduced levels of UNC-45 protein, or in other words, not all of the phenotype can be attributed to reduced UCS activity.

We also measured the steady state protein level of UNC-45's main client, body wall muscle Myosin B (MHC B), because it was reported that the previously characterized *unc-45* mutants have decreased Myosin B, as well as Myosin A, C, and D(28). In Figure 2.7 we show that 4/6 mutants have significantly reduced levels of MHC B at the restrictive temperature (25°C) compared to the permissive temperature (15°C). There was a decline in MHC B in the canonical  $\epsilon 286$  (L822F) mutant, however it was not significant due to the levels of MHC B being already diminished at the permissive temperature. The thick filament staining of the L822F mutant shows some disorganization even at the permissive temperature. The newly identified mutant F724S, which had increased UNC-45 at the restrictive temperature, also had increased MHC B at the restrictive temperature. We can see substantial myosin aggregation and disorganization in the thick filament staining of this mutant, providing further evidence that too much UNC-45 also results in the *unc* phenotype. Interestingly, there was about a 25% loss of MHC B in the wild type strain as well despite there being no significant decline in UNC-45 or thick filament structure organization at 25°C.

### **Discussion:**

The folding of myosin and the assembly of a functional sarcomere requires the molecular chaperone UNC-45B. Despite its relevance, little is known about the molecular mechanisms of its chaperoning function. Through collaboration with the Oberhauser lab at the University of Texas Medical Branch (UTMB), we have used a combination of

biophysical and biological experimental tools to analyze conserved residues/regions of UNC-45 and obtain a better understanding of the molecular mechanisms by which the UCS domain of UNC-45 chaperones myosin. We engineered mutations (Table 2.1) in the chaperoning domain of the human UNC-45B designed to test 1) if the putative “client-binding” groove in the UCS domain of human UNC-45B is functional by mutating highly conserved residues (the Groove, Y737W, and 2xW mutants); and 2) whether our homology-modeled loop is important for binding and holding myosin (the DEL and PRO mutants). We also introduced the R805W mutation to test the hypothesis that the stability of the salt bridge between R805-E767 plays a role in UCS-client interactions (41). We also analyzed six, two of which are new, temperature sensitive *unc-45* mutants that all have mutations at conserved residues within highly conserved regions of UNC-45 (primarily the UCS domain).

We found that mutating several conserved residues in the “putative client-binding” groove did not alter the UCS domain secondary structure (60%  $\alpha$ -helix content) or structural stability ( $T_m$  40°C) but reduced its chaperoning activity (Table 2.1). These groove mutants had a significantly lower heat-shock protecting effect of the ATPase activity of myosin S1 (51% for Y737W and 61% for 2xW) or the CS enzymatic activity (83% for Y737W and 69% for 2xW) when subjected to heat stress (Table 1). We found that these groove mutations also significantly altered the structure and organization of the worm sarcomeres (Figure 2.4; Figure 2.5). Overall, these data strongly support our first hypothesis that the putative “client-binding” groove in the UCS domain of human UNC-45B is indeed functional and does play an important role in the UCS domain chaperoning activity of myosin.

Next, we studied the effects of the two loop mutations (PRO and DEL) on the structure and function of the human UCS domain. We predicted that the PRO mutation, which replaces several partially conserved residues to prolines (KFSKQ / PPGPP), should lead to a weaker interaction with the client and lower chaperoning function of the UCS domain (because of lower flexibility of the highly disordered loop). This mutation did not affect the structure and stability as assayed by CD (circular dichroism) (Table 2.1) but significantly decreased the chaperoning function of the UCS domain when using myosin S1 as a client but not when using CS as a client. We speculate that this chaperoning difference may result from discriminatory interactions of this region of UCS with the non-native substrates (citrate synthase is a commonly used generic substrate to test any given chaperone for its ability to protect from thermal aggregation).

Our biophysical data show that removing the N584-D614 loop caused a significant decrease in the  $\alpha$ -helix character (from 58 to 42%) and a significantly weaker chaperoning function on protecting S1 or CS from heat shock (Table 2.1). The SAXS (small-angle X-ray scattering) data revealed that deletion of the loop lead to a significant conformational change of the UCS domain and a large increase in the stability of the dimeric conformations; the estimated KDs are 11 mM for the WT and >0.2 mM for the DEL. At the concentrations used in the CD and chaperoning assays (1–2 mM), the WT would be 10% dimer, whereas the DEL would be 90% dimer. These large changes in shape and monomer-dimer equilibrium may hinder the access of unfolded or partially folded myosin to the groove. Our results are consistent with the *in vivo* findings by Gazda et al. that deletion of this loop mutation neither rescued the defect in *C. elegans* sarcomere organization nor bound to myosin in immunoprecipitation experiments. Overall, these

data strongly support our second hypothesis, namely that the homology-modeled loop in the human UCS domain is essential for interacting and holding myosin.

The *in vivo* data show that the R805W mutation had the most drastic disorganizing effect on the structure and organization of the worm sarcomeres (Figure 2.4; Figure 2.5). This mutation does not affect UCS secondary structure or its structural stability but significantly impairs its chaperoning activity on protecting S1 or CS from thermal aggregation (53 and 24% lower activity than WT, respectively). The findings that the autosomal dominant mutation R805W segregates with human congenital and infantile cataracts and that this mutant expressed in zebrafish embryonic eyes results in aberrant lens maturation suggest an important role of the R805 residue in the UCS domain conformation, stability, and/or client interaction(29). As suggested by Hansen et al., this mutation may disrupt a salt bridge between R805-E767 (homology model in Fig. 2 B). This salt bridge is highly conserved, from worms (R819-E781) and flies to mice and humans. To better understand how the R805W mutation may alter the *in vitro* chaperoning activity and the *in vivo* function of the UCS domain, we employed SAXS to determine its solution conformation. Like the WT, the R805W mutant has a dimeric conformation (probably via head-to-head interactions). Using a monomer-dimer equilibrium analysis of the R805W SAXS, we estimated an equilibrium constant  $K_D$  of 21 mM, with 40% dimer at 0.8 mg/mL. This  $K_D$  is similar to the WT (11 mM). These relatively small changes in the UCS domain solution properties do not explain the large functional effects (chaperone activity and sarcomere structure) introduced by the R805W mutation. It is possible that this and some of the other mutations (e.g., 2xW) reduce the UCS domain chaperone activity by an allosteric mechanism; this would be the subject of future

experiments using the experimental approach described in this work. Our results may have offered insights into the folding and repair of the many classes of myosin molecules that are expressed in non-muscle tissues. In fact, the expression and function of UNC-45 is not limited to just striated muscle but is very likely to be crucial for the folding of myosin heads of the large myosin superfamily containing at least 35 different classes of myosins, some of which are expressed in nearly all cell types. UNC-45 is required for early embryonic development in *C. elegans* (30, 31) and is involved in cell division and cell migration of ovarian and breast carcinoma (epithelial cells)(32-34); in both of these cases, UNC-45 likely aids the folding of non-muscle myosin II. A better understanding of the mechanisms by which UNC-45 helps fold myosin heads is likely to lead to new therapies for several diseases, especially those due to mutations in myosin, as well as shine some light on our understanding of the UNC-45B interactome.

Temperature-sensitive (ts) mutants of a gene are ones in which there is a marked drop in the level or activity of the encoded protein when the gene is expressed at the restrictive temperature. At the lower permissive temperature, the phenotype of the mutant is very similar to that of the WT. Ts-mutants provide an extremely powerful tool for studying protein function in model organisms like *Saccharomyces cerevisiae*, *C. elegans*, and *Drosophila* which do not maintain their internal temperatures and were instrumental in identifying the *unc-45* gene in *C. elegans*(10). However, the molecular mechanisms underlying temperature sensitivity have remained elusive. In the case of the myosin chaperone UNC-45, these mutations may alter protein stability, chaperone activity, interactions with myosin, or both. After first identifying two new *unc-45* ts mutants in the chaperone UCS domain, namely, G703R and F724S, we assessed the steady state

levels of UNC-45 in a total of 6 *unc-45* ts missense mutants. All the mutants show decreased levels of UNC-45 protein compared to wild type (Figure 2.1D). The total of six ts-mutations, G427E, L559S, G703R, F724S, E781K, and L822F all are located in highly conserved regions (Figure 2.3, Table 2.2), and are located at residues that are conserved between nematode UNC-45 and human UNC-45B. *E. coli* was used to express and purify human UNC-45B with the comparable mutations. These amino acid changes in UNC-45B do not have a large impact on its thermal stability as measured by CD and DSF spectroscopy. Two ts-mutations (i.e., F711S and E767K) slightly decrease the thermal stability of UNC-45B by about 3°C. Interestingly, these two mutations are located in the center of the UCS domain (helices 13H1 and 14H2, respectively) and nearby to the “putative myosin-binding” groove region, helix 13H3.21 We speculate that these two mutations may destabilize the compact structure of the groove region leading to a local structural change and a small overall destabilization. However, all the mutants exhibit a significantly lower chaperoning activity on protecting myosin heads from heat damage.

Even though it has been known for some time that the structure and function of UNC-45 is conserved in the animal kingdom, it was only recently that humans with muscle disease were found to have mutations in UNC-45B, the muscle specific UNC-45 protein in mammals. Donkervoort et al. reported 10 patients who had bi-allelic variants in the UNC45B gene that presented with childhood-onset progressive muscle weakness and muscle eccentric core histology(35). Two of the mutations, R754Q and R778W, are nonconservative changes in the UCS domain close to mutations found in nematode *unc45(m94)* (in human UNC-45B, E767K) and *unc-45(e286)* (in human UNC-45B, L808F).

In terms of biochemical activities, our results are basically consistent with those by Hellerschmied et al., who found that four ts-mutations G427E, L559S, E781K, and L822F have the same or even slightly higher thermal stability than the *C. elegans* WT UNC-45 chaperone(24). Using a cellular chaperone assay that measures the production of soluble myosin in insect cells, they found that these four UNC-45 ts-mutations had a negative effect on the myosin folding activity. Overall, our results indicate that the ts mutations in UNC-45 lead to reduced and abnormal thick filament assembly by a combination of reduced UNC-45 protein stability and reduced UNC-45 chaperoning function. One potential reason for a difference in in vivo versus in vitro mutant protein stability is that the mutations result in a change of posttranslational modifications that ultimately lead to increased degradation. Evidence for this idea can be seen in Figure 2.6C, that shows that both in wild type and the *unc-45* mutants, there are two protein bands detected by western blot, one of which is of lower mobility than the predicted molecular weight. In fact, this larger species increases in the mutants when grown at the restrictive temperature, which could be interpreted as temperature induced unfolding of the mutant proteins lead to further post translational modification. One of the likely PTMs is ubiquitination, which has been reported to occur on UNC-45 and is involved in its degradation(36). The unfolding may alter UNC-45's interaction with another protein that normally covers a PTM site or causes residues to be slightly more or less exposed for modification. This may provide evidence that these conserved residues not only play a role in chaperoning activity, but also in vivo UNC-45 stability and/or regulation.

## Materials and Methods:

### C. elegans Strains:

Standard growth conditions for *C. elegans* were used(37). Wild-type nematodes were the N2 (Bristol) strain. For wild-type and each of the mutant *unc-45* plasmids, three independently generated extrachromosomal array transgenic lines were created by SunyBiotech (Fuzhou, China) by co-injection into wild-type N2 Bristol of pPD95.86- HA-UNC-45 and the transformation marker plasmid pTG96 (*psur-5::sur5::nlsGFP*, which expresses GFP in most somatic cell nuclei). These transgenic lines have the following strain names: for UNC-45 wild-type, GB297-299; for UNC-45 Groove, GB300-302; for UNC-45 R805W, GB303-305; for UNC-45 Pro, GB306-308; and for UNC-45 2xW, GB309-311. The following strains were also used in this study: *unc-45(e286)*, *unc-45(m94)*, *unc-45(b131)*, *unc-45(su2002)*, *unc-45(gk576605)*, *unc-45(gk615477)*, and *unc-45:mNeonGreen*. *e286*, *m94*, *b131*, and *su2002* were obtained from the Caenorhabditis Genetics Center. VC40328 (*unc-45(gk576605)*, G703R) and VC40392 (*unc-45(gk615477)*, F724S) were 2 of 6 strains obtained from the million mutation project (MMP)(27) that had missense mutations in conserved residues of the UCS domain and showed disorganized thick filaments when grown at 25°C. They were outcrossed with N2 wild type five times to eliminate most of the background mutations of a typical MMP strain, to create strain GB337 for *unc-45(gk576605)* [G703R], and strain GB338 for *unc-45(gk615477)* [F724S]. The strain PHX789, *unc-45(syb789)*, is a CRISPR generated strain which expresses UNC-45 with a C-terminal mNeonGreen tag. PHX789 was created by SunyBiotech (<http://www.sunybiotech.com>). PHX789 was outcrossed 2X to wild type to generate strain GB319.

### Immunostaining of adult body wall muscle:

Adult nematodes were fixed and immunostained according to the method described by Nonet et al. and described in further detail by Wilson et al.(38, 39). The following primary antibodies were used: anti-MHC A at 1:200 (mouse monoclonal 5-6 (13)), anti-UNC-95 at 1:100 (rabbit polyclonal Benian-13 (40)), anti-GFP at 1:200 (rabbit polyclonal (A-11122; Invitrogen and Thermo Fisher Scientific)), and anti-HA (mouse monoclonal clone HA-7 (cat. no. H3663; Sigma-Aldrich)). Secondary antibodies, used at 1:200 dilution, included anti-rabbit Alexa 488 (Invitrogen and Thermo Fisher Scientific) and anti-mouse Alexa 594 (Invitrogen). Images were captured at RT with a Zeiss confocal system (LSM 510) equipped with an Axiovert 100M microscope and an Apochromat 63/1.4 numerical aperture oil immersion objective in 2.5 zoom mode (Zeiss, Oberkochen, Germany). The color balances of the images were adjusted by using Photoshop (Adobe, San Jose, CA).

### Generation of antibodies to UNC-45 and Western Blots:

Glutathione S-transferase (GST) and maltose binding protein (MBP) fusions of the 123 C-terminal residues of UNC-45 were expressed in *E. coli* after cloning into pGEX-KK1 and pMAL-KK1, respectively. The GST fusion protein was supplied to Noble Life Sciences (Woodbine, Maryland) for production of rabbit antibodies. Anti- UNC-45 was affinity-purified using Affigel (BioRad)- conjugated to the MBP fusion, as described previously(41). The method of Hannak et al. was used to prepare total protein lysates from wild type and the 6 *unc-45* mutant strains(42). Equal amounts of total protein from these strains were separated on 4–15% gradient polyacrylamide-SDS Laemmli gels, transferred to nitrocellulose membranes, and reacted with affinity-purified rabbit polyclonal anti-UNC-45 at 1:5,000, or mouse monoclonal anti-MHC B. (5–13;8 gift of

Henry F. Epstein, now deceased) at 1:50,000, and then with goat anti-rabbit immunoglobulin G conjugated to HRP, or with goat anti-mouse immunoglobulin G conjugated to HRP at 1:10,000 and visualized by ECL. The quantitation of steady-state levels of protein was performed as described in Miller et al(43). The relative amount of each of these proteins in each lane was normalized to the total protein visualized by Ponceau S staining.

#### Statistical Analysis:

Unless otherwise stated, data are reported as mean  $\pm$  SE of the mean. Western Blot statistical analyses were made using GraphPad Prism Software (version 4.0). Comparisons of three or more means used one-way ANOVA and Bonferroni-adjusted unpaired t tests. Statistical significance was assigned as not-significant for  $p > 0.05$ , \* for  $p \leq 0.05$ , and \*\*\* for  $p \leq 0.001$ .

## Figures and Tables:

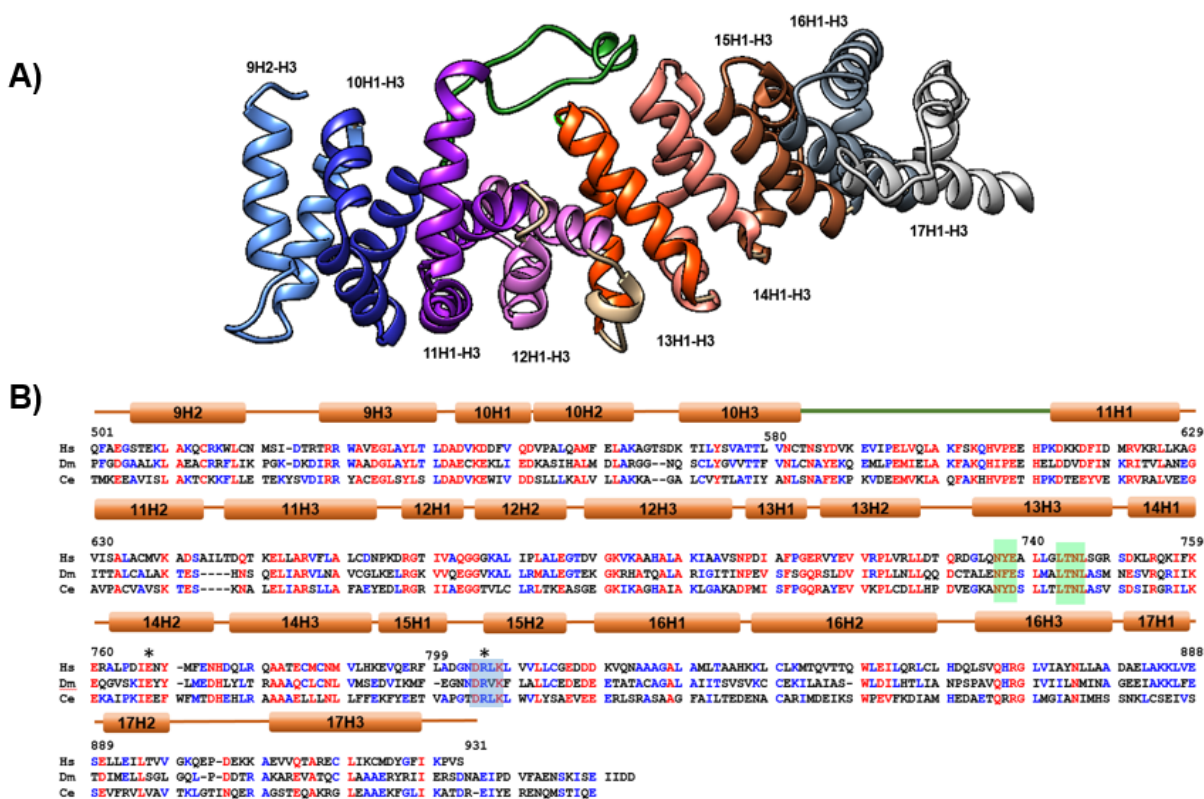


**Figure 2.1.** A) Homology model of the human UCS domain based on the *D. melanogaster* 3D structure (PDB ID: 3NOW), highlighting the different ARM repeats (9 to 17). Phyre2(44), SWISS-MODEL(45) and UCSF Chimera(46) were used for making the human model. B) Sequence alignment of the UCS domains from UNC-45 proteins from *Homo sapiens* (Hs; E1P642), *Drosophila melanogaster* (Dm; Q9VHW4) and *C. elegans* (Ce; Q09981). Red residues are highly conserved in all three sequences; blue are low consensus residues. Green boxed residues are highly conserved residues in the groove region. Blue boxed residues are highly conserved residues in repeat 15. \* denotes conserved inter-repeat interacting ion pair Glu768 and Arg805 residues. The overall sequence identity between the HsUNC-45 and the other listed UNC-45 proteins is about 36%. ClustalOmega(47) and Multalin(48) were used for the alignment.

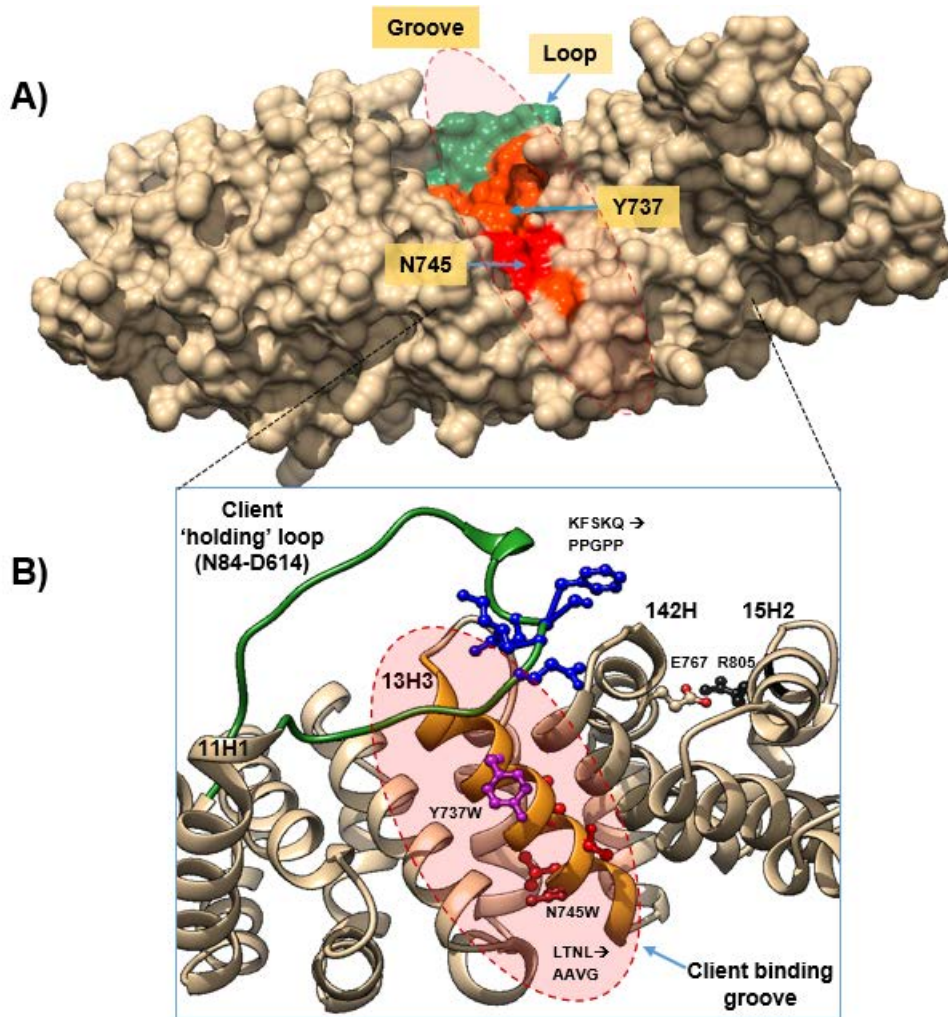


**Figure 2.2.** (A) Surface representation of the human UCS domain highlighting the loop region (in green) and the highly conserved residues in the groove region, 736 NYEaLTNL 746 (red patch). (B) Location of the different residues mutated in the UCS domain: the deleted loop is in green (N584-D614), the mutations in the loop 600 KFSKQ 604 are in blue, and the mutations in the groove region Y737 (in purple), N745 (in red), and R805 (in black). Chimera(46) was used to make the representation.

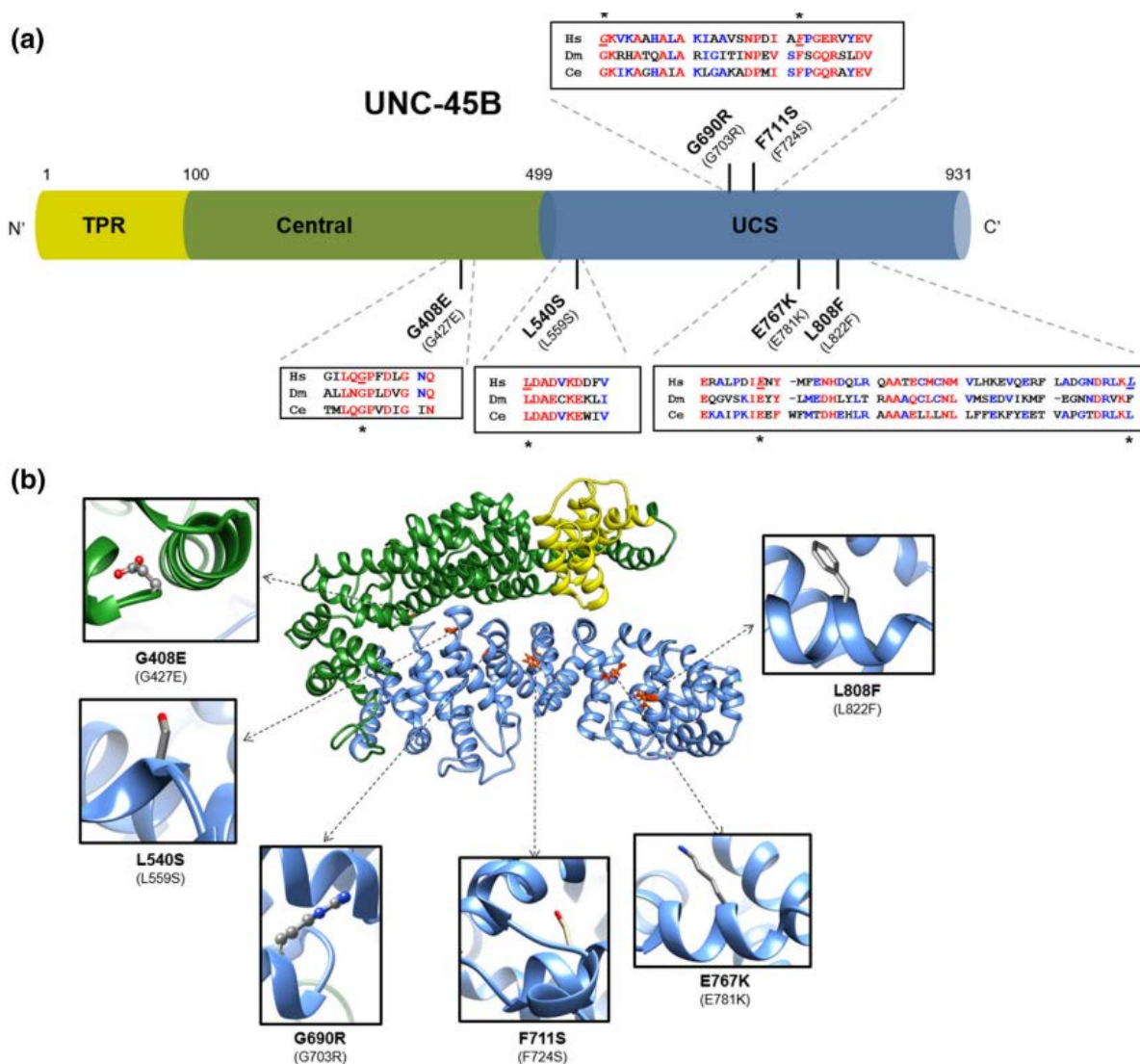


**Figure 2.3. Location of the temperature-sensitive mutations in the human UNC-45B sequence and structure.** (a) Human UNC-45B is made of three distinct domains: a 100-amino-acid N-terminal TPR domain (in yellow), a 400-amino-acid Central domain (in green), and a 431-amino-acid UCS domain (in blue). The equivalent ts mutations in the *C. elegans* UNC-45 sequence are shown in parenthesis. Rectangular boxes show sequence alignment of UNC-45 proteins from *Homo sapiens* (Hs; Q81WX7), *Drosophila melanogaster* (Dm; Q9VHW4) and *C. elegans* (Ce; Q09981). Red residues are strictly conserved in all three sequences; blue are lower consensus residues. ClustalOmega(47) and Multalin(48) were used for the alignment. Mutated residues are marked by an asterisk (\*) and underlined. (b) The homology model of the human UNC-45 protein structure was made using Phyre2(44) and SWISS-MODEL(45) domain using the *C. elegans* 3D structure (PDB ID: 4i2z) as a reference crystal structure. The three domains are colored yellow (TPR), green (central) and blue (UCS). The corresponding temperature-sensitive residues were mutated in Chimera(46). The equivalent ts mutations in the *C. elegans* UNC-45 sequence are shown in parenthesis.

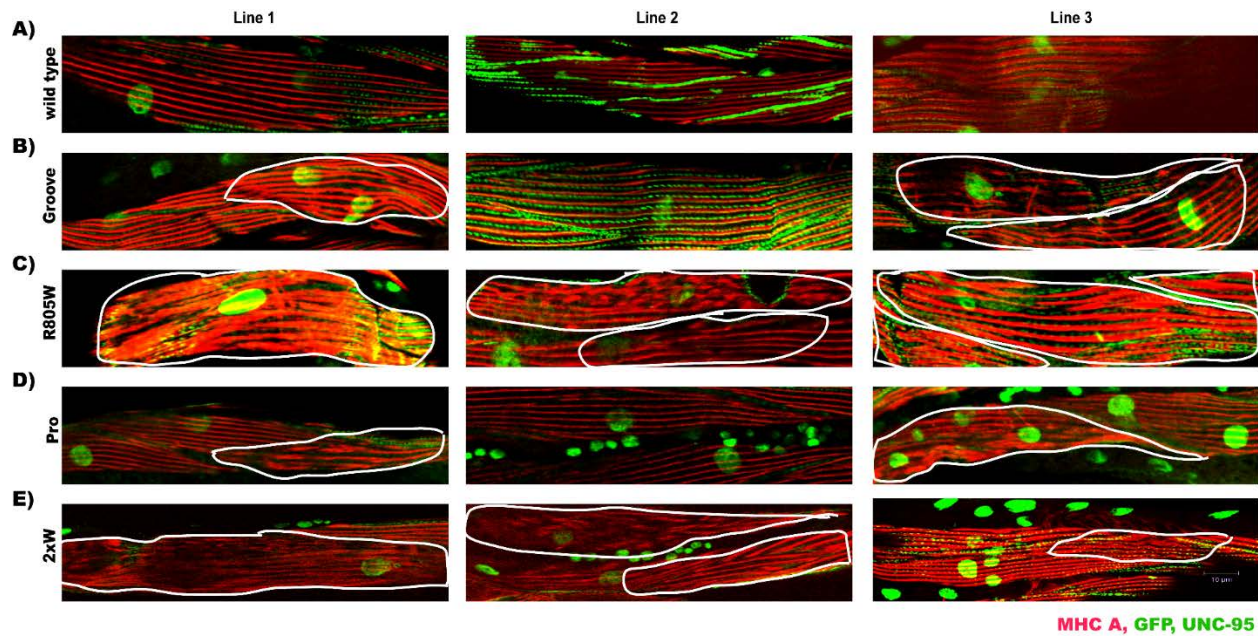


**Figure 2.4: The effects of expression of UNC-45-containing mutations in the UCS domain in vivo.** Shown is the immunostaining of *C. elegans* transgenic strains expressing either extrachromosomal WT (A), Groove (B), R805W (C), PRO (D), or 2xW (E) UNC-45. “Lines 1, 2, and 3” represent three independently generated transgenic lines for each type of UNC-45. Myosin A (MHC A), which localizes to the A-bands of the muscle cells, is shown in red. UNC-95, which localizes to the base of the integrin adhesion complexes in muscle cells and was used to identify the myofibrillar region of muscle cells independent of A-band organization, is shown in green. Nuclear GFP expressed from the transformation marker *sur-5::GFP* was used to identify which muscle cells inherited and expressed the transgene. Although *sur-5::GFP* is expressed in nearly all somatic cells, the single nucleus found in a body-wall muscle cell was identified by its size, shape, and position. White boundaries were drawn around areas of A-band disruption and disorganization.

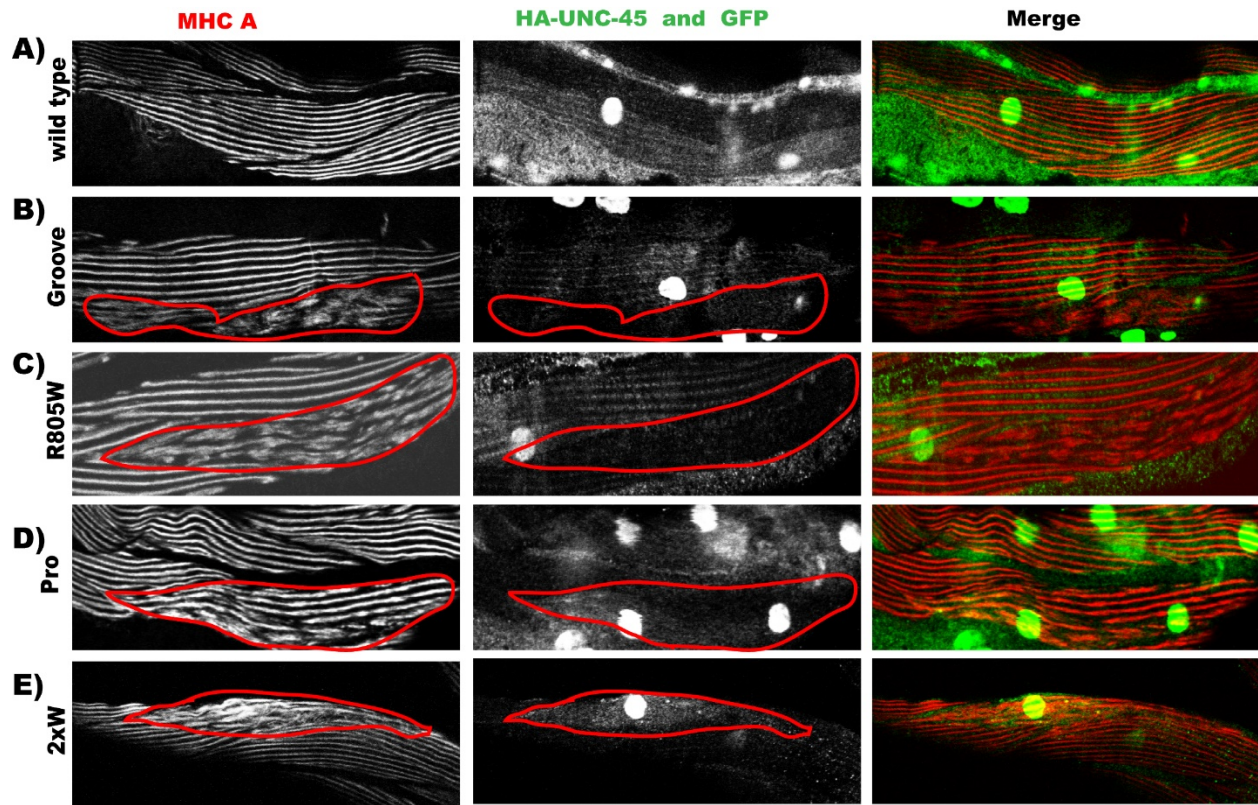


**Figure 2.5. The localization of HA-tagged UNC-45 in the muscle cells of transgenic strains.** Immunostaining of five *C. elegans* strains expressing either extrachromosomal Wildtype (A), Groove (B), R805W (C), Pro (D), or 2xW (E) HA tagged UNC-45. Myosin A (MHC A), which localizes to the A-bands of the muscle cells, is shown in red. HA staining recognizing transgenic form of UNC45 is shown in green. GFP, which localizes to the nucleus of all muscle cells expressing the transgenic array (transformation marker *sur-5::GFP*), is also shown in green. White boundaries have been drawn around areas of A-band disruption/disorganization.

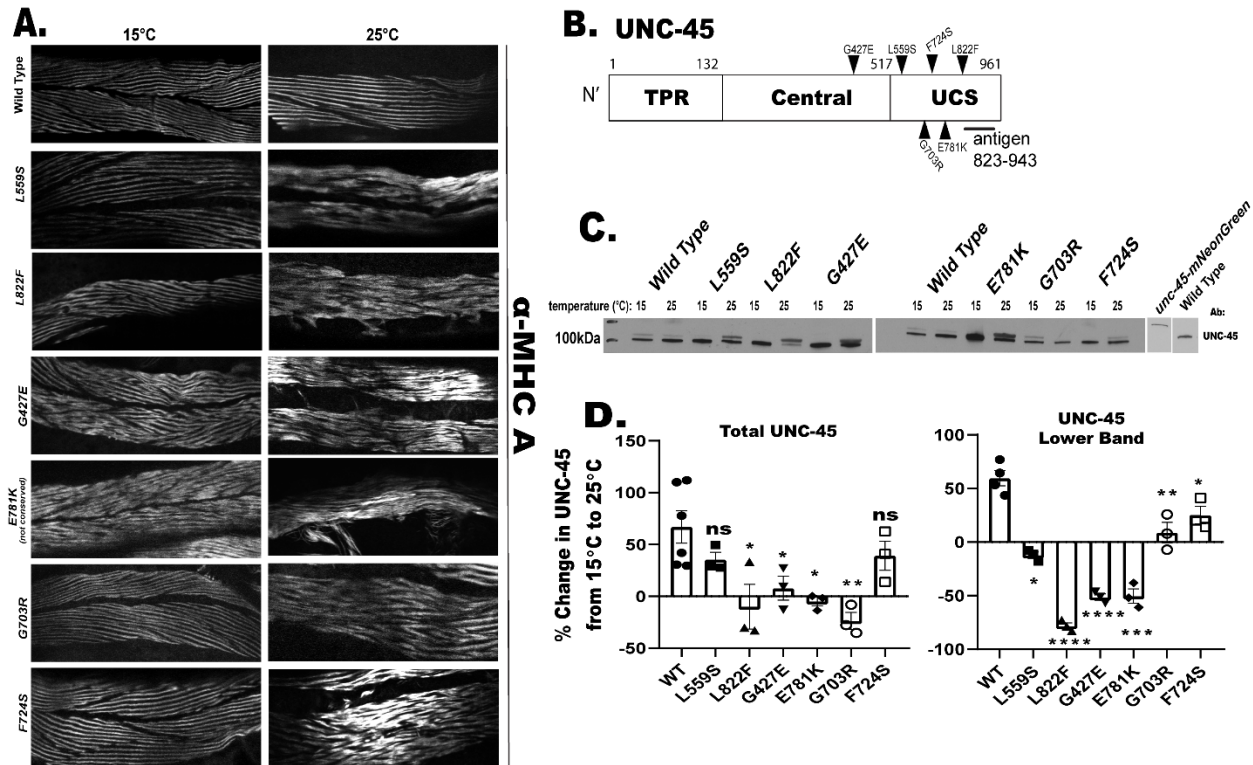


**Figure 2.6. Effects of *unc-45* temperature-sensitive (*ts*) mutations on sarcomere organization and UNC-45 protein levels.** (a) Immunostaining of A-bands with antibodies to MHC A for wild type and the 6 *unc-45* mutant strains raised at 15°C and 25°C. For simplicity only the amino acid changes in the mutant UNC-45 proteins are used to distinguish the mutants (see Table 2 for mutant allele names). Except for wild type, all mutants showed more severe disorganization of sarcomeric A-bands at 25°C. Three alleles, with mutations in F724S, G703R, and L559S, show normal organization of A-bands at 15°C. (b) Schematic of UNC-45 domain organization, location of 6 *ts* mutations examined, and the location of the antigen used to raise rabbit polyclonal antibodies to UNC-45. (c) Representative western blots examining the levels of UNC-45 in wild type and the 6 *ts* *unc-45* mutants at permissive (15°C) and restrictive (25°C) temperatures. The second from the last lane contains an extract from *unc-45(syb789)*, which is a CRISPR engineered strain that expresses UNC-45 with an mNeonGreen tag fused to the C-terminus of UNC-45. Note the shift in size of this band (134 kDa) compared to the size (107 kDa) of UNC-45 bands from wild type and the mutants demonstrating the specificity of the antibody. (d) Graphical representation of the % change in levels of total UNC-45, and lower band of UNC-45 of *unc-45* mutant alleles when shifted from 15°C to 25°C.

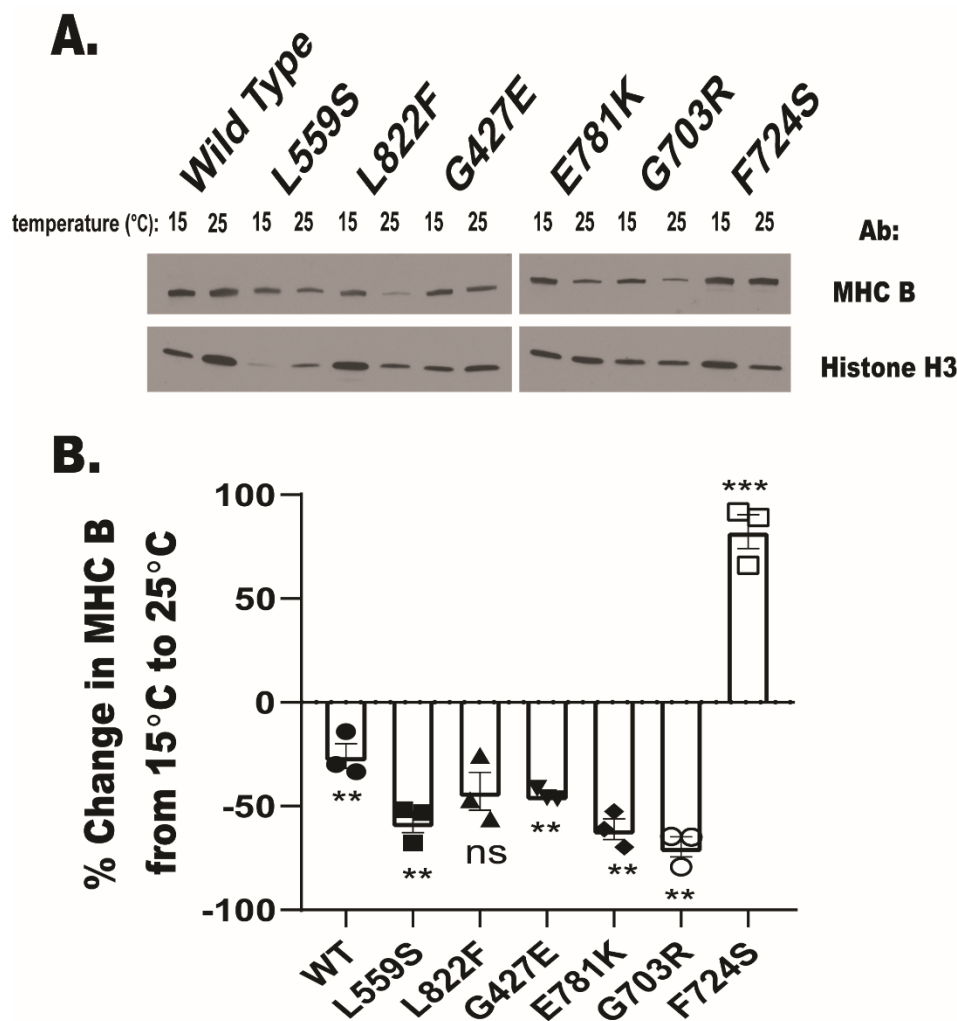


**Figure 2.7. Effects of unc-45 temperature-sensitive (ts) mutations on myosin MHC B protein levels.** (a) Representative western blots examining the levels of myosin MHC B in wild type and the 6 ts unc-45 mutants at permissive (15°C) and restrictive (25°C) temperatures. (b) Graphical representation of the % change in MHC B levels of unc-45 mutant alleles when shifted from 15°C to 25°C.

**Table 2.1 Summary of the In Vitro and In Vivo Effects of UCS Mutations**

Protein Name	$\alpha$ (%)	$\beta$ (%)	S1 Assay <sup>a</sup>	CS Assay <sup>a</sup>	Worm Sarcomere Phenotype	Predicted Effects of the Mutation on UCS Domain Structure and Function
WT	58	4	100	100	normal	
DEL	42	14	39	62	<sup>b</sup>	These discontinue the substrate cleft and reduce the interaction with client and lead to a reduced chaperone activity.
PRO	62	6	40	99	disrupted (2/3)	The addition of Pro residues should increase rigidity of “holding” loop and lead to a reduced chaperone activity.
Groove	<sup>c</sup>		<sup>c</sup>	<sup>c</sup>	disrupted (2/3)	These reduce the interaction with client and lead to negligible or no chaperone activity.
Y737W	61	4	51	83	<sup>d</sup>	The addition of large side chains should interfere with client binding and hence lead to a reduced chaperoning activity.
2xW	63	2	61	69	disrupted (2/3)	The addition of two large side chains should lead to decreased interaction with client and hence a weaker chaperoning activity.
R805W	62	6	47	76	disrupted (3/3)	Altered chaperoning (higher or lower) is because of the ion pair instability between helices.

**Table 2.2. Summary of the impact of ts mutations on the biophysical properties of human UNC-45 chaperone and on *C. elegans* protein levels**

Human UNC-45 ts-mutant name	<i>C. elegans</i> ts-mutant (allele)	Location of the mutation (ARM repeat)	Protein stability CD /SYPRO (T <sub>m</sub> )	ATPase protection (% relative to WT)	Change total UNC-45 (and UNC-45 lower band) from 15 to 25° C as compared to wild type
UNC45B-WT	WT		39°C/47°C	100	Increased (increased)
UNC45B-G408E	G427E ( <i>b131</i> )	Highly conserved aa in sequence between 6H3 and 7H1	41°C/47°C	80	Decreased (decreased)
UNC45B-L540S	L559S ( <i>su2002</i> )	Highly conserved aa in in loop between 9H3 and 10H1	43°C/47°C	75	No change (decreased)
UNC45B-G690R	G703R ( <i>gk576605</i> ) <sup>a</sup>	Highly conserved aa in 12H3	37°C/45°C	67	Decreased (decreased)
UNC45B-F711S	F724S ( <i>gk615477</i> ) <sup>a</sup>	Highly conserved aa in loop between 12H3 and 13H2	35°C/42°C	73	No change (decreased)
UNC45B-E767K	E781K ( <i>m94</i> )	Highly conserved aa in 14H2	36°C/42°C	76	Decreased (decreased)
UNC45B-L808F	L822F ( <i>e286</i> )	Conserved aa in 15H2 (F in Dm)	41°C/47°C	75	Decreased (decreased)

<sup>a</sup>New mutations obtained from the million mutation project.

### Acknowledgements

This study was supported by National Institutes of Health grant R01GM118534 to Guy M. Benian and Andres F. Oberhauser, and also supported in-part by the Emory Initiative Biological Discovery Through Chemical Innovation (BDCI) to Guy M. Benian. We thank Drs. Luis Holthausen and Pawel Bujalowski for their invaluable help with the CD experiments.

### Literature Cited:

1. Crawford GL & Horowitz R (2011) Scaffolds and chaperones in myofibril assembly: putting the striations in striated muscle. *Biophysical reviews* 3(1):25-32.
2. Benian GM & Epstein HF (2011) Caenorhabditis elegans muscle: a genetic and molecular model for protein interactions in the heart. *Circulation research* 109(9):1082-1095.
3. Epstein HF & Benian GM (2012) Paradigm Shifts in Cardiovascular Research From Caenorhabditis elegans Muscle. *Trends in Cardiovascular Medicine* 22(8):201-209.
4. Chow D, Srikakulam R, Chen Y, & Winkelmann DA (2002) Folding of the Striated Muscle Myosin Motor Domain\*. *Journal of Biological Chemistry* 277(39):36799-36807.
5. Srikakulam R, Liu L, & Winkelmann DA (2008) Unc45b forms a cytosolic complex with Hsp90 and targets the unfolded myosin motor domain. *PloS one* 3(5):e2137.
6. Pokrzywa W & Hoppe T (2013) Chaperoning myosin assembly in muscle formation and aging. *Worm* 2(3):e25644.
7. Hellerschmied D & Clausen T (2014) Myosin chaperones. *Current opinion in structural biology* 25:9-15.
8. Lee CF, Melkani GC, & Bernstein SI (2014) The UNC-45 myosin chaperone: from worms to flies to vertebrates. *International review of cell and molecular biology* 313:103-144.
9. Smith DA, Carland CR, Guo Y, & Bernstein SI (2014) Getting Folded: Chaperone Proteins in Muscle Development, Maintenance and Disease. *The Anatomical Record* 297(9):1637-1649.
10. Epstein HF & Thomson JN (1974) Temperature-sensitive mutation affecting myofilament assembly in Caenorhabditis elegans. *Nature* 250(467):579-580.
11. Barral JM, Bauer CC, Ortiz I, & Epstein HF (1998) Unc-45 mutations in Caenorhabditis elegans implicate a CRO1/She4p-like domain in myosin assembly. *The Journal of cell biology* 143(5):1215-1225.
12. Venolia L, Ao W, Kim S, Kim C, & Pilgrim D (1999) unc-45 gene of Caenorhabditis elegans encodes a muscle-specific tetratricopeptide repeat-containing protein. *Cell motility and the cytoskeleton* 42(3):163-177.
13. Miller DM, 3rd, Ortiz I, Berliner GC, & Epstein HF (1983) Differential localization of two myosins within nematode thick filaments. *Cell* 34(2):477-490.
14. Ao W & Pilgrim D (2000) Caenorhabditis elegans UNC-45 is a component of muscle thick filaments and colocalizes with myosin heavy chain B, but not myosin heavy chain A. *The Journal of cell biology* 148(2):375-384.
15. Gazda L, et al. (2013) The myosin chaperone UNC-45 is organized in tandem modules to support myofilament formation in C. elegans. *Cell* 152(1-2):183-195.
16. Barral JM, Hutagalung AH, Brinker A, Hartl FU, & Epstein HF (2002) Role of the myosin assembly protein UNC-45 as a molecular chaperone for myosin. *Science (New York, N.Y.)* 295(5555):669-671.
17. Ni W, Hutagalung AH, Li S, & Epstein HF (2011) The myosin-binding UCS domain but not the Hsp90-binding TPR domain of the UNC-45 chaperone is essential for function in Caenorhabditis elegans. *Journal of cell science* 124(Pt 18):3164-3173.

18. Nicholls P, *et al.* (2014) Chaperone-mediated reversible inhibition of the sarcomeric myosin power stroke. *FEBS letters* 588(21):3977-3981.
19. Bujalowski PJ, Nicholls P, Garza E, & Oberhauser AF (2018) The central domain of UNC-45 chaperone inhibits the myosin power stroke. *FEBS open bio* 8(1):41-48.
20. Fratev F, Osk Jonsdottir S, & Pajeva I (2013) Structural insight into the UNC-45-myosin complex. *Proteins* 81(7):1212-1221.
21. Groves MR & Barford D (1999) Topological characteristics of helical repeat protein. *Current opinion in structural biology* 9(3):383-389.
22. Conti E & Kuriyan J (2000) Crystallographic analysis of the specific yet versatile recognition of distinct nuclear localization signals by karyopherin  $\alpha$ . *Structure* 8(3):329-338.
23. Tewari R, Bailes E, Bunting KA, & Coates JC (2010) Armadillo-repeat protein functions: questions for little creatures. *Trends in cell biology* 20(8):470-481.
24. Hellerschmied D, *et al.* (2019) Molecular features of the UNC-45 chaperone critical for binding and folding muscle myosin. *Nature communications* 10(1):4781.
25. Shi H & Blobel G (2010) UNC-45/CRO1/She4p (UCS) protein forms elongated dimer and joins two myosin heads near their actin binding region. *Proceedings of the National Academy of Sciences* 107(50):21382-21387.
26. Gieseler K, Qadota H, & Benian GM (2017) Development, structure, and maintenance of *C. elegans* body wall muscle. *WormBook : the online review of C. elegans biology 2017*:1-59.
27. Thompson O, *et al.* (2013) The million mutation project: a new approach to genetics in *Caenorhabditis elegans*. *Genome research* 23(10):1749-1762.
28. Landsverk ML, *et al.* (2007) The UNC-45 chaperone mediates sarcomere assembly through myosin degradation in *Caenorhabditis elegans*. *The Journal of cell biology* 177(2):205-210.
29. Hansen L, *et al.* (2014) The myosin chaperone UNC45B is involved in lens development and autosomal dominant juvenile cataract. *European journal of human genetics : EJHG* 22(11):1290-1297.
30. Kachur T, Ao W, Berger J, & Pilgrim D (2004) Maternal UNC-45 is involved in cytokinesis and colocalizes with non-muscle myosin in the early *Caenorhabditis elegans* embryo. *Journal of cell science* 117(Pt 22):5313-5321.
31. Kachur TM & Pilgrim DB (2008) Myosin assembly, maintenance and degradation in muscle: Role of the chaperone UNC-45 in myosin thick filament dynamics. *International journal of molecular sciences* 9(9):1863-1875.
32. Bazzaro M, *et al.* (2007) Myosin II co-chaperone general cell UNC-45 overexpression is associated with ovarian cancer, rapid proliferation, and motility. *The American journal of pathology* 171(5):1640-1649.
33. Guo W, Chen D, Fan Z, & Epstein HF (2011) Differential turnover of myosin chaperone UNC-45A isoforms increases in metastatic human breast cancer. *Journal of molecular biology* 412(3):365-378.
34. Lehtimäki JI, *et al.* (2017) UNC-45a promotes myosin folding and stress fiber assembly. *The Journal of cell biology* 216(12):4053-4072.

35. Donkervoort S, *et al.* (2020) Pathogenic Variants in the Myosin Chaperone UNC-45B Cause Progressive Myopathy with Eccentric Cores. *American journal of human genetics* 107(6):1078-1095.
36. Hoppe T, *et al.* (2004) Regulation of the myosin-directed chaperone UNC-45 by a novel E3/E4-multiubiquitylation complex in *C. elegans*. *Cell* 118(3):337-349.
37. Brenner S (1974) The genetics of *Caenorhabditis elegans*. *Genetics* 77(1):71-94.
38. Nonet ML, Grundahl K, Meyer BJ, & Rand JB (1993) Synaptic function is impaired but not eliminated in *C. elegans* mutants lacking synaptotagmin. *Cell* 73(7):1291-1305.
39. Wilson KJ, Qadota H, & Benian GM (2012) Immunofluorescent localization of proteins in *Caenorhabditis elegans* muscle. *Methods in molecular biology (Clifton, N.J.)* 798:171-181.
40. Qadota H, Mercer KB, Miller RK, Kaibuchi K, & Benian GM (2007) Two LIM domain proteins and UNC-96 link UNC-97/pinch to myosin thick filaments in *Caenorhabditis elegans* muscle. *Molecular biology of the cell* 18(11):4317-4326.
41. Mercer KB, *et al.* (2003) *Caenorhabditis elegans* UNC-98, a C2H2 Zn finger protein, is a novel partner of UNC-97/PINCH in muscle adhesion complexes. *Molecular biology of the cell* 14(6):2492-2507.
42. Hannak E, *et al.* (2002) The kinetically dominant assembly pathway for centrosomal asters in *Caenorhabditis elegans* is gamma-tubulin dependent. *The Journal of cell biology* 157(4):591-602.
43. Miller RK, *et al.* (2009) CSN-5, a component of the COP9 signalosome complex, regulates the levels of UNC-96 and UNC-98, two components of M-lines in *Caenorhabditis elegans* muscle. *Molecular biology of the cell* 20(15):3608-3616.
44. Kelley LA & Sternberg MJE (2009) Protein structure prediction on the Web: a case study using the Phyre server. *Nature protocols* 4(3):363-371.
45. Schwede T, Kopp J, Guex N, & Peitsch MC (2003) SWISS-MODEL: An automated protein homology-modeling server. *Nucleic acids research* 31(13):3381-3385.
46. Pettersen EF, *et al.* (2004) UCSF Chimera—A visualization system for exploratory research and analysis. *Journal of computational chemistry* 25(13):1605-1612.
47. Chenna R, *et al.* (2003) Multiple sequence alignment with the Clustal series of programs. *Nucleic acids research* 31(13):3497-3500.
48. Corpet F (1988) Multiple sequence alignment with hierarchical clustering. *Nucleic acids research* 16(22):10881-10890.

### **Chapter 3: UNC-45 has a crucial role in maintaining muscle sarcomeres during aging in *C. elegans***

Matheny CJ, Qadota H, Kemelman M, Oberhauser AF, Benian GM. UNC-45 has a crucial role in maintaining muscle sarcomeres during aging in *Caenorhabditis elegans*. *Aging Cell*. 2022.  
*Under revision.*

**Introduction:**

Sarcopenia, the decline in skeletal muscle mass and function without any underlying disease, is a major contributor to physical disability, poor quality of life, and death among the elderly (1). 40-50% of individuals over 80 years of age suffer from this loss of muscle mass and function (2, 3). The molecular mechanisms responsible for this age-related condition remain uncertain (4). Resistance training and dietary changes are recognized as the gold standard therapy but have only a modest effect (5). There is a direct association between poor hand grip strength, reduced physical function and a higher risk of falling (6). Intriguingly, even in middle age (40-69), there is a correlation between reduced grip strength and all-cause mortality and incidence of and mortality from cardiovascular disease, respiratory disease, and cancer (7). Elderly individuals at a higher risk of falling are at a higher risk of vertebral and non-vertebral fractures (6) – leading to surgeries, hospitalization, and increased medical complications and risks. Additionally, the increased risk of respiratory illness in individuals over 65 years of age may be partially explained by the ageing-related weakening of the diaphragm muscle resulting in non-productive coughs and more severe respiratory illnesses (8). With the ever-increasing population of elderly and the predicted strain on the healthcare system (9), it is crucial we understand the molecular mechanisms responsible for age-related diseases like sarcopenia so that we can develop more effective therapies and prevention methods.

Sarcopenic patients exhibit a loss of myofibrils, which are comprised of thin and thick filaments. The thin filaments are predominantly composed of filamentous actin while thick filaments are predominantly composed of myosin (10). There is a superfamily of myosins composed of at least 30 classes of myosins, but all myosins consist of 3 regions:

a “head”, a “neck”, and a “tail” (11). The head is a complex structure that converts the energy of ATP hydrolysis to the mechanical work of binding and moving along F-actin tracks (11). The chaperone UNC-45 is required to fold the myosin head initially after translation and, likely, to re-fold the myosin head after stress results in unfolding (12-15). UNC-45 may also be crucial in mature muscle because of the physical stress muscle cells undergo throughout life and the relatively slow turnover rate of myosin in established thick filaments (16). UNC-45, which is conserved across all eukaryotes, was first identified in *Caenorhabditis elegans* and named for the uncoordinated (impaired movement) phenotype observed in mutant animals (17). Mis-regulation of UNC-45 is associated with several diseases including myopathies, cardiomyopathies, cataracts, and cancer metastasis (18-24). UNC-45 is comprised of a C-terminal UCS domain responsible for binding myosin, an N-terminal tetratricopeptide repeat (TPR) domain that interacts with the heat shock co-chaperone protein HSP-90 (15), and a central domain that acts as an inhibitor of the myosin power stroke (25). These authors put forth the following model: Under normal conditions, the UCS domain of UNC-45 is bound to the myosin head and the TPR domain is bound to HSP-90. Under stress conditions, HSP-90 detaches from the TPR domain, causing a conformational change in UNC-45 that allows the Central domain to bind to the myosin neck resulting in inhibition of the myosin power stroke while the UCS domain re-folds the myosin head. After refolding of the myosin head, HSP-90 then rebinds the TPR domain, causing the Central domain to release the myosin neck, allowing movement of the myosin motor (25).

*C. elegans* is an excellent genetic model organism to study sarcomere assembly, maintenance and regulation (26), and conserved mechanisms of aging (27). The *C.*

*C. elegans* model provides the shortest lifespan and largest possible sample size among the models used to study sarcopenia. Their short lifespan (average 18-21 days) makes them particularly convenient for aging studies. Muscle function is easy to monitor in worms since they require functioning body wall muscles for locomotion. Additionally, nematode muscle does not contain stem cells and thus provides an opportunity to investigate how the assembled muscle contractile apparatus is maintained and functions during aging in the absence of regeneration. Monica Driscoll's lab was the first to report that *C. elegans* undergo an age-dependent decline in whole animal locomotion and deterioration of the muscle myofilament lattice and thus *C. elegans* is a good model for sarcopenia (28).

Here we have verified and expanded upon evidence that *C. elegans* develop sarcopenia as they age. We observe early onset of sarcopenia when UNC-45 is perturbed at the beginning of adulthood in a temperature sensitive mutant, providing evidence that UNC-45 is important during adulthood and that UNC-45 may play a role in sarcopenia pathology. We have characterized the change in mRNA and protein levels of UNC-45, its co-chaperone HSP-90, and its myosin clients during aging. Additionally, we have identified a new UNC-45 post translational modification that may play a role in its protein regulation and found evidence that HSP-90 stabilizes UNC-45.

## **Results:**

*C. elegans* develop sarcopenia and show decreased numbers of assembled thick filaments during aging:

We have verified and extended the results reported in Herndon et al. (2002) by performing immunostaining on wild type worms using an antibody to MHC A (one of the

myosin heavy chain isoforms in body wall muscle), and also examined earlier and additional time points. We observe that the number of A-bands, or assembled thick filaments, declines with age (Figure 3.1A-F). We began counting A-bands once maturity was reached at day 1 of adulthood and continued until the majority of animals reached a sarcopenic state at day 16. A significant loss of A-band number can be seen by day 8 of adulthood. Elderly animals also show a decline in thick filament organization at days 12 and 16 (Figure 3.1 D&E), similar to *unc-45* missense mutants (29). These results support the notion that *C. elegans* experience a loss of muscle mass with age, beginning at the midpoint of life and continuing until death, analogous to humans. We also measured whole animal locomotion or motility using a crawling assay and found that motility declines by day 4 of adulthood and continues to decline until there is almost no significant mobility by day 16 (Figure 3.1G). Interestingly, muscle function appears to decline before muscle mass loss is seen. This may suggest that some thick filaments are rendered less functional before they are lost and/or, very likely, that loss of muscle mass is not the sole contributor to loss of muscle function with age.

UNC-45 has a role in maintaining assembled thick filaments and nematode motility during adulthood:

To assess the importance of UNC-45 within *C. elegans* adult muscle we utilized the canonical *unc-45(e286)* temperature sensitive mutant. This strain is relatively normal when grown at 15°C, but has a mutation (L822F) within the UCS domain of UNC-45 that renders it non-functional/reduced when grown at 25°C. When allowed to develop at 25°C, this strain has lower steady state levels of both thick filament isoforms of myosin heavy chain, MHC A and MHC B, and fewer assembled thick filaments (29, 30), similar to aged

worms. We have shown, using our own antibody to UNC-45, that this mutant does in fact have significantly reduced levels of UNC-45 when grown at 25°C (31). For our purposes, we allowed the animals to develop normally at 15°C and transferred them to the restrictive temperature of 25°C only after muscle maturity had been reached (referred to as day 0 of adulthood). We observed a decline in assembled thick filaments (A-band number) beginning at day 4 of adulthood assessed by anti-MHC A staining (Figure 3.2A and Figure S3.1), as opposed to day 8 in the wildtype strain (Figure 3.1F). The animals grown at the restrictive temperature also show a decline in motility at day 1 of adulthood (Figure 3.2B), as opposed to day 4 in both the wildtype (Figure 3.1G) and the mutant grown at the permissive temperature (Figure 3.2B). As shown in Figure S3.2, the growth of wild type animals at 25° does not significantly affect worm locomotion compared to worms grown at 15° when sampled at numerous time points from day 1 to day 16 of adulthood. Within 24 hours of being transitioned to the restrictive temperature perturbed thick filaments can be seen via immunostaining of MHC A in *unc-45(e286)*(Figure 3.2C-J). We would describe this phenotype as an early onset of sarcopenia in *unc-45(e286)* mutant animals. This provides evidence that UNC-45 is essential to muscles during adulthood.

As adults age, there is a sequential decline of HSP-90, UNC-45 and myosin:

Using quantitative western blotting we have found that at day 3 of adulthood, there is a drop in the level of HSP-90 protein (Figure 3.3A). At day 4 of adulthood there is a drop in the level of UNC-45 protein (Figure 3.3B). By day 8 of adulthood, there is a drop in the level of MHC B protein, the major client of UNC-45 (Figure 3.3C). The level of MHC A protein shows a more gradual decline beginning at day 1 (Figure 3.3D). Although the decline in the level of HSP-90 protein at day 3, may be

causally related to the decline in *hsp-90* mRNA at day 2 (Figure 3.3E), the decline in UNC-45 and MHC-B proteins may be more related to the degradation of UNC-45 and MHC B proteins, rather than the declines in their mRNAs: There is a significant decline in *unc-45* mRNA by day 2 (Figure 3.3F), and a significant decline in *unc-54* (encodes MHC B) mRNA by day 1 (Figure 3.3G), and the levels of these mRNAs remain low throughout the remainder of adulthood. It is noteworthy that the loss of UNC-45 protein at day 4 (Figure 3.3B) correlates with the onset of reduced whole worm locomotion at day 4 (Figure 3.1G).

#### UNC-45 phosphorylation increases with aging:

Using gradient SDS-PAGE gels, we noticed that during adult aging, as the protein band corresponding to UNC-45 (107 kDa) declines, a higher molecular weight band appears and increases (Figure 3.4). We suspect that this higher molecular weight UNC-45 protein band is the result of post-translational modification. In an attempt to identify this post translational modification, we ran protein lysates from different aged wildtype worms on a SuperSep™ Phos-tag™ electrophoresis gel, which separates proteins based on both molecular weight and phosphorylation status (more phosphate groups cause the protein to run slower through a gel containing the Phos-tag organic molecule which binds to phosphates, including phosphorylated proteins). Using this gel followed by western blotting and reaction with anti-UNC-45 antibodies shows that with age there is an increase in UNC-45 protein bands that run more slowly in the gel beginning at day 3 of adulthood, consistent with an increase in the phosphorylation of UNC-45 with aging (Figure 3.5A). Further evidence that these slower running UNC-45 bands are phosphorylated was provided by showing that they are eliminated upon treatment of the protein lysates with lambda phosphatase (Figure 3.5B).

We also immunoprecipitated endogenous UNC-45::mNeonGreen from a CRISPR generated strain using magnetic beads coupled to anti-mNeonGreen nanobodies, and reacted the eluted bound fraction with different anti-phospho-antibodies. We found increased phospho-serine/threonine and phospho-tyrosine at day 4 of adulthood, which is when we observe the dramatic decline of UNC-45. Based on the phospho-antibodies and the motifs they are reported to react with, UNC-45 is potentially being phosphorylated by multiple kinases, including PKC, AMPK, PKA, and AKT, which all recognize similar phosphorylation motifs. Additional phosphorylated protein(s) appear to be pulled down with the UNC-45::mNeonGreen immunoprecipitation and react with the phospho-antibodies (Figure 3.5C). The band running around 250kDa is likely one or more Myosin isoforms, and the band running around 60kDa could be HSP-70, which is known to complex with UNC-45(15, 32, 33). To identify the site or sites of phosphorylation on UNC-45, we immunoprecipitated UNC-45::mNeonGreen from a large quantity of worms of mixed developmental stages, including adults of different ages. This UNC-45::mNeonGreen was sent for mass spectrometry analysis. After cleavage with trypsin and GluC, peptides covering about 94% of the UNC-45 protein sequence were analyzed and the only site of phosphorylation was serine 111. As shown in Figure 3.6, this residue lies close to the C-terminus of the TPR domain and could conceivably interfere with binding to the HSP-90 C-terminus. Intriguingly, serine 111, though in a highly conserved region, is not a conserved residue. In fact, in *Drosophila* it is an aspartic acid and in humans and zebrafish it is a glutamic acid – both negatively charged residues. Perhaps the negative charge here is important and the residue evolved to have an inherent negative charge. We tried to immunoprecipitate UNC-45::mNeonGreen from day 4 adults,

but were not able to obtain enough protein for mass spectrometry analysis. Thus, a caveat is that we do not know whether S111 is the site that is phosphorylated during adult muscle aging.

A delayed onset of sarcopenia is associated with increased UNC-45 and HSP-90:

It is well-established that genetic disruption of the insulin-like signaling pathway results in increased longevity of *C. elegans* (34, 35). The *age-1(hx546)* strain has a mutation in the phosphatidylinositol 3-kinase catalytic subunit (PI3KCA) of the insulin like signaling pathway that results in animals living ~7-9 fold longer (36). We have found that these animals experience a delayed onset of sarcopenia, with the number of assembled thick filaments only marginally declining by day 16 of adulthood (Figure 3.7F). Intriguingly, although it has been reported that these animals move more in liquid media early in life (37), we found a slight decline in spontaneous movement on agar plates at days 1 and 4 (Figure 3.7G). This does not necessarily correlate to muscle health as it could be due to uncharacterized neuronal or metabolic changes caused by this mutation. When stimulated by poking with a toothpick, the animals display normal, healthy sinusoidal movement on the agar surface until at least day 8 of adulthood. These mutant animals not only retain their HSP-90, UNC-45 and MHC B protein levels longer than wildtype, but the steady state levels of these proteins continue to increase past day 0 of adulthood (Figure 3.8A-C). This is not surprising since we observe that the steady state transcripts of *hsp-90* and *unc-54* continue to increase past day 0 of adulthood, spiking around days 2 and 3, as if the animals are still developing. In contrast, we don't see much change in *unc-45* transcript levels between wildtype and the long-lived animals. We once

again found that the decline in UNC-45 protein occurs independently of its transcript and after the decline in HSP-90 protein.

The interaction of HSP-90 with UNC-45 may stabilize UNC-45:

The TPR domain of UNC-45 binds to HSP-90 (Barral et al. 2002). Intriguingly, we have found that the *hsp-90(p673)* temperature sensitive mutant has significantly less UNC-45 protein when grown at the restrictive temperature of 25°C (Figure 3.9B and D). This loss of protein appears to be independent of steady state mRNA since *unc-45* mRNA increases at the restrictive temperature of 25°C (Figure 3.9E). This also provides evidence that *unc-45* transcription may be sensitive to heat stress, and potentially other types of stress. The *hsp-90(p673)* mutation (E292K) is speculated to potentially disrupt interactions with some clients and/or co-chaperones(38). The mutation is located on the surface of the middle domain (MD) of the protein (Figure 3.9A), while the ATPase region is in the N-terminal domain (NTD)(39) and UNC-45 binds to the conserved MEEVD sequence towards the end of the C-terminal domain (CTD)(15). Because this mutant HSP-90 results in such a dramatic loss of UNC-45 protein, we speculate that this mutation is somehow affecting HSP-90's ability to interact with UNC-45. However, since the known binding site of HSP-90 in its C-terminus (CTD) to UNC-45 is so distant from the mutation site in its MD, perhaps the mutation causes some conformational change that is transmitted from the MD to the CTD. The *unc-45(e286); hsp-90(p673)* double mutant displays reduced motility to that of *unc-45(e286)* alone at the permissive temperature of 15°C (Figure 3.9F). This would suggest that the additional mutation is enough to exacerbate the Unc phenotype even at the permissive temperature. Above 15°C, all three strains exhibit little to no crawling motility.

**Discussion:**

With conserved pathways, a short lifespan, large sample sizes, and a plethora of easy genetic techniques available, *C. elegans* have become a vital model organism in the pursuit of studying the molecular mechanisms responsible for many aging associated pathologies, including sarcopenia. With age, we begin to lose our ability to generate new muscle cells due to the dwindling population of satellite stem cells. This makes the maintenance of already existing muscle fibers key to maintaining muscle health with age. With this in mind, the nematode becomes an even more intriguing model to use for sarcopenia studies since they do not have satellite cells to replenish their muscle cells. In this study we have used *C. elegans* to identify changes in the myosin head chaperone UNC-45 during aging that may prove crucial to the decline in muscle maintenance with age.

Previously, UNC-45 had only been shown to be crucial during muscle development, but not during adulthood (17). However, since then more evidence has emerged that suggests that myosin may require its chaperone UNC-45 to maintain its integrity in the face of damage that accumulates with age. We now know that sarcomere proteins assembled into the thick filament have a low protein turnover rate(16) and it has been shown that the reduction in myofibrillar synthesis rate in old (61-74yr) vs. young (22-31yr) human muscle is not caused by reduced myosin mRNA(40). This suggests that the myosin assembled into thick filaments requires a mechanism to retain its structure after denaturing events (chemical, thermal, and physical stress) that occur within the muscle. Barral et al. have shown that UNC-45 prevents thermal aggregation of myosin heads in vitro (15). Etard et al. have shown that Unc-45b, the skeletal muscle specific isoform,

localizes to the Z-discs normally and moves to thick filaments during stress (cold and heat shock, chemical, and physical) in zebrafish skeletal muscle (13). We find that perturbation of UNC-45 during adulthood is enough to cause an early onset of sarcopenia-like pathology. Thus, our results demonstrate that UNC-45 is crucial to maintaining muscle health specifically during adulthood.

We then sought to characterize the changes in total steady state protein and transcript levels of UNC-45, its co-chaperone HSP-90, and its clients within body wall muscle, MHC A and MHC B (Figure 3.3). We found that *hsp-90* transcript declines at day 2 of adulthood, directly before the decline in HSP-90 protein. The loss of HSP-90 at day 3 directly precedes a loss of UNC-45 protein at day 4 of adulthood. Then, there is a major decline in MHC B, the main client of UNC-45 and more abundant body wall muscle myosin isoform, at day 8 of adulthood. We theorize that the decline in UNC-45 protein is due primarily to protein degradation. The decline in UNC-45 that we observe during adulthood may be due to increased ubiquitination followed by proteasomal degradation. It has been reported that *C. elegans* UNC-45 is polyubiquitinated by CHN-1 and CDC-48 resulting in degradation by the 26S proteasome (41). One study found that aged sarcopenic rat skeletal muscle contains higher levels of CHIP and p97, which are the mammalian homologs of CHN-1 and CDC-48(42). The authors found no significant change in *unc-45b* mRNA between young adult and aged muscle samples but found that Unc-45B protein was decreased in the aged muscle compared to young adult muscle(42). We observe what appears to be an increase in post-translational modification of UNC-45 with age (Figure 3.4) and have identified that one of these modifications is phosphorylation (Figure 3.5). Phosphorylation may be related to the already known ubiquitylation of UNC-

45 and its degradation by the proteasome (19). Through mass spectrometry, we have identified serine 111 as a site of phosphorylation. Adding a bulky negative charged molecule added to this region of UNC-45's TPR domain could be interfering with the interaction between UNC-45 and HSP-90. Though in a conserved region, serine 111 is not a conserved residue. In humans this residue is actually a glutamic acid, which would act like a phosphomimetic. This raises the question of why this residue evolved from being phosphorylated to being constitutively negatively charged. Perhaps this site is crucial to the regulation of UNC-45 protein levels within cells. Whether it interferes with HSP-90 binding or leads to degradation of UNC-45 remains unexplored.

The *age-1(hx546)* longevity mutant shows a delay in the loss of assembled thick filaments but not spontaneous crawling motility (Figure 3.7). A major characteristic of aging muscle and sarcopenia pathology is the loss of muscle mass, which does not begin to occur in these animals until day 16 of adulthood (day 8 in wildtype). The amount of UNC-45, HSP-90, and MHC B protein continues to increase in these animals well past day 0 of adulthood. *Hsp-90* and *unc-54* transcripts remain above wildtype levels while *unc-45* transcript has the same trend as in the wildtype animals. Since one theory behind the improved stress resistance of this strain is an increase in heat shock proteins and chaperones(43, 44), it is not surprising that the *hsp-90* mRNA is upregulated. However, we do still observe a decline in HSP-90 protein back to wildtype levels by day 8 of adulthood, which precedes a decline in UNC-45 protein back to wildtype levels by day 12 of adulthood. This delay in the loss of UNC-45 protein may be one of the mechanisms that allow this long-lived mutant to have an extended health span as well as lifespan.

Having increased UNC-45 to maintain myosin heads during aging would be beneficial to refold the myosin head after stress if there is also equivalent HSP-90 available to re-bind the TPR domain so as not to cause aberrant inhibition of the myosin power stroke. We find that in a loss of function *hsp-90* mutant there is significantly reduced UNC-45 protein, but not transcript. This suggests that interaction with HSP-90 is important for the protein stability of UNC-45 and that in the absence of HSP-90, UNC-45 is left more susceptible to degradation. This leads us to theorize that during aging there is a loss of HSP-90, which leaves regions of UNC-45 more open to post translational modifications, like phosphorylation, and leads to increased degradation of UNC-45. At least for *C. elegans*, the crystal structure of UNC-45 (Gazda et al., 2013) shows that it forms linear multimers in which the length of the repeating unit is similar to the repeating unit in the staggered display of pairs of myosin heads on the surface of thick filaments. In addition, antibodies to UNC-45 co-localize with MHC B myosin on the major portions of the thick filament in already assembled sarcomeres of adult muscle (Ao and Pilgrim, 2000; Gazda et al., 2013). Thus, in adult muscle, UNC-45 is positioned on the thick filament to re-fold any myosin heads that are damaged by thermal or chemical stress. Therefore, our model is that during adult aging, the loss of HSP-90, followed by the loss of the myosin head chaperone UNC-45, leads to fewer myosin heads being re-folded, and these myosin molecules and even thick filaments are removed from the sarcomere, forming aggregates and/or being degraded. Because of the low level of myosin transcripts and translation, there is not enough new myosin protein available to replenish the myosin within existing thick filaments, or to form new thick filaments. This results in an overall decline in thick filament number, sarcomere size and number, and muscle function.

As we age, we experience a loss of our satellite cells (muscle stem cells) and the maintenance of our existing muscle cells becomes crucial to maintaining our mobility. UNC-45 is the conserved myosin head chaperone responsible for the initial folding and assemblage of myosin heads into the thick filament, and *most likely* refolding the myosin head after stress causes it to unfold. Humans have two UNC-45 homologs, A and B. UNC45-A is expressed ubiquitously and UNC-45B is expressed primarily in striated muscles – skeletal and cardiac. The results presented here suggest that increased expression and/or increased activity of UNC45B might be a strategy for prevention and treatment of sarcopenia, and even age-associated heart failure.

## **Materials and Methods:**

### *C. elegans* Strains

Standard growth conditions for *C. elegans* were used (45). Wildtype Bristol N2, *age-1(hx546)*, *GB319*, and *GB350* were grown at 20°C. As described in the above results, temperature sensitive mutants *unc-45(e286)* and *hsp-90(p673)* were grown at 15°C, 20°C, or 25°C. Adult worms were separated from their progeny daily by allowing the adults to sink in M9 buffer in glass tubes, removing the supernatant containing the L1s, and washing several times before returning to NGM plates. The double mutant *unc-45(e286); hsp-90(p673)* was generated by genetic crossing. *GB319* is the 2X outcrossed derivative of *PHX789 (unc-45(syb789))* which is a CRISPR-generated strain that expresses UNC-45-mNeonGreen and was described previously (31). The strain, *PHX501 (hsp-90(syb501))*, is a CRISPR-generated strain which expresses HSP-90 with a C-terminal mKate2 tag. *PHX501* was created by SunyBiotech

(<http://www.sunybiotech.com>). PHX501 was outcrossed 2X to wild type to generate strain GB350.

#### Immunostaining in adult body-wall muscle

Adult nematodes were fixed and immunostained according to the method described by Nonet et al. and described in further detail by Wilson et al. (46, 47). The following primary antibodies were used: anti-MHC A at 1:200 (mouse monoclonal 5-6; Miller et al., 1983), anti-MHC B at 1:200 (mouse monoclonal 5-8 (30)), and anti-UNC-95 at 1:100 (rabbit polyclonal Benian-13 (48)). Secondary antibodies, used at 1:200 dilution, included anti-rabbit Alexa 488 (Invitrogen, Thermo Fisher Scientific) and anti-mouse Alexa 594 (Invitrogen). Images were captured at room temperature with a Zeiss confocal system (LSM510) equipped with an Axiovert 100M microscope and an Apochromat x63/1.4 numerical aperture oil immersion objective in x2.5 zoom mode. The color balances of the images were adjusted by using Photoshop (Adobe, San Jose, CA). A minimum of 10 animals were used for A-band counting.

#### Motility crawling assays

Adult worms were collected at different ages using M9 buffer containing 0.2g/L gelatin. They were transferred to a 1.5mL microcentrifuge tube, allowed to settle to the bottom, and washed 3X with M9 buffer containing 0.2g/L gelatin. 5 $\mu$ L of worm suspension was added to the center of a 6cm unseeded NGM plate. Worms were allowed to adapt for 5 minutes before a video recording of their crawling was made using a dissecting stereoscopic microscope fitted with a CMOS camera (Thorlabs). Several 10 second videos (a minimum of 15, but up to 30, with less videos needed for paralyzed animals) were recorded for each sample and analyzed by Image J FIJI WrmTracker software to

obtain body bends per second (BBPS). Statistical significance was determined using a student's T-test.

### Quantitative Real-Time PCR

Worms from two 10cm NGM plates were collected using M9 buffer and frozen as a dry packed worm pellet. Lysis buffer from the Qiagen RNeasy Plus Mini Kit (cat. 74134) was added, the sample was freeze-thawed in liquid nitrogen five times to crack the worm cuticle, and then vortexed with MagnaLyser beads (Roche) for 1 minute. The samples were centrifuged, and the supernatant was used to extract RNA with the Qiagen RNeasy Plus Mini Kit. The NCBI primer designing tool (<https://www.ncbi.nlm.nih.gov/tools/primer-blast/>) was used to create primer pairs specific for each gene of interest that also had at least one intron separating the primer pair (see Table S1). 1µg of cDNA was synthesized from the RNA using BioRad iScript Reverse Transcription Supermix (cat. 1708840). The cDNA was then diluted 1/10 in nuclease free water and 2.5µL was used per reaction with 10µL of qRT-PCR master mix (1.25µL of each primer, 1.25µL of nuclease free water, and 6.25 µL of SybrGreen supermix (Biorad cat. 1708880)). A BioRad CFX Real-Time PCR thermal cycler was used. Fold change was determined using the  $2^{-\Delta\Delta Ct}$  method (49). *ges-1* and *gapdh-2* were used for normalization. Statistical significance was determined using a student's T-test.

### Production and purification of antibodies

The generation of rabbit polyclonal antibodies to the C-terminal 120 residues of UNC-45 was described previously (31). A 149 residue region (aa 553-702) at the C-terminus of HSP-90 ("HSP-90 antigen")(Figure S4A) was expressed in *E. coli* as a GST fusion protein and sent to Noble Life Sciences for antibody production in rats. After approx. 3 months,

we received the antisera, and affinity purified anti-HSP-90 antibodies by use of an MBP-HSP-90 antigen coupled to Affigel matrix (BioRad), using a procedure previously published (50). Both antibodies work well in western blots, detecting a polypeptide of expected size for UNC-45 (107 kDa) and HSP-90 (80 kDa), and no detectable extraneous bands at a 1:5,000 or 1:2,500 dilution, respectively. In addition, we demonstrated that anti-HSP-90 antibodies detect a protein of expected size of approximately 100 kDa from a lysate prepared from animals that express HSP-90-mKate2 (Figure S3.3B).

#### Western blots and quantitation of protein levels

We used the procedure of Hannak et al. (51) to prepare total protein lysates from wild-type, *hsp-90(p673)*, and *age-1(hx546)* strains. When comparing wild-type and mutant strains, we loaded approximately equal amounts of protein extract estimated by finding volumes of extracts that would give equal intensity of banding after Coomassie staining. We used quantities of extracts and dilutions of antibodies that would place us into the linear range of detection by ECL and exposure to film. The following antibodies and dilutions were used: rabbit anti-UNC-45(31) at 1:5,000; rat anti-HSP-90 at 1:2,500; mouse monoclonal 5-8 (30) for MHC B at 1:40,000; mouse monoclonal 5-6 ascites (30) for MHC A at 1:5,000; Phospho-(Ser/Thr) Kinase Substrate Antibody Sampler Kit (cell signaling) at 1:1,000; Phospho-Tyrosine (4G10, cell signaling) mouse mAb at 1:1,1000. The quantitation of steady-state levels of protein was performed as described in Miller et al. (2009)(52). The relative amount of each of these muscle proteins in each lane was normalized to the amount of Histone H3 detected using anti-Histone H3 (abcam, cat. ab1791) at 1:40,000 dilution. The amount of Histone H3 at different ages was compared to Ponceau S staining to ensure no significant changes throughout aging (Figure S3.5).

BioRad precast Mini-PROTEAN TGX Stain-Free Gels were used (4-20%, cat. 4568093, 12%, cat. 4568041). The BioRad Precision Plus Protein™ Kaleidoscope™ Prestained Protein Standards (cat. 1610375) were used on all standard SDS-PAGE gels.

### Immunoprecipitation

Worms were collected from 2 to 4 10cm NGM plates with M9 and frozen. 500µL – 1mL of IP buffer (25mM Tris pH 7.5, 150mM NaCl, 1mM EDTA, 0.5% NP40, 5% glycerol, 1X Halt protease & phosphatase inhibitor cocktail (ThermoFisher)) was added to each sample. They were then freeze-thawed in liquid nitrogen 3-5X to crack the cuticle, added to MagnaLyser beads, and vortexed for 1 minute. The samples were centrifuged, and the lysate supernatant was added to 25µL of mNeonGreen-Trap Magnetic Agarose suspension (cat. no. ntma-10, Chromotek, Inc.) in which nanobodies to mNeonGreen had been coupled to magnetic agarose beads. They were then incubated on a spinning wheel at 4°C for 1 hour, washed 3X with IP buffer, and eluted with 2X Laemmli buffer with βME by boiling for 5 minutes at 95°C.

### Phosphorylation analysis

SuperSep™ phos-tag™ SDS gels (Fuji Film 198-17981, 195-17991) were used per product instructions. Samples were prepared using the IP method described above and cleaned with Amicon centrifugal filters. The WIDE-VIEW™ Prestained Protein Size Marker III (Fuji Film, 230-02461) was used with all SuperSep™ phos-tag™ SDS gels. Lambda protein phosphatase (New England BioLabs, P0753S) was used per product instructions.

### Mass Spectrometry Analysis

Samples were immunoprecipitated from 3 generous scoops of worm powder (extensively ground in a mortar and pestle in liquid nitrogen) made from a mixed population of UNC-45::mNeonGreen worms using the above immunoprecipitation method. Initially, the elution was run on a 4-20% SDS-PAGE, and the resulting bands were excised and sent to the mass spectrometry facility at the University of Texas Medical Branch (Galveston, Texas), where they were analyzed by Dr. Aaron Bailey. Because of the purity of the initial samples, we then sent Dr. Bailey the in solution elution to analyze.

### Homology modeling of nematode HSP-90

For HSP-90 protein structure modeling, CLUSTALW version 1.2.2 (<https://www.ebi.ac.uk/Tools/msa/clustalw2/>), SWISS-MODEL version July 2021 (<https://swissmodel.expasy.org/>;(53)) online tools were used. Human Hsp-90 (5fwm.pdb; (54)) was used as template crystal structure and the *C. elegans* HSP-90 sequence as the target. Molecular graphics were generated by using Chimera version 1.15 (<https://www.cgl.ucsf.edu/chimera/>; (55))

### Statistical Analysis

Unless otherwise stated, data are reported as mean  $\pm$  SE of the mean. Western Blot statistical analyses were made using GraphPad Prism Software (version 4.0). Comparisons of three or more means used one-way ANOVA and Bonferroni-adjusted unpaired t tests. Statistical significance was assigned as not-significant for  $p > 0.05$ , \* for  $p \leq 0.05$ , \*\* for  $p \leq 0.005$ , \*\*\* for  $p \leq 0.001$ , and \*\*\*\* for  $p \leq 0.0005$ .

## Figures and Figure Legends:

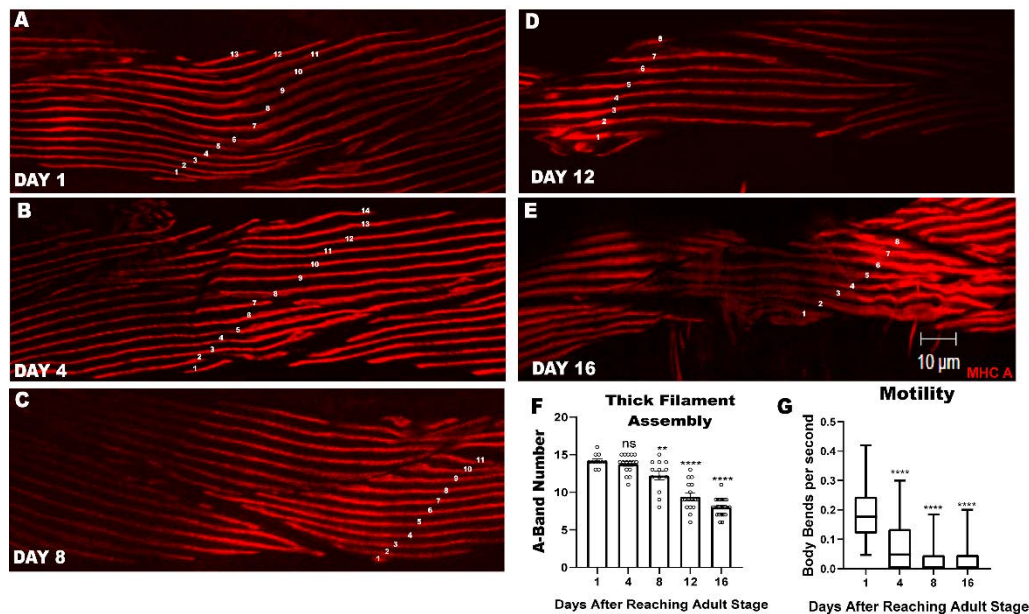


**Figure 3.1.** The number of assembled thick filaments (A-bands) and whole nematode motility decline with age A-E) are representative images of body wall muscle near the vulva immunostained with anti-MHC A at different ages of adulthood (day 1, 4, 8, 12, 16) with an A-band count depicted as white numbers along the A-bands. F) is the quantification of A-band number at different ages of adulthood. G) is the quantification of agar crawling motility assays at different ages of adulthood measured in body bends per second. Statistic depicted are that day of adulthood (4,8,12, or 16) compared to day 1 of adulthood. There was no statistical differences between days 8 and 16 motility. \*p-value <0.05, \*\*p-value < 0.005, \*\*\*p-value < 0.0005\*\*\*\* p-value < 0.0001.

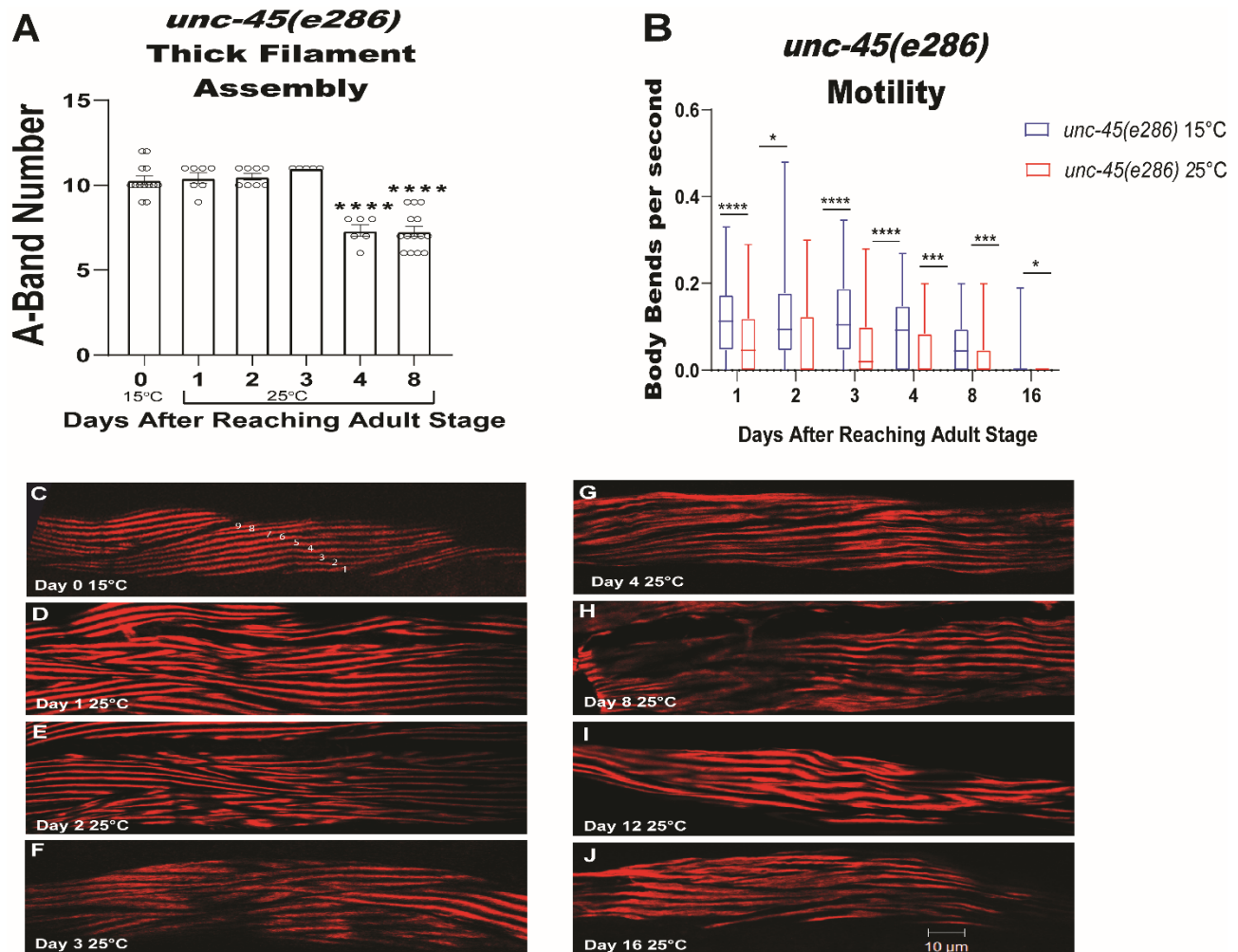


**Figure 3.2. UNC-45 has a role in maintaining assembled thick filaments (A-bands) and nematode motility during adulthood** The canonical *unc-45* temperature sensitive mutant, *e286*, was allowed to develop normally at the permissive temperature of 15°C and shifted to the restrictive temperature of 25°C on day 0 of adulthood. A) is the quantification of A-band number at different ages of adulthood. B) is the quantification of crawling motility assays at different adult ages at the permissive (15°C) and restrictive (25°C) temperatures. C) is a representative image of body wall muscle immunostained with anti-MHC A at day 0 of adulthood after the animal was allowed to develop at 15°C. D-J) are representative images of body wall muscle from animals grown at 25°C immunostained with anti-MHC A at different adult ages (day 1, 4, 8, 12, 16) with an A-band count depicted as white numbers for cells with parallel thick filaments (D-G). \*p-value < 0.05, \*\*p-value < 0.005, \*\*\*p-value < 0.0005 \*\*\*\* p-value < 0.0001.

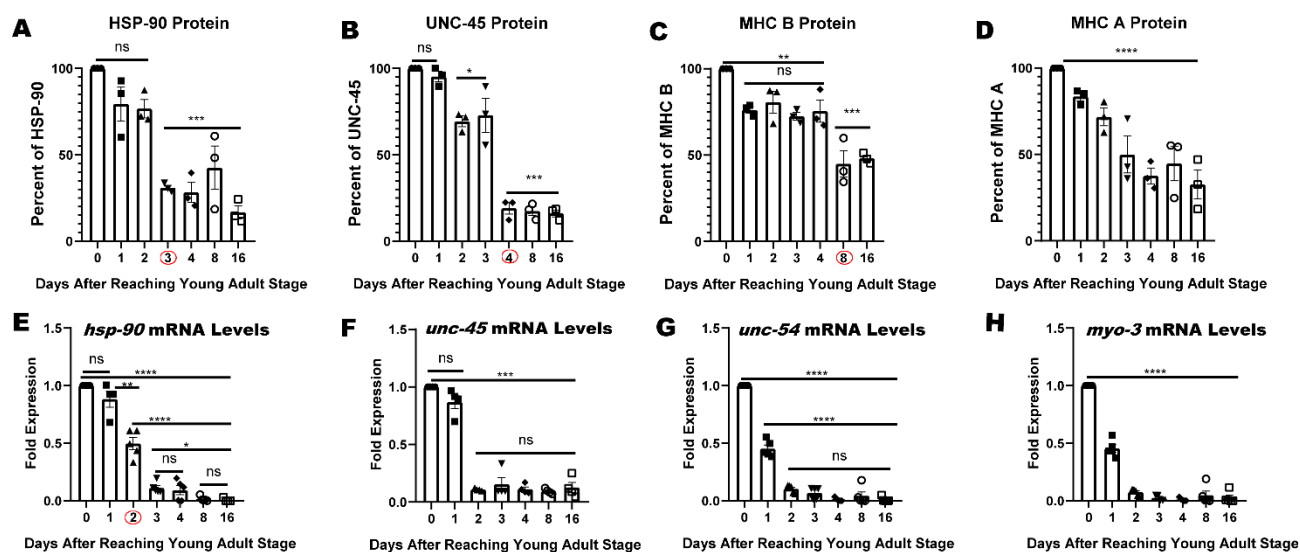


**Figure 3.3. The Sequential Decline of HSP-90, UNC-45, and Myosin with Age** (A-D) Graphical quantification of steady state protein levels of HSP-90, UNC-45, MHC B, and MHC A (myosin isoforms). Data are shown as a percentage of protein relative to Histone H3 protein. E-H) Steady state mRNA fold expression of *unc-45*, *hsp-90*, *unc-54* (MHC B), and *myo-3* (MHC A) during aging relative to *gpdh-2* (GAPDH). Days of significant protein or mRNA decline are circled with red circles. \* p-value < 0.05 \*\*p-value < 0.005, \*\*\*p-value < 0.0005 \*\*\*\* p-value < 0.0001

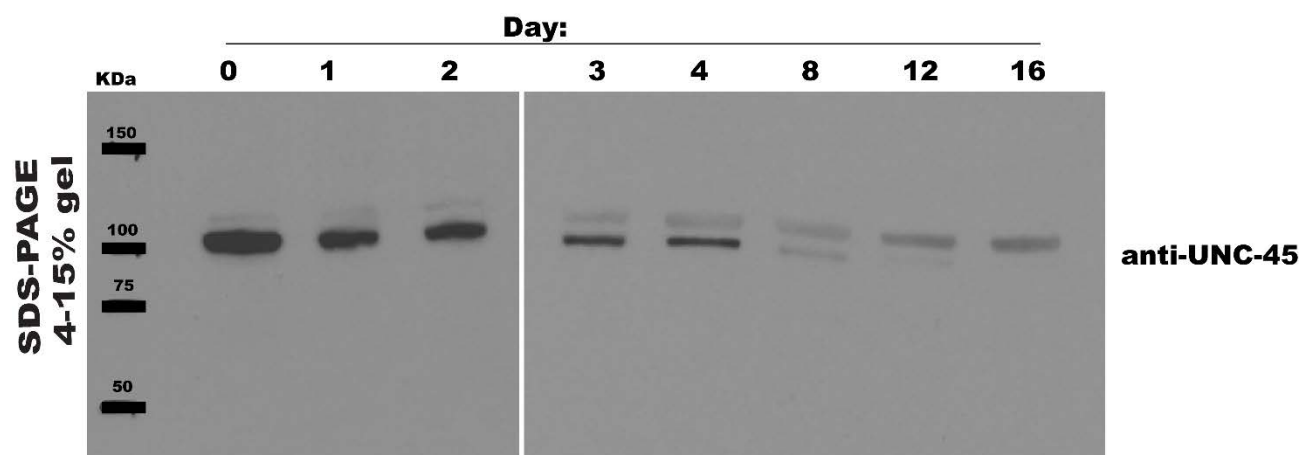


**Figure 3.4. A higher molecular weight UNC-45 band accumulates as the expected sized UNC-45 band declines with aging.** Protein lysate from day 0, 1, 2, 3, 4, 8, 12, and 16 old worms were run on a 4-20% gradient gel, transferred to a nitrocellulose blot, and reacted with the UNC-45 antibody to reveal a higher molecular weight UNC-45 band.

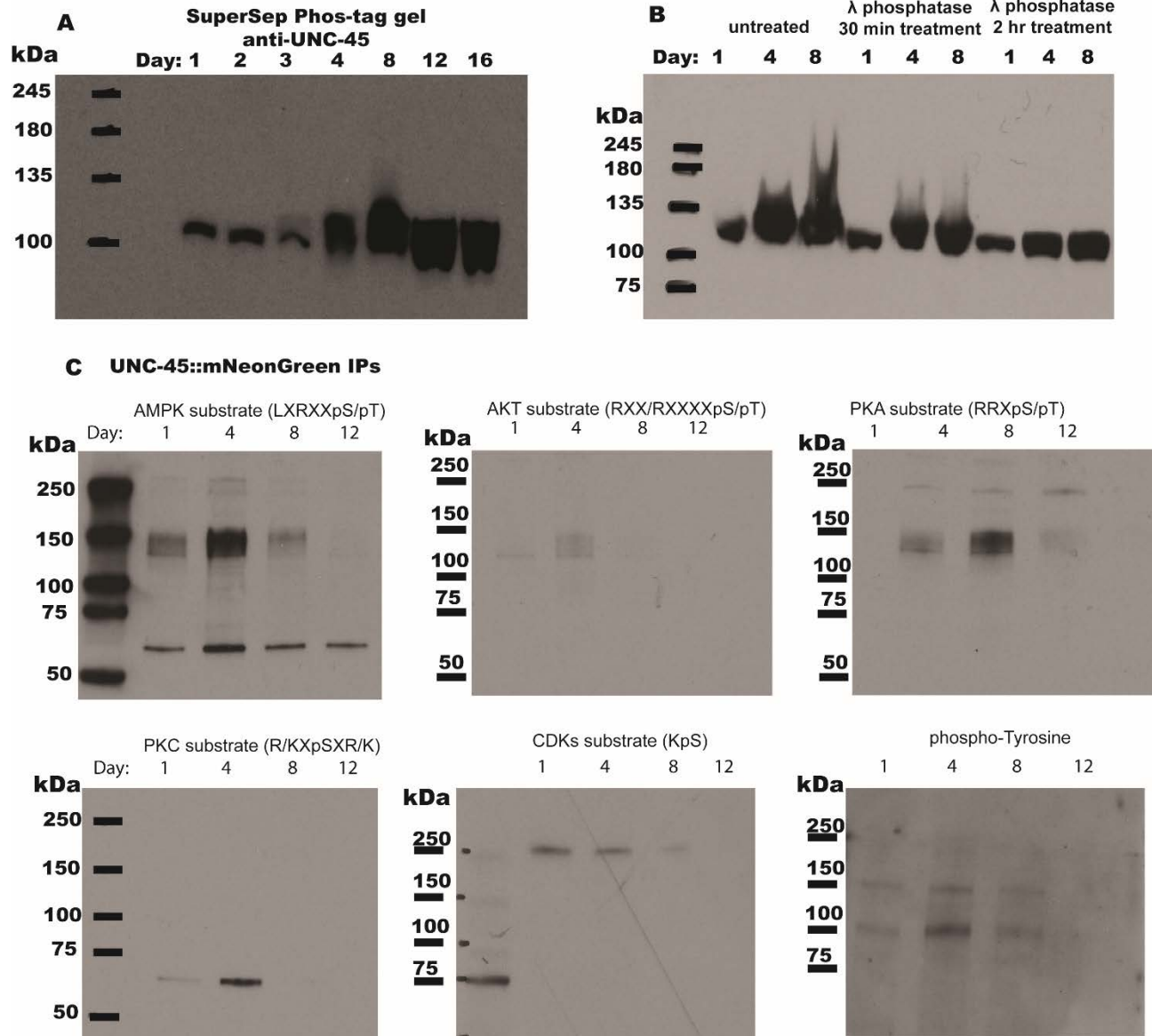


**Figure 3.5. UNC-45 phosphorylation increases with age.** A) Wildtype samples at different ages run on SuperSep Phos-tag gels and blotted with anti-UNC-45. The first blot (left) shows the change in phosphorylation of UNC-45 from day 1 to 16 in wildtype animals (7.5% gel). B) shows the putative phosphorylation pattern disappearing after treatment with  $\lambda$  phosphatase (12% gel). C) UNC-45 was immunoprecipitated from CRISPR generated *unc-45::mNeonGreen* worms using nanobodies to mNeonGreen pre-conjugated to magnetic beads and the elutions were run on SDS-PAGE and blotted with different anti-phospho antibodies specific for different phosphorylation motifs.

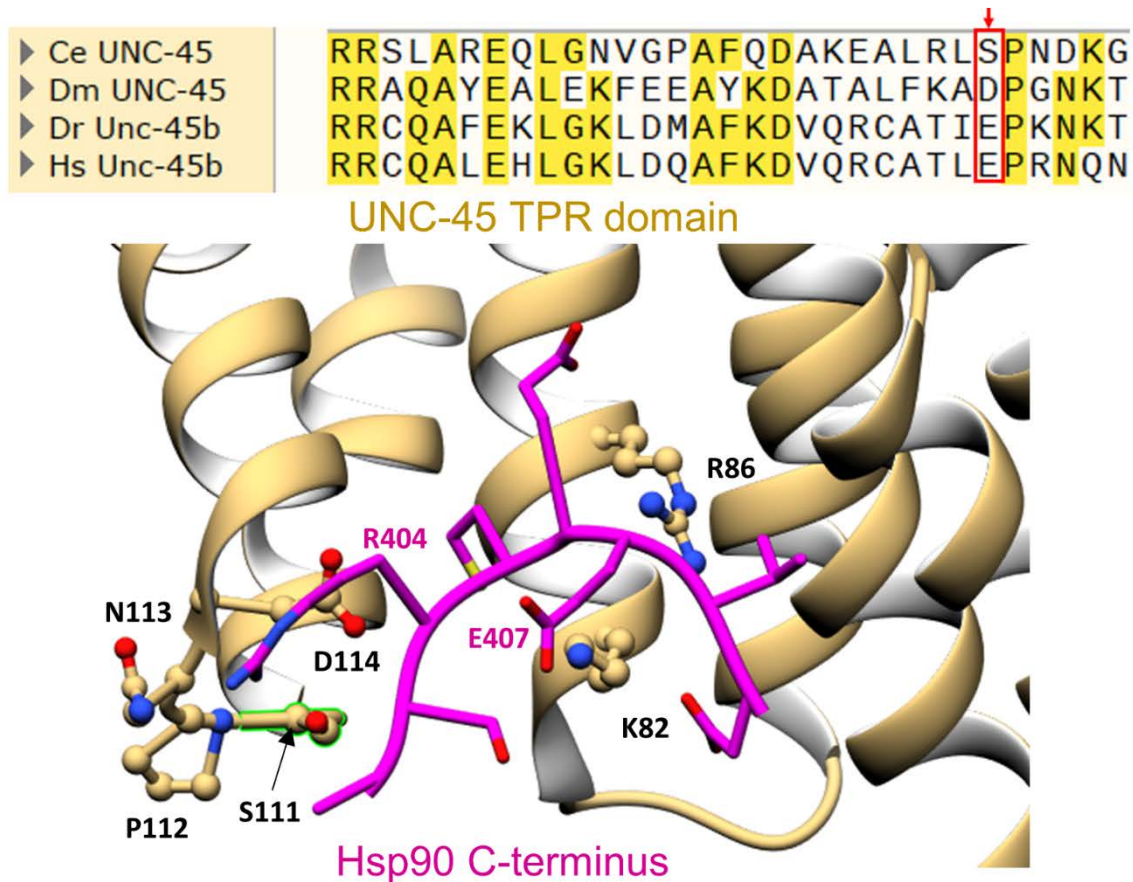


**Figure 3.6. UNC-45 is phosphorylated at Serine 111.** Sequence alignment of *C. elegans*, *Drosophila*, zebrafish, and human UNC-45/Unc-45b at the end of the TPR domain. The site of *C. elegans* phosphorylation, S111, is indicated with a red arrow and the sequence alignment is boxed in red. Below the alignment is the crystal structure of the UNC-45 – HSP-90 interaction site in *C. elegans* modified from Gazda et al. (56). The area of interaction closest to the phosphorylation site is circled in red.

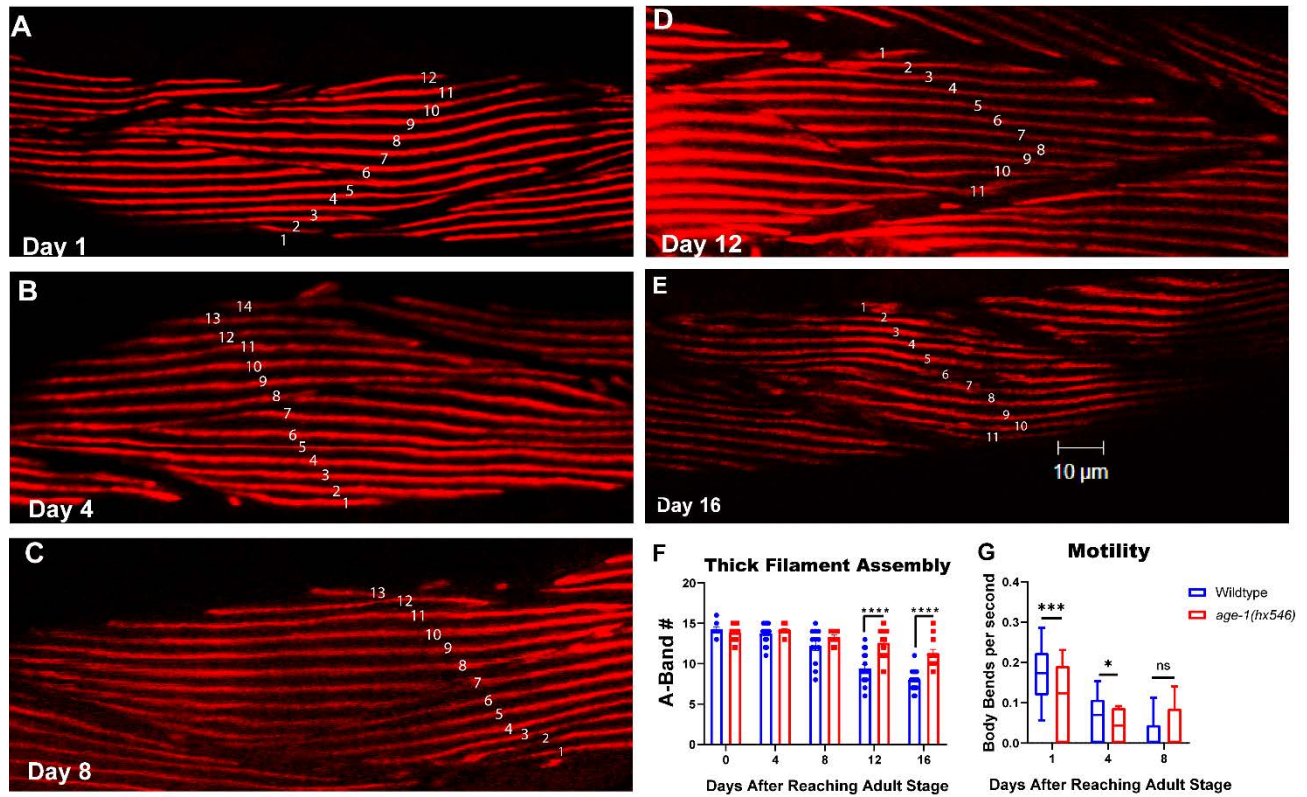


**Figure 3.7. The *age-1(hx546)* longevity mutant has a delayed loss of assembled thick filaments but not motility.** A-E) are representative images of body wall muscle near the vulva immunostained with anti-MHC A at different ages of adulthood (day 1, 4, 8, 12, 16) with an A-band count depicted as white numbers along the A-bands. F) is the quantification of A-band number at different ages of adulthood compared to N2 wildtype. G) is the quantification of agar crawling motility assays at different ages of adulthood measured in body bends per second compared to N2 wildtype. \* p-value < 0.05 \*\*p-value < 0.005, \*\*\*p-value < 0.0005\*\*\*\* p-value < 0.0001

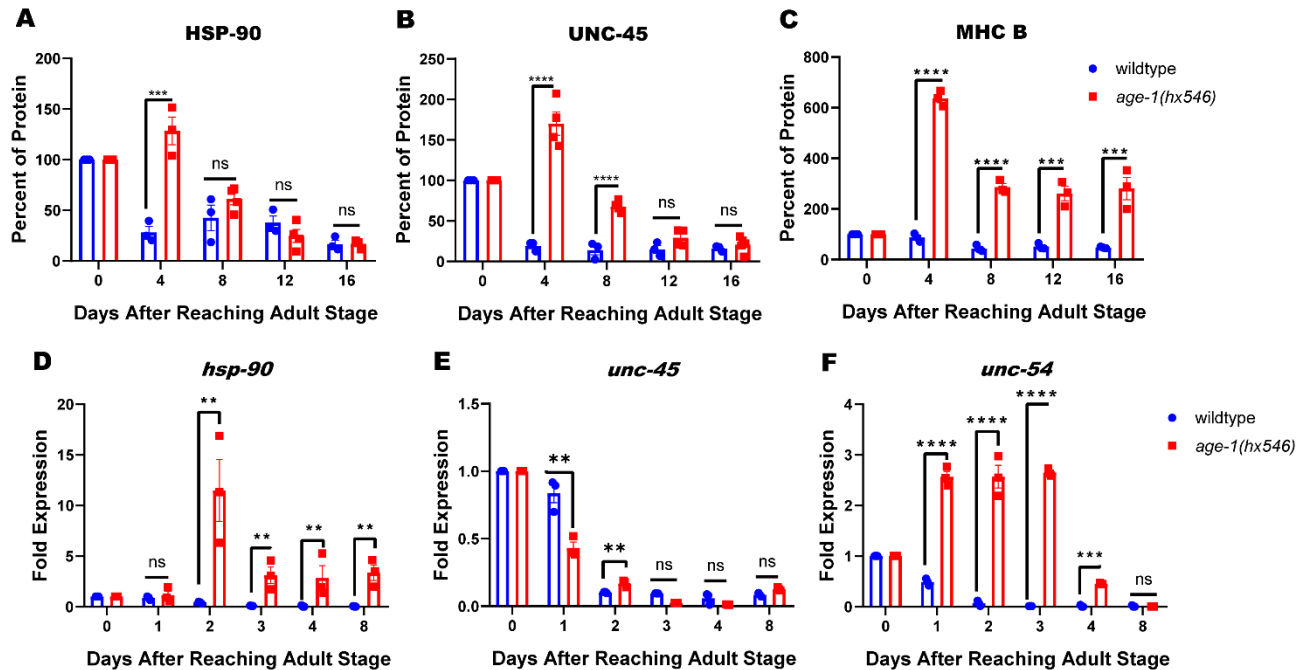


**Figure 3.8. The *age-1(hx546)* longevity mutant has increased levels of UNC-45, HSP-90, and myosin MHC-B.** A-C) Graphical quantification of steady state protein levels of HSP-90, UNC-45, and MHC B (major body wall myosin isoform). Data are shown as a percentage of protein relative to histone H3 protein. D-F) Steady state mRNA fold expression of *unc-45*, *hsp-90* and *unc-54* (MHC B) during aging relative to *gpdh-2* (GAPDH). \* p-value < 0.05 \*\*p-value < 0.005, \*\*\*p-value < 0.0005 \*\*\*\* p-value < 0.0001

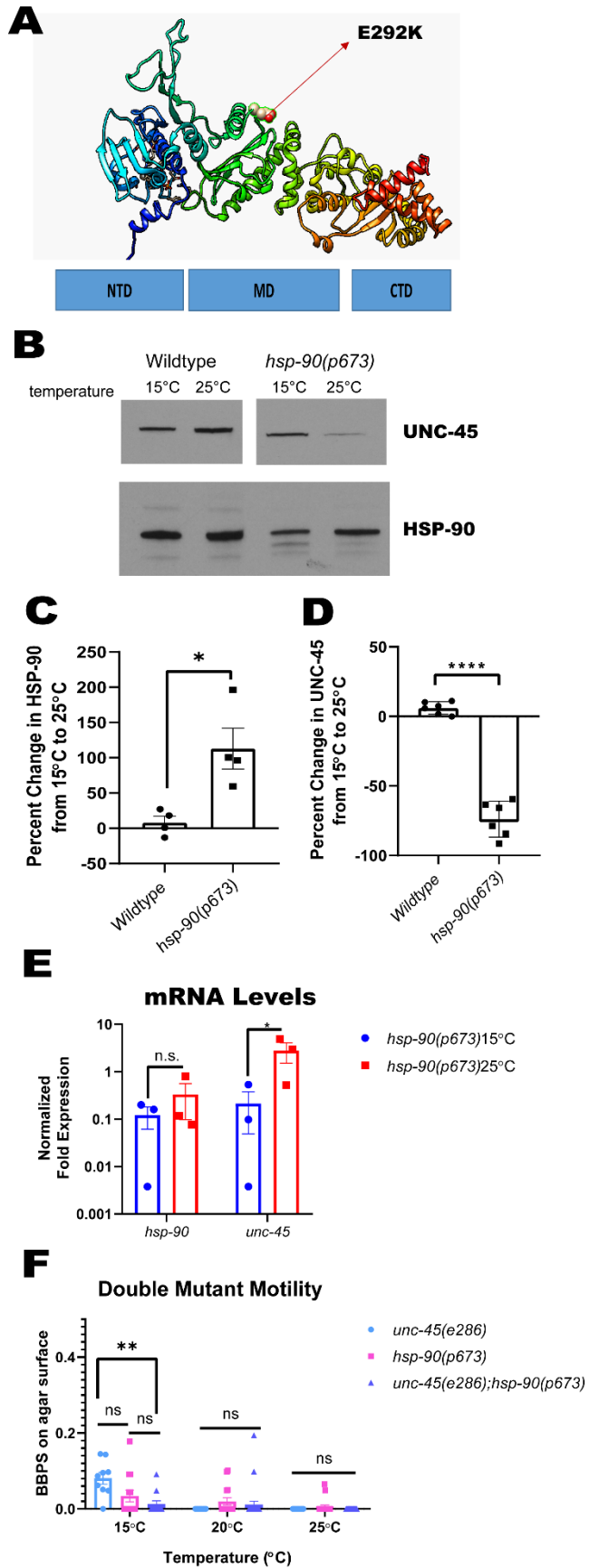


**Figure 3.9. *hsp-90* loss of function temperature sensitive mutant has decreased UNC-45 protein, but not transcript.** A) A homology model of the nematode HSP-90 protein showing the location of the E292K mutation in *hsp-90(p673)*. B) Western blot of UNC-45 and HSP-90 steady state protein levels. Histone H3 was used as the protein loading control. C and D) Quantification of UNC-45 and HSP-90 protein percent reduction at 25°C relative to 15°C from wild type and *hsp-90(p673)*. E) The relative fold expression of *unc-45* and *hsp-90* mRNA levels of the *hsp-90(p673)* strain grown at 15°C and 25°C. *ges-1* (gut esterase) was used to normalize expression. F) The quantification of agar crawling motility of the *unc-45(e286)*, *hsp-90(p673)*, and *unc-45(e286);hsp-90(p763)* measured in body bends per second mutant strains. \* p-value < 0.05 \*\*p-value < 0.005, \*\*\*p-value < 0.0005\*\*\*\* p-value < 0.0001.

### Supplemental Figures and Tables:

**Table S3.1. Primers**

gene	Forward primer	Reverse primer
<i>gapdh-2</i>	5' ACTCTTCACGATTGTCGCTTAGT 3'	5' AACCCACATACGGACGGTTG 3'
<i>ges-1</i>	5' GCTAAAACCGGAGTTCCCCAA 3'	5' CGTCCAGAAAGCGAGAGGT 3'
<i>hsp-90</i>	5' ATTCGCTACCAGGCACTCAC 3'	5' GACAAGATCGGCCTTGGTCA 3'
<i>unc-45</i>	5' TGCTGAAGGTGGAACGGTTT 3'	5' CGTATGCTCGTTGTCCAGGG 3'
<i>unc-54</i>	5' ATCCAAGCCATTCATGCCGA 3'	5' GGTC AACGTGCTGAGAGTGT 3'
<i>myo-3</i>	5' TCCAGAAGATGGATTTCGTCGC 3'	5' GCGGGTTCATCTCTTGGCAT 3'

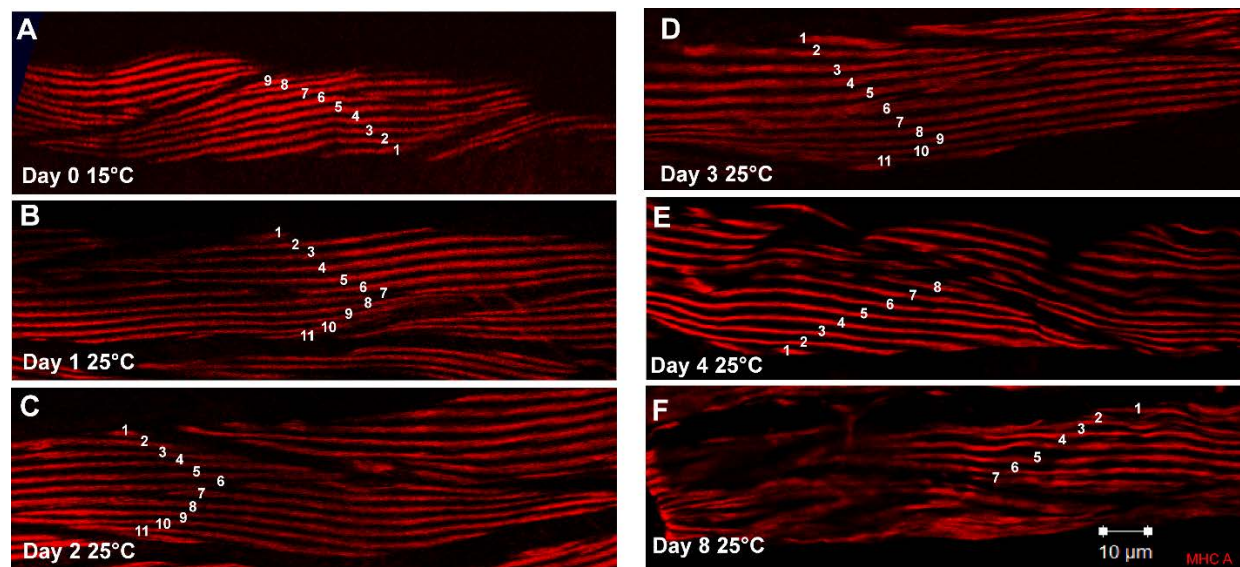


**Figure S3.1. *unc-45(e286)* representative images of MHC A immunostaining to count A-bands as an assessment of assembled thick filament quantity.** A-F) are representative images of body wall muscle near the vulva immunostained with anti-

MHC A at different ages of adulthood (day 0, 1, 2, 3, 4, 8) and grown at either 15°C (A) or 25°C (B-F) with an A-band count depicted as white numbers along the A-bands.

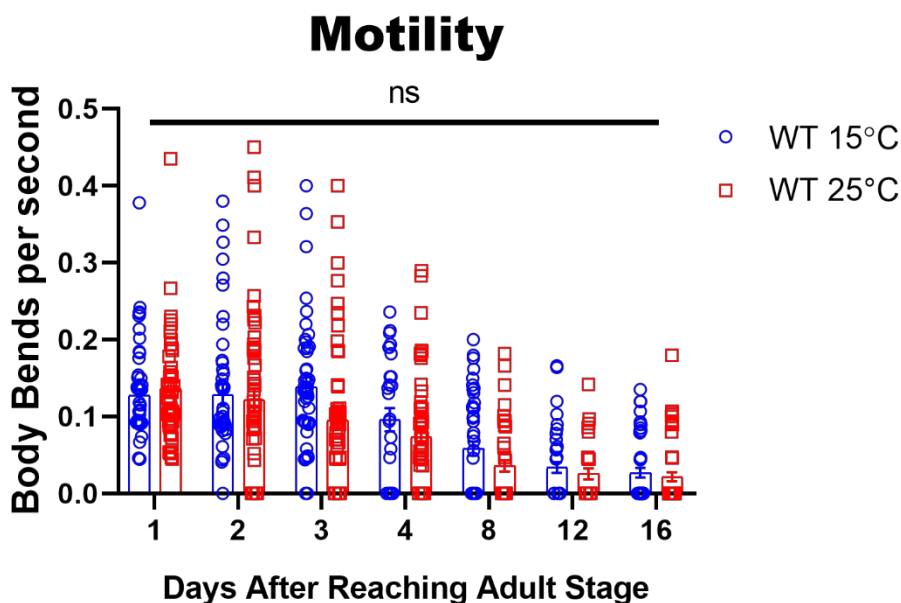


**Figure S3.2. Crawling motility does not change significantly when wildtype worms are grown at 15°C vs. 25°C.** Quantification of agar crawling motility assays at different ages of adulthood and grown at either 15°C or 25°C measured in body bends per second.

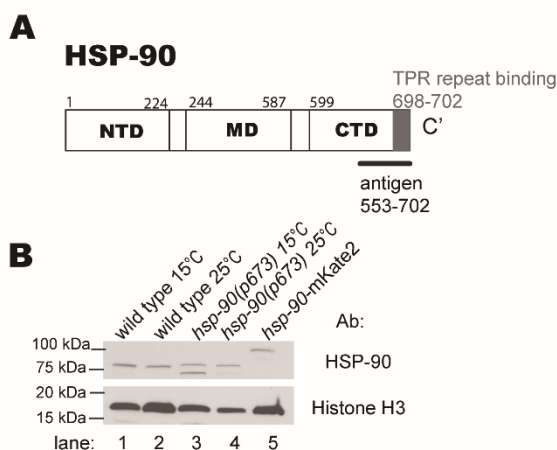


**Figure S3.3. HSP-90 Antibody validation.** A) shows the protein domains of HSP-90 and the epitope that was used as an antigen when creating the antibody. B) shows a Western Blot validating the antibody that was produced. shows HSP-90 loss of function temperature sensitive mutants (lanes 3-4) compared to wild type (lanes 1-2) to show that the mutants have altered HSP-90 and one CRISPR generated fluorescently tagged (mKate2) HSP-90 strain (lane 5) compared to wild type (lanes 1-2) to show that the

antibody recognizes one protein band of the appropriate size (106.3 and 80.3 kDa respectively).

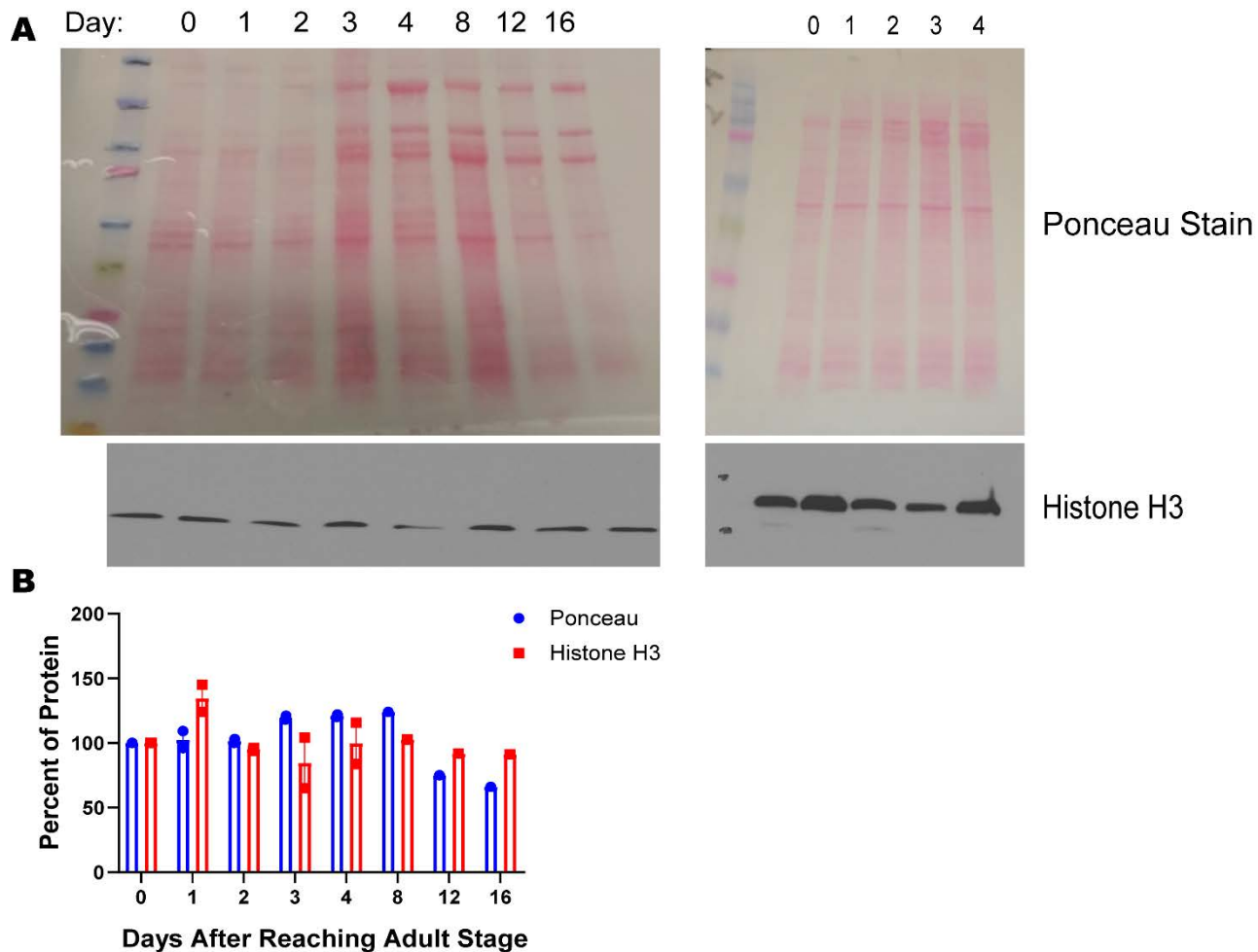


**Figure S3.4. Histone H3 compared to Ponceau S staining.** A) depicts Ponceau S staining above the Histone H3 from the same blot. B) depicts quantification of Ponceau S staining levels compared to Histone H3 levels at different ages. Fiji Image J was used to measure protein levels.

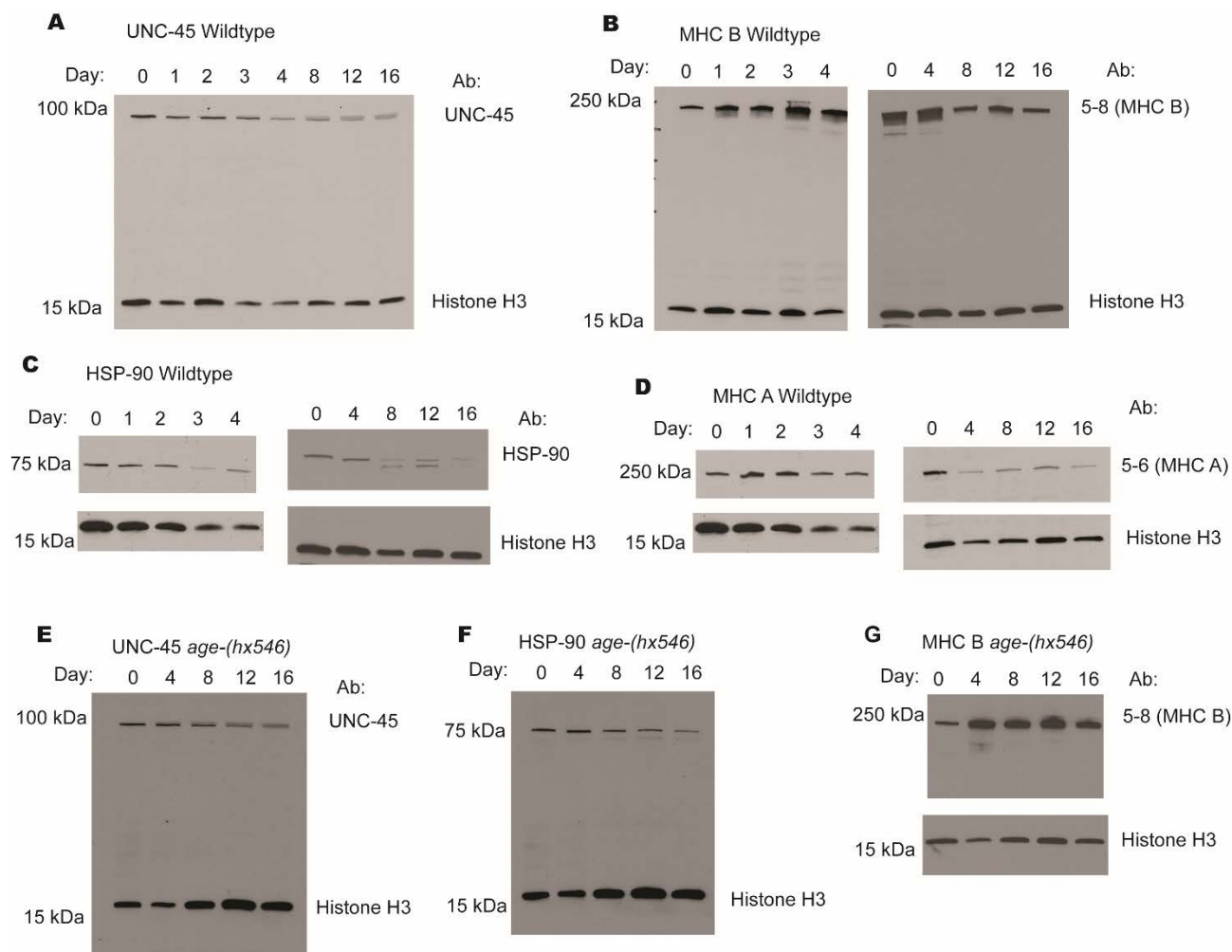


**Figure S3.5. Representative Western Blot images from wildtype and *age-1(hx546)*.** A-D) depict representative images of UNC-45 (A), MHC B (B), HSP-90 (C), and MHC A (D) Western Blots from wildtype worms at different ages. E-G) depict representative images of UNC-45 (E), HSP-90 (F), and MHC B (G) from *age-1(hx546)* worms at different ages. The load control Histone H3 is also shown for each blot. When blots are shown as two images instead of one, it is because a different exposure time was needed for the two different proteins on the blot.

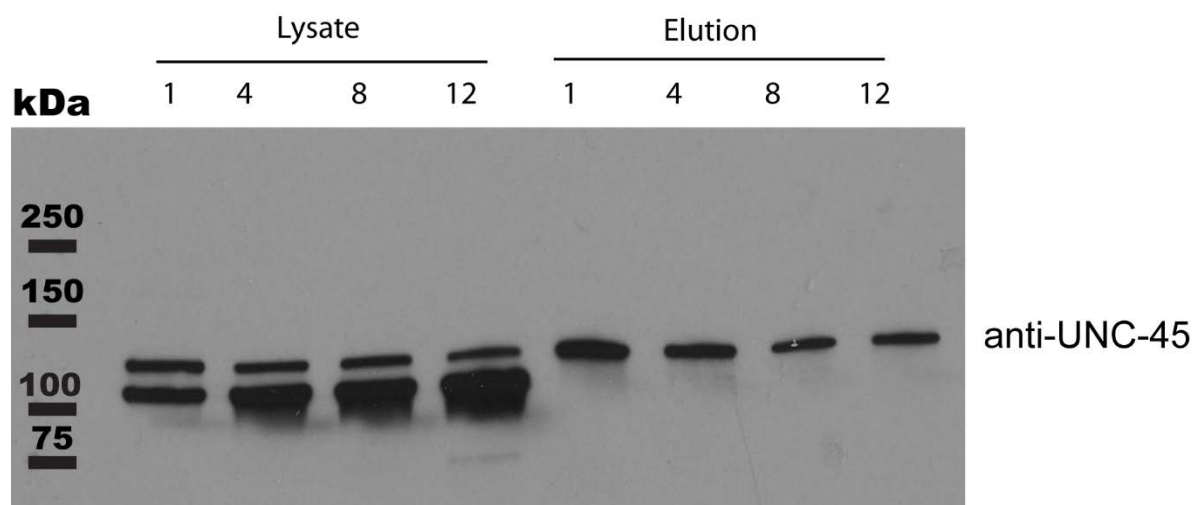


**Figure S3.6. mNeonGreen Immunoprecipitation.** Part of the protein lysate (~1%) of each sample used for the immunoprecipitation (right side of blot) and part of the total elution (~12.5%) from each immunoprecipitation (left side of blot) were run on a 4-20% SDS-PAGE gel, transferred to nitrocellulose, and reacted with the UNC-45 antibody to ensure that UNC-45::mNeonGreen was pulled down with the pre-conjugated mNeonGreen nanobodies magnetic beads.

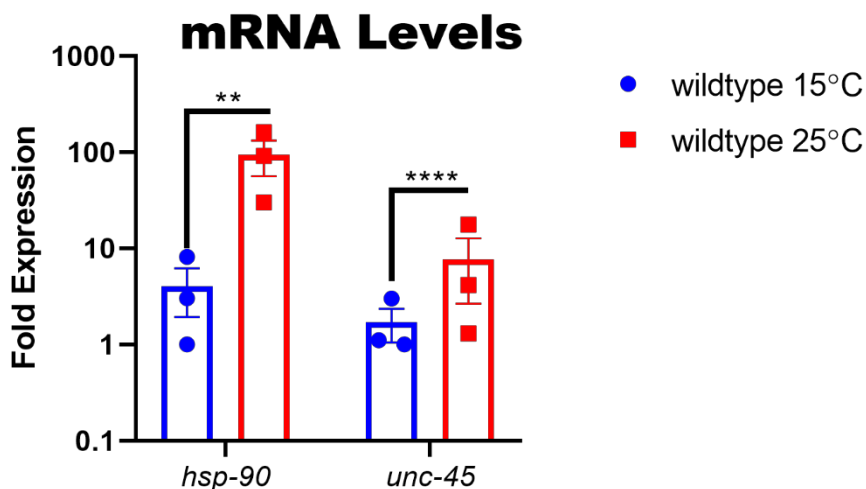
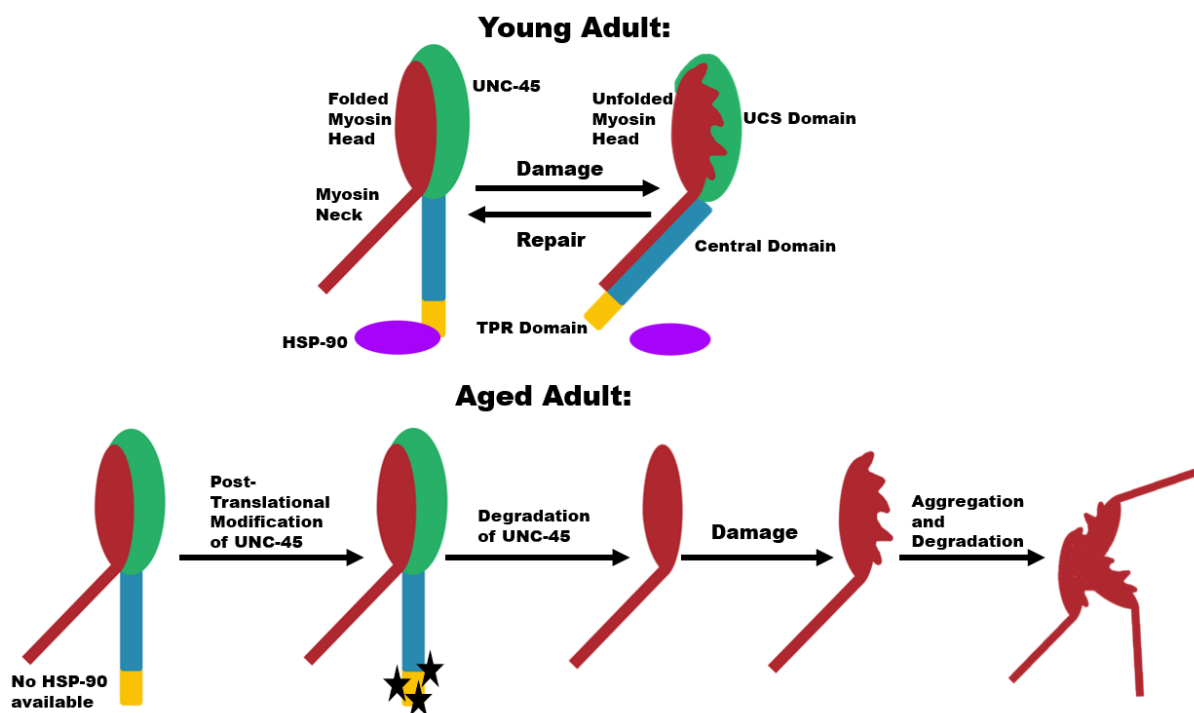


**Figure S7. Steady state transcript expression of *hsp-90* and *unc-45* in Wildtype worms grown at 15°C and 25°C.** The relative fold expression of *unc-45* and *hsp-90* mRNA levels of the N2 wildtype strain grown at 15°C and 25°C. *ges-1* (gut esterase) was used to normalize expression. \*\* p-value <0.005, \*\*\*\* p-value <0.0001.



**Graphical Abstract.** In young adults, under normal conditions the UCS domain of UNC-45 (shown in green) is bound to the myosin head (in red) and the TPR domain (in yellow) is bound to HSP-90 (in purple). Under stress conditions, HSP-90 detaches from the TPR domain, causing a conformational change in UNC-45 that allows the Central domain (in blue) to bind to the myosin neck (in red) resulting in inhibition of the myosin power stroke while the UCS domain protects/re-folds the myosin head. HSP-90 can then rebind the TPR domain, causing the Central domain to release the myosin neck, allowing movement of the myosin motor. However, aged adults experience a loss of HSP-90 and UNC-45 (which has increased post translational modification with aging). The loss of the Myosin chaperones leads to increased aggregation and degradation of Myosin with age. This loss of Myosin at the thick filament results in decline in muscle mass and function, also known as sarcopenia. Note that only the myosin head and neck are shown for simplicity of illustration.

## Acknowledgments

This work was supported in-part by National Institutes of Health grant R01GM118534 to G.M.B. and A.F.O., and also supported in-part by the Emory Initiative Biological Discovery Through Chemical Innovation (BDCI) to G.M.B. Many of the nematode strains used in this work were provided by the Caenorhabditis Genetics Center, which is funded by the NIH Office of Research Infrastructure Programs (P40 OD010440). Monoclonal culture supernatants for 5-6 and 5-8 antibodies were obtained from the University of Iowa Hybridoma Bank, and the 5-6 ascites fluid was kindly provided by Henry F. Epstein (deceased).

## Literature Cited

1. Cruz-Jentoft AJ, *et al.* (2014) Prevalence of and interventions for sarcopenia in ageing adults: a systematic review. Report of the International Sarcopenia Initiative (EWGSOP and IWGS). *Age and ageing* 43(6):748-759.
2. Iannuzzi-Sucich M, Prestwood KM, & Kenny AM (2002) Prevalence of sarcopenia and predictors of skeletal muscle mass in healthy, older men and women. *The journals of gerontology. Series A, Biological sciences and medical sciences* 57(12):M772-777.
3. Barbosa-Silva TG, Bielemann RM, Gonzalez MC, & Menezes AM (2016) Prevalence of sarcopenia among community-dwelling elderly of a medium-sized South American city: results of the COMO VAI? study. *Journal of cachexia, sarcopenia and muscle* 7(2):136-143.
4. Zembron-Lacny A, Dziubek W, Rogowski L, Skorupka E, & Dabrowska G (2014) Sarcopenia: monitoring, molecular mechanisms, and physical intervention. *Physiological research* 63(6):683-691.
5. Candow DG (2011) Sarcopenia: current theories and the potential beneficial effect of creatine application strategies. *Biogerontology* 12(4):273-281.
6. Szulc P, Feyt C, & Chapurlat R (2016) High risk of fall, poor physical function, and low grip strength in men with fracture-the STRAMBO study. *Journal of cachexia, sarcopenia and muscle* 7(3):299-311.
7. Celis-Morales CA, *et al.* (2018) Associations of grip strength with cardiovascular, respiratory, and cancer outcomes and all cause mortality: prospective cohort study of half a million UK Biobank participants. *BMJ (Clinical research ed.)* 361:k1651.
8. Gosselin LE, Johnson BD, & Sieck GC (1994) Age-related changes in diaphragm muscle contractile properties and myosin heavy chain isoforms. *American journal of respiratory and critical care medicine* 150(1):174-178.
9. Statistics FIFoA-R (2012) Older Americans 2012: Key Indicators of Well-Being. *U.S. Government Printing Office; Washington, DC.*
10. Henderson CA, Gomez CG, Novak SM, Mi-Mi L, & Gregorio CC (2017) Overview of the Muscle Cytoskeleton. *Comprehensive Physiology* 7(3):891-944.
11. Squire JM, Paul DM, & Morris EP (2017) Myosin and Actin Filaments in Muscle: Structures and Interactions. *Sub-cellular biochemistry* 82:319-371.
12. Kachur TM & Pilgrim DB (2008) Myosin assembly, maintenance and degradation in muscle: Role of the chaperone UNC-45 in myosin thick filament dynamics. *International journal of molecular sciences* 9(9):1863-1875.
13. Etard C, Roostalu U, & Strahle U (2008) Shuttling of the chaperones Unc45b and Hsp90a between the A band and the Z line of the myofibril. *The Journal of cell biology* 180(6):1163-1175.
14. Barral JM, Bauer CC, Ortiz I, & Epstein HF (1998) Unc-45 mutations in *Caenorhabditis elegans* implicate a CRO1/She4p-like domain in myosin assembly. *The Journal of cell biology* 143(5):1215-1225.
15. Barral JM, Hutagalung AH, Brinker A, Hartl FU, & Epstein HF (2002) Role of the myosin assembly protein UNC-45 as a molecular chaperone for myosin. *Science (New York, N. Y.)* 295(5555):669-671.

16. Solomon V & Goldberg AL (1996) Importance of the ATP-ubiquitin-proteasome pathway in the degradation of soluble and myofibrillar proteins in rabbit muscle extracts. *The Journal of biological chemistry* 271(43):26690-26697.
17. Epstein HF & Thomson JN (1974) Temperature-sensitive mutation affecting myofilament assembly in *Caenorhabditis elegans*. *Nature* 250(467):579-580.
18. Bazzaro M, *et al.* (2007) Myosin II co-chaperone general cell UNC-45 overexpression is associated with ovarian cancer, rapid proliferation, and motility. *The American journal of pathology* 171(5):1640-1649.
19. Janiesch PC, *et al.* (2007) The ubiquitin-selective chaperone CDC-48/p97 links myosin assembly to human myopathy. *Nature cell biology* 9(4):379-390.
20. Wohlgemuth SL, Crawford BD, & Pilgrim DB (2007) The myosin co-chaperone UNC-45 is required for skeletal and cardiac muscle function in zebrafish. *Developmental biology* 303(2):483-492.
21. Bernick EP, Zhang PJ, & Du S (2010) Knockdown and overexpression of Unc-45b result in defective myofibril organization in skeletal muscles of zebrafish embryos. *BMC cell biology* 11:70.
22. Melkani GC, Bodmer R, Ocorr K, & Bernstein SI (2011) The UNC-45 chaperone is critical for establishing myosin-based myofibrillar organization and cardiac contractility in the *Drosophila* heart model. *PLoS one* 6(7):e22579.
23. Hansen L, *et al.* (2014) The myosin chaperone UNC45B is involved in lens development and autosomal dominant juvenile cataract. *European journal of human genetics : EJHG* 22(11):1290-1297.
24. Esteve C, *et al.* (2018) Loss-of-Function Mutations in UNC45A Cause a Syndrome Associating Cholestasis, Diarrhea, Impaired Hearing, and Bone Fragility. *American journal of human genetics* 102(3):364-374.
25. Bujalowski PJ, Nicholls P, Garza E, & Oberhauser AF (2018) The central domain of UNC-45 chaperone inhibits the myosin power stroke. *FEBS open bio* 8(1):41-48.
26. Gieseler K, Qadota H, & Benian GM (2017) Development, structure, and maintenance of *C. elegans* body wall muscle. *WormBook : the online review of C. elegans biology* 2017:1-59.
27. Kenyon CJ (2010) The genetics of ageing. *Nature* 464(7288):504-512.
28. Herndon LA, *et al.* (2002) Stochastic and genetic factors influence tissue-specific decline in ageing *C. elegans*. *Nature* 419(6909):808-814.
29. Landsverk ML, *et al.* (2007) The UNC-45 chaperone mediates sarcomere assembly through myosin degradation in *Caenorhabditis elegans*. *The Journal of cell biology* 177(2):205-210.
30. Miller DM, 3rd, Ortiz I, Berliner GC, & Epstein HF (1983) Differential localization of two myosins within nematode thick filaments. *Cell* 34(2):477-490.
31. Moncrief T, *et al.* (2021) Mutations in conserved residues of the myosin chaperone UNC-45 result in both reduced stability and chaperoning activity. *Protein science : a publication of the Protein Society* 30(11):2221-2232.
32. Srikakulam R & Winkelmann DA (2004) Chaperone-mediated folding and assembly of myosin in striated muscle. *Journal of cell science* 117(Pt 4):641-652.

33. Liu L, Srikakulam R, & Winkelmann DA (2008) Unc45 activates Hsp90-dependent folding of the myosin motor domain. *The Journal of biological chemistry* 283(19):13185-13193.
34. Kenyon C, Chang J, Gensch E, Rudner A, & Tabtiang R (1993) A *C. elegans* mutant that lives twice as long as wild type. *Nature* 366(6454):461-464.
35. Klass MR (1983) A method for the isolation of longevity mutants in the nematode *Caenorhabditis elegans* and initial results. *Mechanisms of ageing and development* 22(3-4):279-286.
36. Ayyadevara S, Alla R, Thaden JJ, & Shmookler Reis RJ (2008) Remarkable longevity and stress resistance of nematode PI3K-null mutants. *Aging cell* 7(1):13-22.
37. Duhon SA & Johnson TE (1995) Movement as an index of vitality: comparing wild type and the age-1 mutant of *Caenorhabditis elegans*. *The journals of gerontology. Series A, Biological sciences and medical sciences* 50(5):B254-261.
38. Birnby DA, *et al.* (2000) A transmembrane guanylyl cyclase (DAF-11) and Hsp90 (DAF-21) regulate a common set of chemosensory behaviors in *caenorhabditis elegans*. *Genetics* 155(1):85-104.
39. Obermann WM, Sondermann H, Russo AA, Pavletich NP, & Hartl FU (1998) In vivo function of Hsp90 is dependent on ATP binding and ATP hydrolysis. *The Journal of cell biology* 143(4):901-910.
40. Welle S, Bhatt K, & Thornton C (1996) Polyadenylated RNA, actin mRNA, and myosin heavy chain mRNA in young and old human skeletal muscle. *The American journal of physiology* 270(2 Pt 1):E224-229.
41. Hoppe T, *et al.* (2004) Regulation of the myosin-directed chaperone UNC-45 by a novel E3/E4-multiubiquitylation complex in *C. elegans*. *Cell* 118(3):337-349.
42. Altun M, *et al.* (2010) Muscle wasting in aged, sarcopenic rats is associated with enhanced activity of the ubiquitin proteasome pathway. *The Journal of biological chemistry* 285(51):39597-39608.
43. Walker GA, *et al.* (2001) Heat shock protein accumulation is upregulated in a long-lived mutant of *Caenorhabditis elegans*. *The journals of gerontology. Series A, Biological sciences and medical sciences* 56(7):B281-287.
44. Shmookler Reis RJ, Ayyadevara S, Crow WA, Lee T, & DeLongchamp RR (2012) Gene categories differentially expressed in *C. elegans* age-1 mutants of extraordinary longevity: new insights from novel data-mining procedures. *The journals of gerontology. Series A, Biological sciences and medical sciences* 67(4):366-375.
45. Brenner S (1974) The genetics of *Caenorhabditis elegans*. *Genetics* 77(1):71-94.
46. Nonet ML, Grundahl K, Meyer BJ, & Rand JB (1993) Synaptic function is impaired but not eliminated in *C. elegans* mutants lacking synaptotagmin. *Cell* 73(7):1291-1305.
47. Wilson KJ, Qadota H, & Benian GM (2012) Immunofluorescent localization of proteins in *Caenorhabditis elegans* muscle. *Methods in molecular biology (Clifton, N.J.)* 798:171-181.
48. Qadota H, Mercer KB, Miller RK, Kaibuchi K, & Benian GM (2007) Two LIM domain proteins and UNC-96 link UNC-97/pinch to myosin thick filaments in *Caenorhabditis elegans* muscle. *Molecular biology of the cell* 18(11):4317-4326.

49. Schmittgen TD & Livak KJ (2008) Analyzing real-time PCR data by the comparative C(T) method. *Nature protocols* 3(6):1101-1108.
50. Benian GM, L'Hernault SW, & Morris ME (1993) Additional sequence complexity in the muscle gene, *unc-22*, and its encoded protein, twitchin, of *Caenorhabditis elegans*. *Genetics* 134(4):1097-1104.
51. Hannak E, *et al.* (2002) The kinetically dominant assembly pathway for centrosomal asters in *Caenorhabditis elegans* is gamma-tubulin dependent. *The Journal of cell biology* 157(4):591-602.
52. Miller RK, *et al.* (2009) CSN-5, a component of the COP9 signalosome complex, regulates the levels of UNC-96 and UNC-98, two components of M-lines in *Caenorhabditis elegans* muscle. *Molecular biology of the cell* 20(15):3608-3616.
53. Waterhouse A, *et al.* (2018) SWISS-MODEL: homology modelling of protein structures and complexes. *Nucleic acids research* 46(W1):W296-w303.
54. Verba KA, *et al.* (2016) Atomic structure of Hsp90-Cdc37-Cdk4 reveals that Hsp90 traps and stabilizes an unfolded kinase. *Science (New York, N.Y.)* 352(6293):1542-1547.
55. Pettersen EF, *et al.* (2004) UCSF Chimera--a visualization system for exploratory research and analysis. *Journal of computational chemistry* 25(13):1605-1612.
56. Gazda L, *et al.* (2013) The myosin chaperone UNC-45 is organized in tandem modules to support myofilament formation in *C. elegans*. *Cell* 152(1-2):183-195.

**Chapter 4: Indole improves aging muscle mass and function and increases myosin in aged nematodes in an AHR-1, HSP-90, and UNC-45 dependent manner**

Matheny CJ, Sonowal R, Qadota H, Kalman D, Benian GM. Indole improves aging muscle mass and function and increases myosin in aged nematodes in an AHR-1, HSP-90, and UNC-45 dependent manner. *In preparation.*

**Introduction:**

As advances in science and medicine extend our lifespans, the issue of increased frailty and age-associated diseases have become a larger concern (1-3). A major ageing disorder that is highly correlated with frailty, morbidity, mortality, and an overall decline in the quality of life is sarcopenia(4). Sarcopenia is defined as the loss of muscle mass and function during aging without any underlying diseases. Improved diet and exercise have a modest effect on improving and maintaining muscle mass and function, but the best diet and resistance training regimen for maintaining muscle health into late adulthood has yet to be determined(5, 6). Increasing essential amino acids, milk-based proteins, creatine monohydrate, essential fatty acids, and even vitamin D have been shown to be beneficial to building and maintaining muscle mass in older adults who are also exercising their muscle(7). One factor that may be key to identifying the ideal diet for muscle growth and maintenance is the microbiome. Our commensal microbiota are necessary for proper nutrient metabolism, as well as maintaining the integrity of the intestinal epithelial barrier and enhancing innate immunity(8-11). Additionally, the bacteria inhabiting our digestive tract secrete metabolites that can improve the overall health of multiple organ systems(12-14).

One such metabolite is indole, which is obtained from plant-based dietary sources and produced by intestinal microbiota, like *Eschericia coli*, via tryptophanase (TnaA)-mediated catalysis of dietary tryptophan(15). Indole can be found in millimolar concentrations in the intestinal tract and its derivatives can be detected throughout the body(16). In mice, *Drosophila*, and *C. elegans*, indole treatment improves mobility, presumably through improved muscle health, in older animals(17). Sonowal et al. found

that indole's ability to extend muscle healthspan in *Drosophila* and *C. elegans* is dependent on the aryl hydrocarbon receptor (AHR), a xenobiotic receptor that can bind to indole(17, 18). The mechanism(s) by which AHR mediates indole's protective effects on muscle health remain unknown.

As we age, our ability to regenerate new muscle cells ("myofibers") from satellite cells (muscle stem cells) becomes impaired and the maintenance of existing muscle cells becomes crucial to maintaining mobility(19). The fundamental unit of muscle contraction, the sarcomere, consists of overlapping thin filaments, primarily composed of actin, and thick filaments primarily composed of myosin. Muscle contraction occurs via the sliding of thin filaments inwards from either side of the sarcomere by the attachment and pulling of myosin heads on the surface of thick filaments with thin filaments. Myosin heads require the chaperone UNC-45 (Unc-45a/b in mammals) to initially fold after translation and for the assembly of myosin molecules into thick filaments. At least for *C. elegans* muscle, UNC-45 remains associated with the thick filaments in mature muscle, and probably is there to re-fold the myosin head after cellular stressors might result in unfolding of myosin heads(20-25). In vitro experiments with purified proteins done by Bujalowski et al. suggest the following model: When the co-chaperone HSP-90 binds to the TPR (N-terminal tetratricopeptide repeat) domain of UNC-45, it is in a state of 'rest' and unable to bind to myosin. When HSP-90 unbinds, UNC-45 undergoes a conformational change to bind to myosin, inhibit the power stroke, and refold the myosin head. Once HSP-90 rebinds the TPR domain, UNC-45 releases myosin so that it can return to the work of muscle contraction(26). Recently our lab (Matheny et al., submitted) has shown that UNC-45 is important for maintaining adult nematode muscle and that UNC-45 protein declines during

aging after a decline in HSP-90. We also found that HSP-90 is important for the protein stability of UNC-45. Logically, UNC-45's protein regulation should be tied to HSP-90 protein levels since in the absence of HSP-90, UNC-45 inhibits the myosin power stroke and can cause paralysis.

Other than UNC-45, HSP-90 has a multitude of binding partners, including the aryl hydrocarbon receptor, AHR-1. AHR-1 is bound in a complex with HSP-90 in the cytoplasm until a ligand binds, at which point AHR-1 dissociates from HSP-90, translocates to the nucleus, and complexes with another transcription factor, ARNT (AHR nuclear translocator), to bind to xenobiotic response elements located upstream of multiple genes (27-29). We hypothesized that when indole binds to AHR-1, it would cause HSP-90 to unbind – increasing the amount of HSP-90 available for other binding partners, like UNC-45. Here, we show that indole treatment prevents the age-associated decline in UNC-45 and myosin protein levels in an AHR-1 and HSP-90 dependent manner and prevents the decline in myosin in an UNC-45 dependent manner. We also observe an increase in UNC-45 associated with HSP-90 after treatment with indole.

## **Results:**

### Indole protects against the age-associated decline in muscle mass and function:

Sonowal et al. (2017) reported that indole improves nematode thrashing motility and pharyngeal pumping and reduces the percentage of elderly paralyzed worms(17). Here we have analyzed whole nematode spontaneous crawling motility on agar plates and used myosin MHC A (myosin heavy chain A) immunostaining to count the number of A-bands or assembled thick filaments. All strains of *E. coli* produce indole. As noted

above, indole is generated by the action of the enzyme tryptophanase on tryptophan. An *E. coli* K12 strain with deletion of tryptophanase ( $\Delta$ tna) produces no indole (Anyanful et al., 2005). To create a most dramatic effect, we compared nematodes grown on extra indole (*E. coli* K12 plus indole supplemented in the NGM agar plates), to nematodes grown with no indole (*E. coli* K12  $\Delta$ tna and no added indole (just methanol solvent)). Previously, our lab found that when wild type nematodes are grown under standard conditions (Brenner, 1974), i.e. NGM agar with *E. coli* OP50, crawling motility declines by day 4 of adulthood (Matheny et al., submitted). However, when grown in the presence of extra indole, crawling motility is maintained up to at least day 8 of adulthood (Figure 4.1A). This is in contrast to worms grown in the absence of indole, which show a decline in motility by day 4 of adulthood, similar to “standard” conditions, which provide some indole from the OP50 *E. coli*. We used MHC A immunostaining to count A-band numbers in individual body wall muscle cells of 1-, 8-, and 12-day old adult worms grown in the presence of extra indole vs. no indole. Wildtype animals grown under standard conditions start to experience a decline in assembled thick filaments by day 8 of adulthood (Matheny et al., submitted). Worms treated with extra indole maintained their total number of assembled thick filaments until at least day 12 of adulthood, while worms grown without indole experienced a decline in assembled thick filaments by day 8 of adulthood, similar to worms grown under standard conditions (Figure 4.1B-G). Therefore, extra indole maintains muscle function and mass during aging.

#### Indole protects against the age-associated decline in UNC-45 and Myosin:

Previously, our lab has found that, under standard growth conditions, during aging, a decline in HSP-90 protein at day 3 of adulthood is followed by a decline in UNC-45

protein at day 4 of adulthood and a decline in body wall myosin MHC B (the major client of UNC-45 chaperone) at day 8 of adulthood (Matheny et al., submitted). We found that the loss of HSP-90 protein is likely due to decreased transcription and the loss of UNC-45 and myosin is likely independent of transcription. Like myosin, *unc-45* has a low steady state transcription rate once adulthood has been reached. This suggests that UNC-45 is stably associated with the thick filament and has a low protein turnover rate, consistent with the known co-immunolocalization of MHC B and UNC-45 to the sarcomeric A-bands (Ao and Pilgrim, 2000; Gazda et al., 2013). We also reported that the level of UNC-45 protein is substantially reduced in the HSP-90 mutant *hsp-90(p673)*, suggesting a major role for HSP-90 in UNC-45 protein stability (Matheny et al., submitted).

When worms are exposed to extra indole, they not only maintain “young” protein levels of UNC-45 and myosin, but they also have a two-fold increase in levels of UNC-45 and myosin at day 8 of adulthood (Figure 4.2 A and C). Worms grown in the absence of indole show a decline in UNC-45 and myosin protein similar to worms grown under standard conditions (Matheny et al., submitted). As expected from our previous studies, the increases in UNC-45 and myosin protein appear to not be caused by an increase in transcription (Figure 4.2D). In fact, curiously, indole treatment results in a decline in *unc-45*, *hsp-90*, and *unc-54* transcript at day 8. Interestingly, extra indole does not seem to affect the total protein level of HSP-90 (Figure 4.2B). However, we know that without available HSP-90 to bind to the TPR domain of UNC-45, UNC-45 is likely degraded. Thus, we postulate that extra indole increases the amount of HSP-90 able to interact with UNC-45 without increasing the total amount of HSP-90 protein.

Indole's protective effects depend on AHR-1, HSP-90, and UNC-45:

Sonowal et al. (2017) reported that the beneficial effects of indole on *C. elegans* swimming motility (thrashing) is dependent on the aryl hydrocarbon receptor (AHR-1), one of the likely receptors for indole (24). We have found that the benefits of extra indole on crawling motility and number of assembled thick filaments are also AHR-1 dependent. We used *ahr-1(ju145)*, a likely null mutant which has a nonsense mutation in the middle of the gene. *ahr-1(ju145)* experiences a decline in crawling motility by day 4 of adulthood and a decline in assembled thick filaments by day 8 of adulthood, regardless of whether the strain was exposed to extra indole or no indole (Figure 4.3). These time points are identical to what we have observed in wild type animals grown under standard conditions (Matheny et al., under revision), and earlier than what we observed with wild type animals grown with extra indole (Figure 4.1).

Since we know that UNC-45 protein stability depends on HSP-90 (Matheny et al., submitted), we also analyzed the *hsp-90(p673)* mutant's crawling motility and number of assembled thick filaments after indole treatment. *hsp-90(p673)* is a temperature sensitive mutant, meaning it has a relatively wildtype phenotype at 15°C but is perturbed at 25°C. This mutant exhibits dauer forming (daf) and uncoordinated (unc) phenotypes at 25°C. We allowed the worms to develop normally at 15°C and transitioned them to 25°C at day 0 of adulthood. We found that, like with the *ahr-1* mutant, extra indole has no protective effects on the muscle health of the *hsp-90* mutant. Motility declines dramatically by day 4 of adulthood and the assembled thick filaments have declined in both number and organization by day 8 of adulthood, regardless of exposure to extra indole or no indole (Figure 4.3). In fact, in *hsp-90(p673)* animals, the presence of extra indole results in a

decline in the number of A-bands at day 8. This provides evidence that indole's ability to facilitate muscle health maintenance is dependent on both AHR-1 and HSP-90.

In order to validate the importance of UNC-45 on indole's effectiveness, we also treated *unc-45(e286)* temperature sensitive mutants with indole. These animals were allowed to develop normally at 15°C and then transitioned to 25°C and to indole or methanol conditions once adulthood was reached. As anticipated, extra indole had no protective effect on the muscle health (motility and number of A-bands) of these animals (Figure 4.3C and F).

We also analyzed the total protein levels of UNC-45, HSP-90, and myosin MHC B in both *ahr-1(ju145)*, *hsp-90(p673)*, and *unc-45(e286)* strains. The increase in total protein levels of UNC-45 and MHC B seen in wildtype animals treated with indole is completely nullified in these mutants (Figure 4.2A and C). These results suggest that increasing Myosin through a mechanism involving AHR-1, HSP-90, and UNC-45 may be one way in which indole is improving muscle health of aging animals.

#### More HSP-90 is associated with UNC-45 when treated with Indole:

We hypothesize that indole binds to AHR-1, causing HSP-90 to be released from an AHR-1/HSP-90 complex and, thus, increasing the amount of available HSP-90 to bind to UNC-45. To test this theory, we performed immunoprecipitation experiments to determine if more HSP-90 was bound to UNC-45 after indole treatment. We used two CRISPR generated strains, one with an mNeonGreen tag on endogenous UNC-45(30) and one with an mKate2 tag on endogenous HSP-90 (Matheny et al., under revision), and magnetic beads conjugated to either mNeonGreen or RFP nanobodies to cleanly pull

down either UNC-45 or HSP-90. We then ran out the elutions on SDS-PAGE gels, blotted, and reacted with antibodies to UNC-45 or HSP-90. HSP-90::mKate2 was immunoprecipitated from day 8 adults grown with or without indole. As shown in Figure 4.4A and C, approximately 2-fold more UNC-45 co-immunoprecipitated in the presence of indole compared to in the absence of indole. We then conducted the reciprocal experiment: UNC-45::mNeonGreen was immunoprecipitated from day 8 adults grown with or without indole. As shown in Figure 4.4B and D, somewhat more HSP-90 was co-immunoprecipitated in the presence of indole, but it was not statistically significant.

### **Discussion:**

Previously, Sonowal et al. showed that treatment with indole improves nematode healthspan (swimming motility and pharyngeal pumping) in an unknown *ahr-1* dependent manner. We have validated their results by demonstrating that indole treatment improves crawling motility and have gone on further to demonstrate that indole maintains the number of assembled thick filaments and increases the steady state level of myosin in aged animals in an *ahr-1*, *hsp-90*, and *unc-45* dependent manner. Wildtype crawling motility declines by day 4 of adulthood when grown under standard conditions (some indole provided in the OP50 *E. coli*). Worms grown on NGM containing indole and fed K12 *E. coli* (extra indole conditions) maintained their crawling motility up to at least day 8 of adulthood (Figure 4.1). Worms grown on NGM containing vehicle (methanol) and fed a  $\Delta$ *tnaA* mutant *E. coli* (no indole conditions) experienced a decline in motility by day 4 of adulthood, similar to wildtype conditions. Wildtype animals grown under standard conditions start to experience a decline in assembled thick filaments by day 8 of adulthood (Matheny et al. under revision). Indole treated worms maintained their total number of

assembled thick filaments until at least day 12 of adulthood, while vehicle (methanol) treated worms did experience a decline in assembled thick filaments by day 8 of adulthood (Figure 4.1). This provides further evidence of indole's ability to maintain muscle health during aging.

When worms are treated with indole, they not only maintain young protein levels of UNC-45 and Myosin, but they have a 2.8-fold increase in levels of UNC-45 and a 4-fold increase in myosin at day 8 of adulthood. The vehicle (methanol) treated control experiences a decline in UNC-45 and Myosin protein similar to wildtype conditions. As expected, the increases in UNC-45 and Myosin protein do not appear to be caused by an increase in steady state transcription. Interestingly, indole treatment does not seem to affect the total protein level of HSP-90. However, we know that without available HSP-90 to bind to the TPR domain, UNC-45 is likely degraded. Thus, we postulate that indole is increasing the amount of freely available HSP-90 without increasing the total protein level of HSP-90. We found that, like with the *ahr-1* mutant, indole has no protective effects on the muscle health of the *hsp-90* or *unc-45* mutants. We also found by co-immunoprecipitation experiments that the UNC-45 from animals grown with indole did in fact have an increase in associated HSP-90. This supports our hypothesis that one of the ways in which indole is acting at a molecular level is by causing more HSP-90 to be released from the complex with AHR-1 and, thus, available to interact with UNC-45, stabilizing UNC-45 and promoting the ability of UNC-45 to chaperone myosin and maintain already assembled sarcomeres in aged adult animals.

## Materials and Methods:

### C. elegans Strains

Standard growth conditions for *C. elegans* were used (31). Wildtype Bristol N2, *ahr-1(ju145)*, *GB319*, and *GB350* were grown at 20°C. As described in the above results, temperature sensitive mutant *hsp-90(p673)* was grown at 15°C during development and transitioned to 25°C at the onset of adulthood. Adult worms were separated from their progeny daily by allowing the adults to sink in M9 buffer in glass tubes, removing the supernatant containing the L1s, and washing several times before returning to NGM plates. *GB319* is the 2X outcrossed derivative of *PHX789 (unc-45(syb789))* which is a CRISPR-generated strain that expresses UNC-45-mNeonGreen and was described previously (30). The strain, *PHX501 (hsp-90(syb501))*, is a CRISPR-generated strain which expresses HSP-90 with a C-terminal mKate2 tag. *PHX501* was outcrossed 2X to wild type to generate strain *GB350*, and was also described previously (Matheny et al., submitted).

### Indole treatment

Worms were grown on NGM agar plates containing either 100µM of indole (Sigma-Aldrich) dissolved in methanol (Sigma-Aldrich) or an equal volume of methanol. Indole plates were seeded with K12 *E. coli* instead of the traditional OP50 bacteria. Methanol plates were seeded with K12Δ*tnaA* as described in Sonowal et al, 2017. Using these methods we thus created conditions in which worms could be grown with more than the usual amount of indole (extra indole)—K12 plus indole in the plates, or no indole--K12Δ*tnaA* and no indole added to the plates.

### Immunostaining in adult body-wall muscle

Adult nematodes were fixed and immunostained according to the method described by Nonet et al. and described in further detail by Wilson et al. (32, 33). anti-MHC A was used at 1:200 (mouse monoclonal 5-6; Miller et al., 1983) and anti-mouse Alexa 594 (Invitrogen) was used at 1:200 dilution(34). Images were captured at room temperature with a Zeiss confocal system (LSM510) equipped with an Axiovert 100M microscope and an Apochromat x63/1.4 numerical aperture oil immersion objective in x2.5 zoom mode. The color balances of the images were adjusted by using Photoshop (Adobe, San Jose, CA).

### Motility crawling assays

Adult worms were collected at different ages using M9 buffer containing 0.2g/L gelatin. They were transferred to a 1.5mL microcentrifuge tube, allowed to settle to the bottom, and washed 3X with M9 buffer containing 0.2g/L gelatin. 5µL of worm suspension was added to the center of a 6cm unseeded NGM plate. Worms were allowed to adapt for 5 minutes before a video recording of their crawling was made using a dissecting stereoscopic microscope fitted with a CMOS camera (Thorlabs). Several 10 second videos were recorded for each sample and analyzed by Image J FIJI WrmTracker software to obtain body bends per second (BBPS). Statistical significance was determined using a student's T-test.

### Quantitative Real-Time PCR

Worms from two 10cm NGM plates were collected using M9 buffer and frozen as a dry packed worm pellet. Lysis buffer from the Qiagen RNeasy Plus Mini Kit (cat. 74134) was added, the sample was freeze-thawed in liquid nitrogen five times to crack the worm

cuticle, and then vortexed with MagnaLyser beads (Roche) for 1 minute. The samples were centrifuged, and the supernatant was used to extract RNA with the Qiagen RNeasy Plus Mini Kit. The NCBI primer designing tool (<https://www.ncbi.nlm.nih.gov/tools/primer-blast/>) was used to create primer pairs specific for each gene of interest that also had at least one intron separating the primer pair (see Table S1). 1µg of cDNA was synthesized from the RNA using BioRad iScript Reverse Transcription Supermix (cat. 1708840). The cDNA was then diluted 1/10 in nuclease free water and 2.5µL was used per reaction with 10µL of qRT-PCR master mix (1.25µL of each primer, 1.25µL of nuclease free water, and 6.25 µL of SybrGreen supermix (Biorad cat. 1708880)). A BioRad CFX Real-Time PCR thermal cycler was used. Fold change was determined using the  $2^{-\Delta\Delta Ct}$  method (35). *gapdh-2* was used for normalization. Statistical significance was determined using a student's T-test.

#### Western blots and quantitation of protein levels

We used the procedure of Hannak et al. (36) to prepare total protein lysates from wild-type, *hsp-90(p673)*, and *ahr-1(ju145)* strains. When comparing wild-type and mutant strains, we loaded approximately equal amounts of protein extract estimated by finding volumes of extracts that would give equal intensity of banding after Coomassie staining. We used quantities of extracts and dilutions of antibodies that would place us into the linear range of detection by ECL and exposure to film. The following antibodies and dilutions were used: rabbit anti-UNC-45(30) at 1:5,000; rat anti-HSP-90 (Matheny et al., submitted) at 1:2,500; mouse monoclonal 5-8 ascites (34) for MHC B at 1:40,000. The quantitation of steady-state levels of protein was performed as described in Miller et al. (2009)(37). The relative amount of each of these muscle proteins in each lane was

normalized to the amount of Histone H3 detected using anti-Histone H3 (abcam, cat. ab1791) at 1:40,000 dilution. BioRad precast Mini-PROTEAN TGX Stain-Free Gels were used (4-20%, cat. 4568093, 12%, cat. 4568041). The BioRad Precision Plus Protein™ Kaleidoscope™ Prestained Protein Standards (cat. 1610375) were used on all standard SDS-PAGE gels.

### Immunoprecipitation

Worms were collected from 2 10cm NGM plates with M9 and frozen. 500µL of IP buffer (25mM Tris pH 7.5, 150mM NaCl, 1mM EDTA, 0.5% NP40, 5% glycerol, 1X Halt protease & phosphatase inhibitor cocktail (ThermoFisher)) was added to each sample. They were then freeze-thawed in liquid nitrogen 3-5X to crack the cuticle, added to MagnaLyser beads, and vortexed for 1 minute. The samples were centrifuged, and the lysate supernatant was added to 25µL of mNeonGreen-Trap or RFP-Trap Magnetic Agarose suspension (cat. no. ntma-10 and rtma10, Chromotek, Inc.) in which nanobodies to mNeonGreen or RFP (red fluorescent protein) had been coupled to magnetic agarose beads. They were then incubated on a spinning wheel at 4°C for 1 hour, washed 3X with IP buffer, and eluted with 2X Laemmli buffer with β-mercaptoethanol.

### Statistical Analysis

Unless otherwise stated, data are reported as mean ± SE of the mean. Western Blot statistical analyses were made using GraphPad Prism Software (version 4.0). Comparisons of three or more means used one-way ANOVA and Bonferroni-adjusted unpaired t tests. Statistical significance was assigned as not-significant for  $p > 0.05$ , \* for  $p \leq 0.05$ , and \*\*\* for  $p \leq 0.001$ .

## Figures:

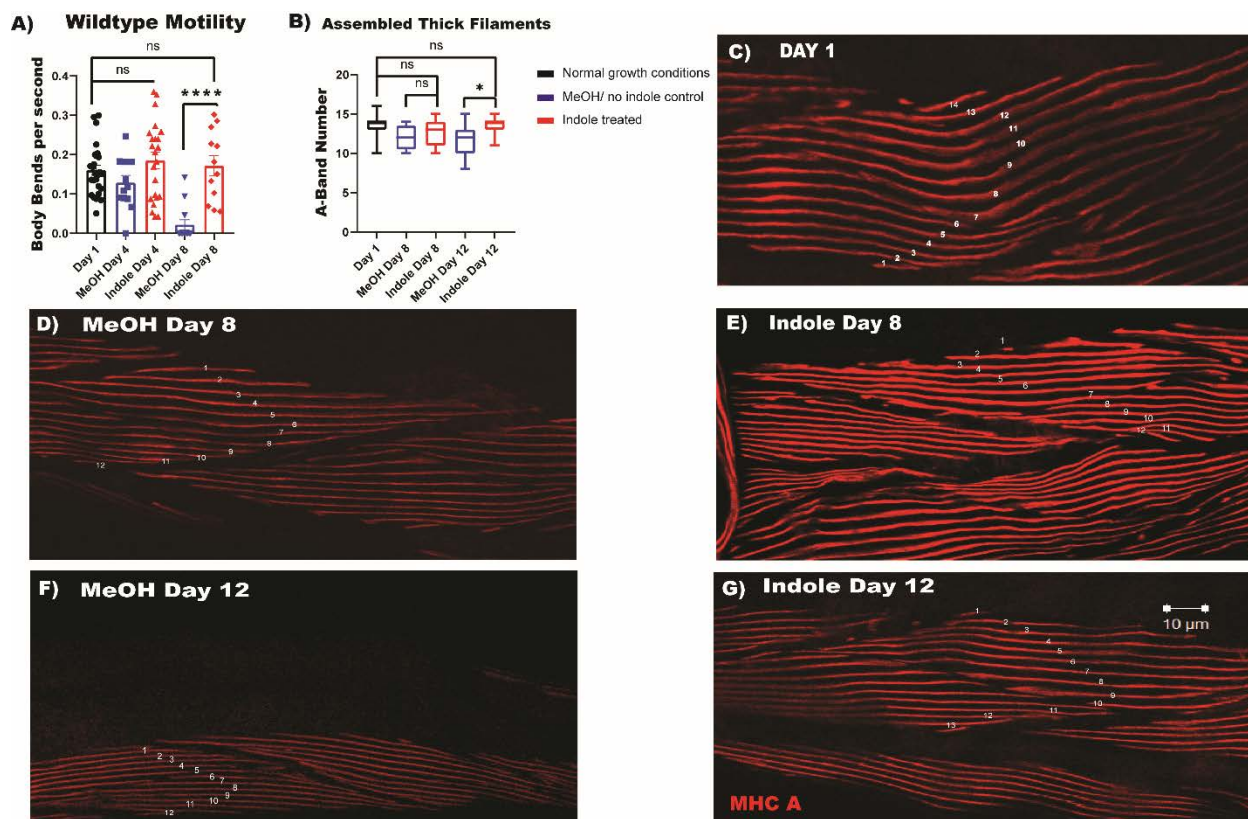


**Figure 4.1. Indole protects against the age-associated decline in whole nematode motility and the number of assembled of thick filaments (A-bands).** A) is the quantification of agar crawling motility assays at different ages of adulthood (days 1, 4, and 8) under normal conditions at day 1 and then treated with either methanol (vehicle control) or indole measured in body bends per second. B) is the quantification of A-band number at different ages of adulthood (days 1, 8, and 12) under normal conditions at day 1 and then treated with either methanol (vehicle control) or indole. C-G) are representative images of body wall muscle near the vulva immunostained with anti-MHC A at different ages of adulthood (days 1, 8, and 12) and treated with either methanol (vehicle control) or indole. \*\*p-value < 0.005, \*\*\*p-value < 0.0005\*\*\*\* p-value < 0.0001.

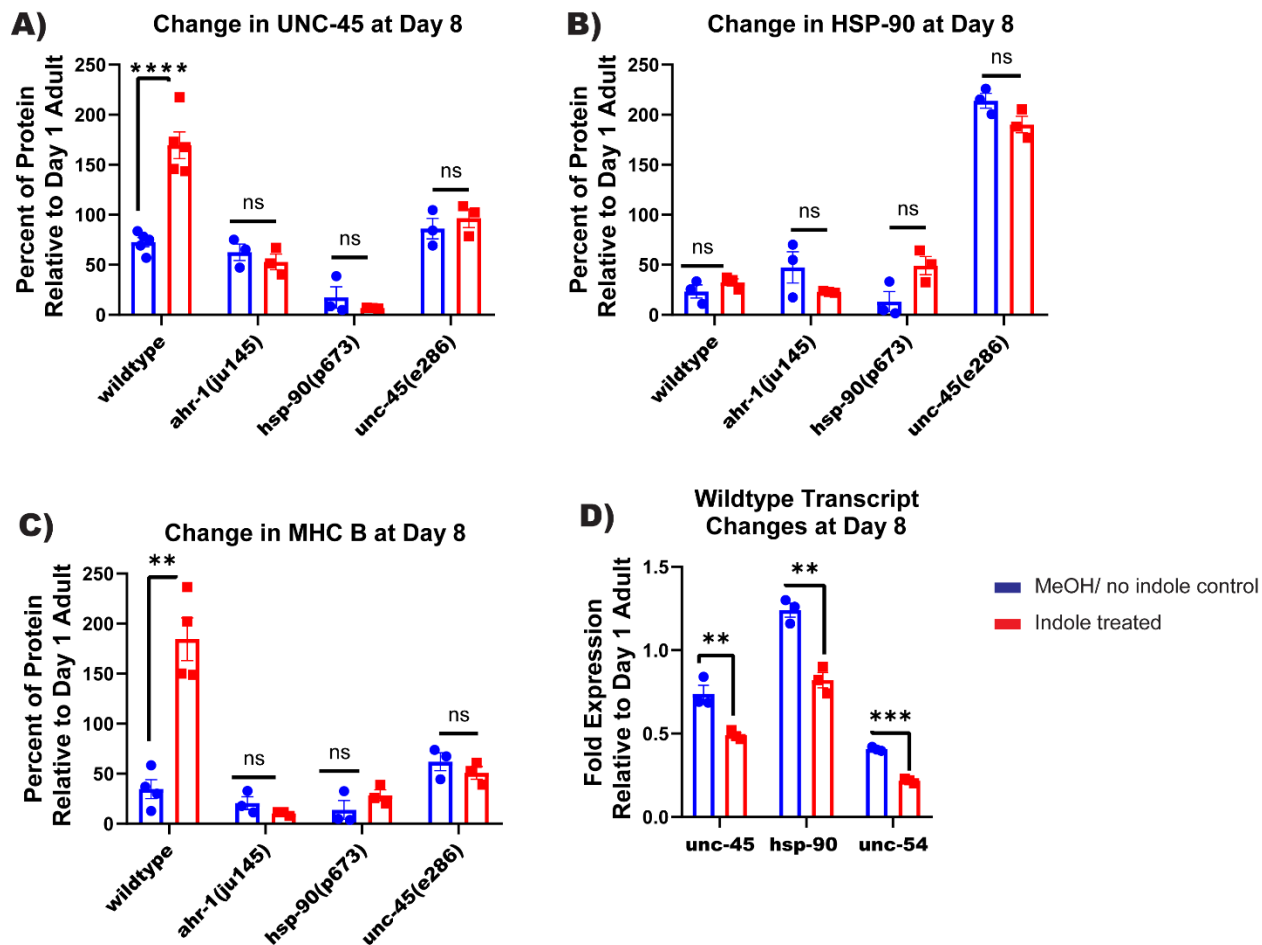


**Figure 4.2. Indole protects against the age-associated decline of Myosin MHC-B protein in an AHR-1/HSP-90/UNC-45 dependent manner.** A-C) Graphical quantification of steady state protein levels UNC-45, HSP-90, and MHC B (major body wall myosin isoform) of wildtype, *ahr-1(ju145)*, *hsp-90(p673)*, and *unc-45(e286)* animals at different ages of adulthood (day 1 and 8) and treated with either methanol (vehicle control) or indole. Note that *hsp-90(p673)* and *unc-45(e286)* were grown at 25°C. Data are shown as a percentage of protein relative to histone H3 protein. D) Steady state mRNA fold expression of *unc-45*, *hsp-90* and *unc-54* (MHC B) relative to *gpdh-2* (GAPDH) of wildtype animals at different ages of adulthood (day 1 and 8) and treated with either methanol (vehicle control) or indole. \*\*p-value < 0.005, \*\*\*p-value < 0.0005\*\*\*\* p-value < 0.0001.

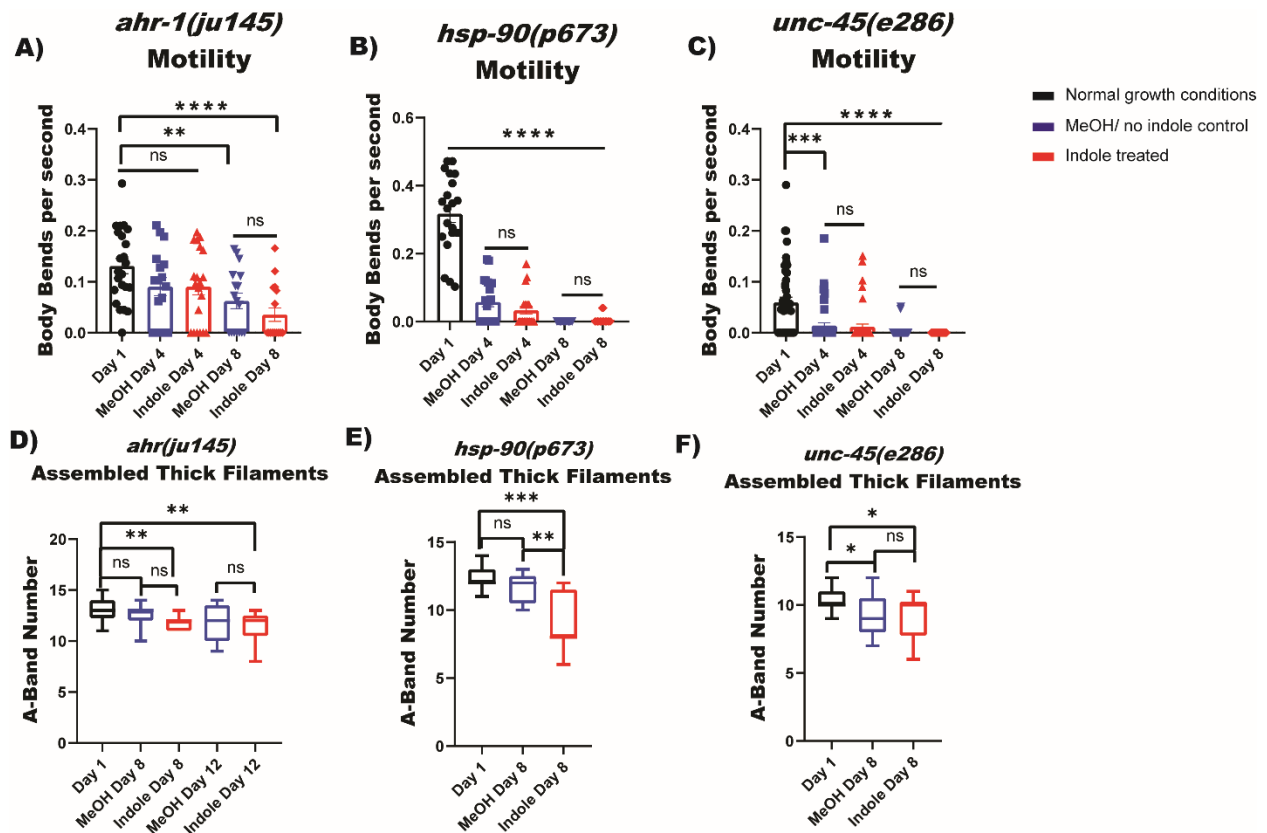


**Figure 4.3. Indole's protective effects against the age-associated decline in whole nematode motility and the number of assembled of thick filaments (A-bands) are dependent on AHR-1, HSP-90, and UNC-45.** A-C) is the quantification of agar crawling motility assays of *ahr-1(ju145)*, *unc-45(e286)*, and *hsp-90(p673)* animals at different ages of adulthood (days 1, 4, and 8) under normal conditions at day 1 and then treated with either methanol (vehicle control) or indole measured in body bends per second. D-F) is the quantification of A-band number of *ahr-1(ju145)*, *unc-45(e286)*, and *hsp-90(p673)* animals at different ages of adulthood (days 1, 8, and 12) under normal conditions at day 1 and then treated with either methanol (vehicle control) or indole.

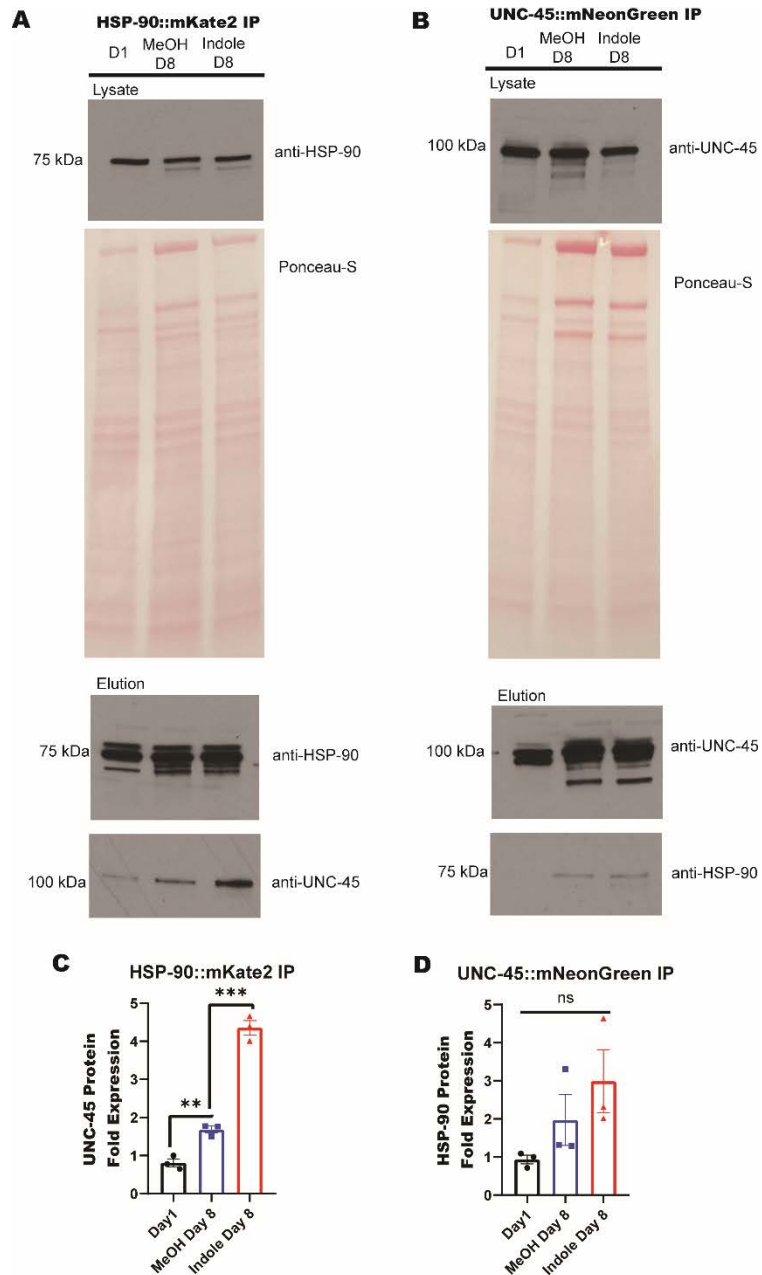


**Figure 4.4. More UNC-45 is associated with HSP-90 after indole treatment.** A and B) Representative Western Blots and the lysate Ponceau-S staining from HSP-90::mKate2 and UNC-45::mNeonGreen immunoprecipitations. Lysates were reacted with anti-HSP-90 for the HSP-90::mKate2 IP and with anti-UNC-45 for the UNC-45::mNeonGreen IP. Elutions from both IPs were reacted with anti-HSP-90 and anti-UNC-45. C and D) Graphical quantification of the amount of UNC-45 pulled down in the HSP-90::mKate2 IP and the amount of HSP-90 pulled down in the UNC-45::mNeonGreen IP. \*\* p-value < 0.005, \*\*\* p-value < 0.0005

## Supplemental Figures

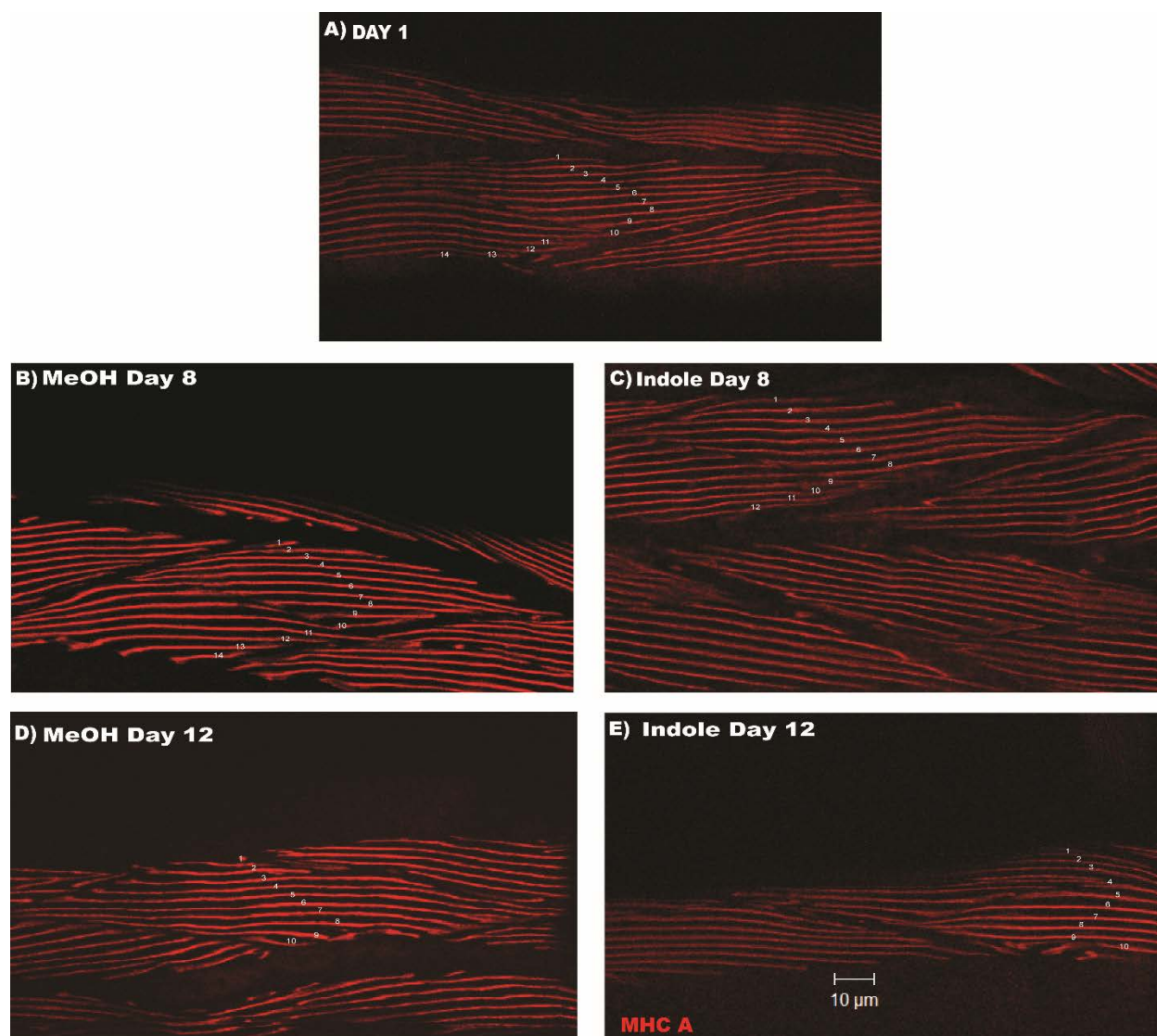


**Figure S4.1. Representative images from MHC A immunostaining of *ahr-1(ju145)*.** A-E) are representative images of body wall muscle near the vulva immunostained with anti-MHC A at different ages of adulthood (day 1, 8, 12) and grown on either regular OP50, Methanol control (B,D), or Indole treatment plates(C,E) with an A-band count depicted as white numbers along the A-bands.

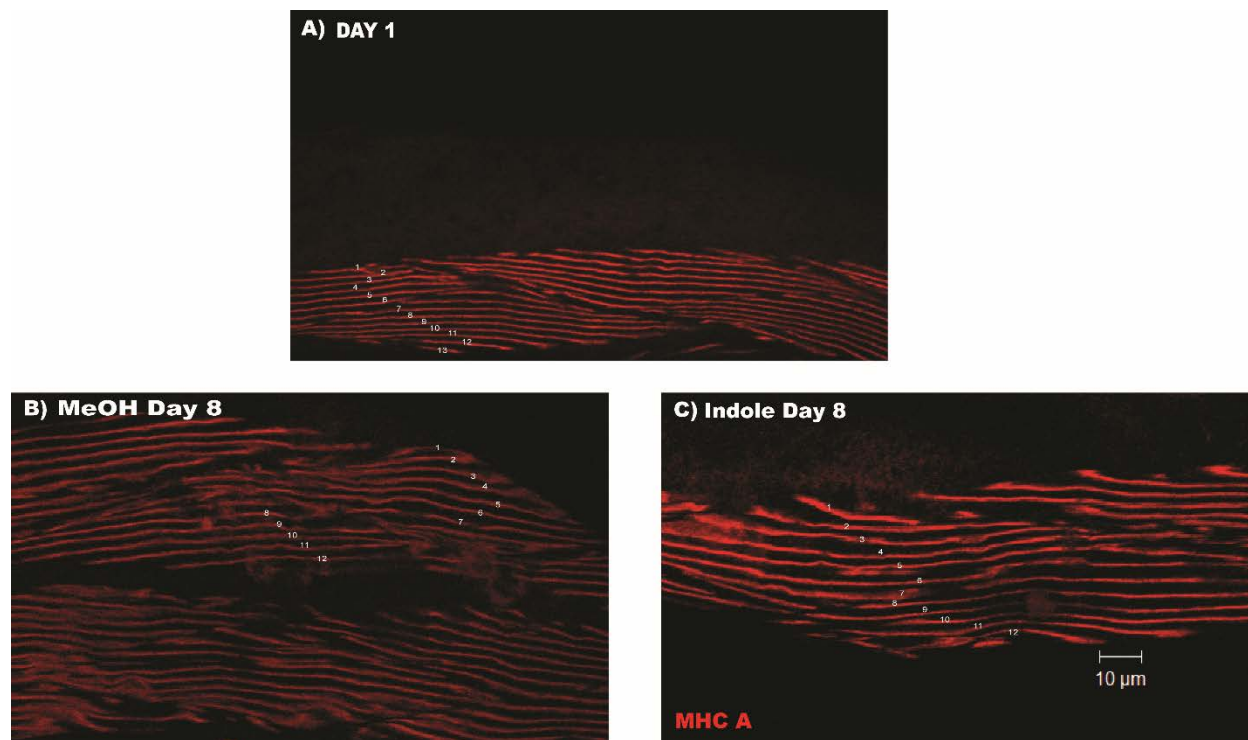


**Figure S4.2. Representative images from MHC A immunostaining of *hsp-90(p673)*.** A-C) are representative images of body wall muscle near the vulva immunostained with anti-MHC A at different ages of adulthood (day 1, 8) and grown on either regular OP50 plates (A), Methanol control (B), or Indole treatment plates (C) at 15°C (A) or 25°C (B,C) with an A-band count depicted as white numbers along the A-bands.

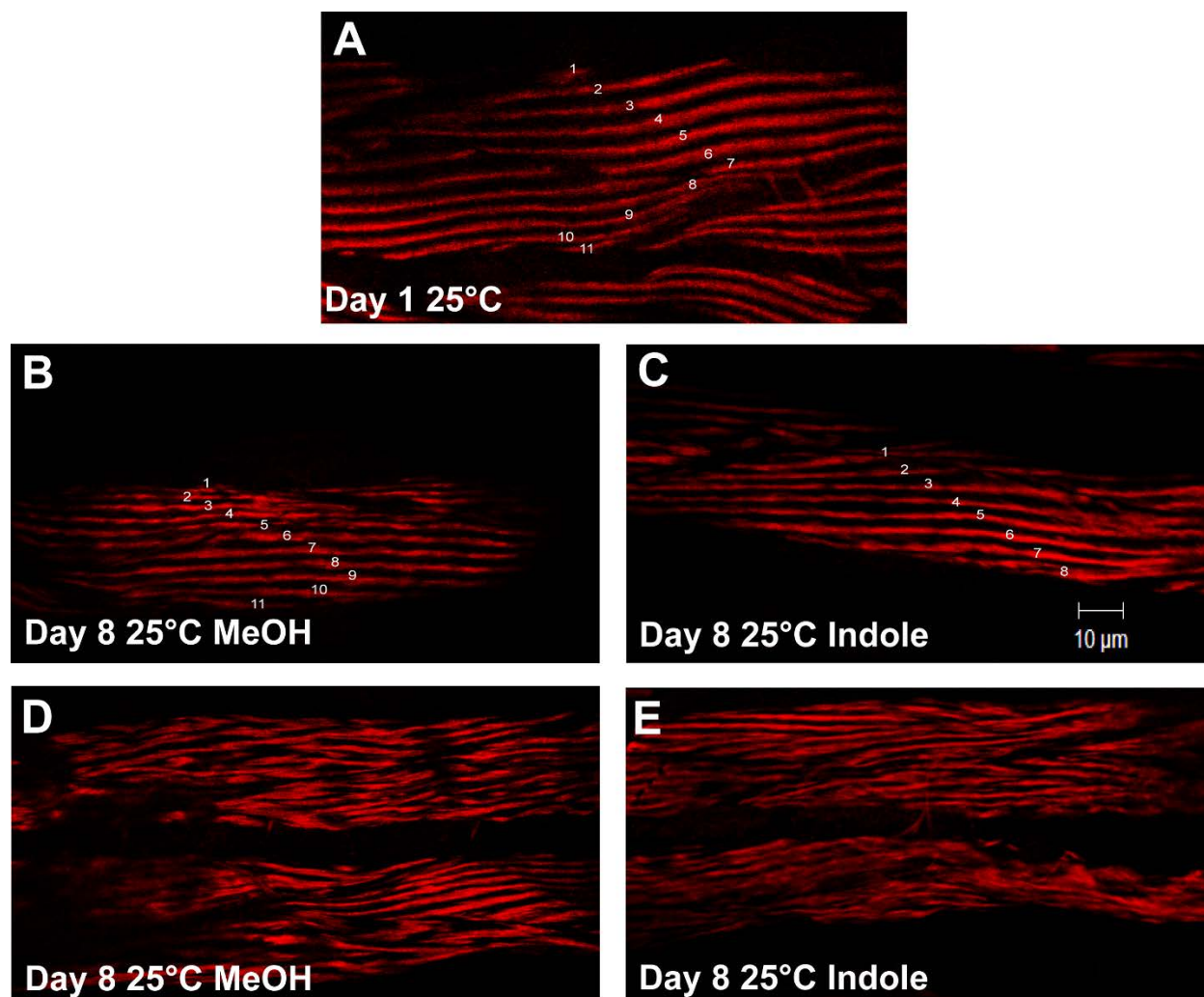


**Figure S4.3. Representative images from MHC A immunostaining of *unc-45(e286)*.** A-E) are representative images of body wall muscle near the vulva immunostained with anti-MHC A at different ages of adulthood (day 1, 8) and grown on either regular OP50 plates (A), Methanol control (B,D), or Indole treatment plates (C,E) at 15°C (A) or 25°C (B – E). A-C) depict muscle cells that an A-band count was possible, the A-band count is depicted as white numbers along the A-bands. D and E) depict disorganized muscle cells at day 8.

## **Acknowledgments**

This work was supported in-part by National Institutes of Health grant R01GM118534 to G.M.B., and also supported in-part by the Emory Initiative Biological Discovery Through Chemical Innovation (BDCI) to G.M.B. Many of the nematode strains used in this work were provided by the *Caenorhabditis* Genetics Center, which is funded by the NIH Office of Research Infrastructure Programs (P40 OD010440). Monoclonal culture supernatants for 5-6 and 5-8 antibodies were obtained from the University of Iowa Hybridoma Bank, and the 5-6 ascites fluid was kindly provided by Henry F. Epstein (deceased).

### Literature Cited

1. Meara E, White C, & Cutler DM (2004) Trends in medical spending by age, 1963-2000. *Health affairs (Project Hope)* 23(4):176-183.
2. Kahn JH, Magauran BG, Jr., Olshaker JS, & Shankar KN (2016) Current Trends in Geriatric Emergency Medicine. *Emergency medicine clinics of North America* 34(3):435-452.
3. Statistics FIFoA-R (2012) Older Americans 2012: Key Indicators of Well-Being. U.S. Government Printing Office; Washington, DC.
4. Cruz-Jentoft AJ, *et al.* (2014) Prevalence of and interventions for sarcopenia in ageing adults: a systematic review. Report of the International Sarcopenia Initiative (EWGSOP and IWGS). *Age and ageing* 43(6):748-759.
5. Candow DG (2011) Sarcopenia: current theories and the potential beneficial effect of creatine application strategies. *Biogerontology* 12(4):273-281.
6. Forbes SC, Little JP, & Candow DG (2012) Exercise and nutritional interventions for improving aging muscle health. *Endocrine* 42(1):29-38.
7. Candow DG, *et al.* (2012) Effect of nutritional interventions and resistance exercise on aging muscle mass and strength. *Biogerontology* 13(4):345-358.
8. Hooper LV & Gordon JI (2001) Commensal host-bacterial relationships in the gut. *Science (New York, N.Y.)* 292(5519):1115-1118.
9. LeBlanc JG, *et al.* (2017) Beneficial effects on host energy metabolism of short-chain fatty acids and vitamins produced by commensal and probiotic bacteria. *Microbial cell factories* 16(1):79.
10. Fukuda S, *et al.* (2011) Bifidobacteria can protect from enteropathogenic infection through production of acetate. *Nature* 469(7331):543-547.
11. Mazmanian SK, Liu CH, Tzianabos AO, & Kasper DL (2005) An immunomodulatory molecule of symbiotic bacteria directs maturation of the host immune system. *Cell* 122(1):107-118.
12. Lee WJ & Hase K (2014) Gut microbiota-generated metabolites in animal health and disease. *Nature chemical biology* 10(6):416-424.
13. Wei GZ, *et al.* (2021) Tryptophan-metabolizing gut microbes regulate adult neurogenesis via the aryl hydrocarbon receptor. *Proceedings of the National Academy of Sciences of the United States of America* 118(27).
14. Saeedi BJ, *et al.* (2020) Gut-Resident Lactobacilli Activate Hepatic Nrf2 and Protect Against Oxidative Liver Injury. *Cell metabolism* 31(5):956-968.e955.
15. Kumari A & Singh RK (2019) Medicinal chemistry of indole derivatives: Current to future therapeutic prospectives. *Bioorganic chemistry* 89:103021.
16. Lee JH, Wood TK, & Lee J (2015) Roles of indole as an interspecies and interkingdom signaling molecule. *Trends in microbiology* 23(11):707-718.
17. Sonowal R, *et al.* (2017) Indoles from commensal bacteria extend healthspan. *Proceedings of the National Academy of Sciences of the United States of America* 114(36):E7506-e7515.
18. Hubbard TD, *et al.* (2015) Adaptation of the human aryl hydrocarbon receptor to sense microbiota-derived indoles. *Scientific reports* 5:12689.

19. Yamakawa H, Kusumoto D, Hashimoto H, & Yuasa S (2020) Stem Cell Aging in Skeletal Muscle Regeneration and Disease. *International journal of molecular sciences* 21(5).
20. Barral JM, Bauer CC, Ortiz I, & Epstein HF (1998) Unc-45 mutations in *Caenorhabditis elegans* implicate a CRO1/She4p-like domain in myosin assembly. *The Journal of cell biology* 143(5):1215-1225.
21. Barral JM, Hutagalung AH, Brinker A, Hartl FU, & Epstein HF (2002) Role of the myosin assembly protein UNC-45 as a molecular chaperone for myosin. *Science (New York, N.Y.)* 295(5555):669-671.
22. Kachur TM & Pilgrim DB (2008) Myosin assembly, maintenance and degradation in muscle: Role of the chaperone UNC-45 in myosin thick filament dynamics. *International journal of molecular sciences* 9(9):1863-1875.
23. Wohlgemuth SL, Crawford BD, & Pilgrim DB (2007) The myosin co-chaperone UNC-45 is required for skeletal and cardiac muscle function in zebrafish. *Developmental biology* 303(2):483-492.
24. Melkani GC, Bodmer R, Ocorr K, & Bernstein SI (2011) The UNC-45 chaperone is critical for establishing myosin-based myofibrillar organization and cardiac contractility in the *Drosophila* heart model. *PloS one* 6(7):e22579.
25. Gazda L, *et al.* (2013) The myosin chaperone UNC-45 is organized in tandem modules to support myofilament formation in *C. elegans*. *Cell* 152(1-2):183-195.
26. Bujalowski PJ, Nicholls P, Garza E, & Oberhauser AF (2018) The central domain of UNC-45 chaperone inhibits the myosin power stroke. *FEBS open bio* 8(1):41-48.
27. Coumailleau P, Poellinger L, Gustafsson JA, & Whitelaw ML (1995) Definition of a minimal domain of the dioxin receptor that is associated with Hsp90 and maintains wild type ligand binding affinity and specificity. *The Journal of biological chemistry* 270(42):25291-25300.
28. Hankinson O (1995) The aryl hydrocarbon receptor complex. *Annual review of pharmacology and toxicology* 35:307-340.
29. Carver LA & Bradfield CA (1997) Ligand-dependent interaction of the aryl hydrocarbon receptor with a novel immunophilin homolog in vivo. *The Journal of biological chemistry* 272(17):11452-11456.
30. Moncrief T, *et al.* (2021) Mutations in conserved residues of the myosin chaperone UNC-45 result in both reduced stability and chaperoning activity. *Protein science : a publication of the Protein Society* 30(11):2221-2232.
31. Brenner S (1974) The genetics of *Caenorhabditis elegans*. *Genetics* 77(1):71-94.
32. Nonet ML, Grundahl K, Meyer BJ, & Rand JB (1993) Synaptic function is impaired but not eliminated in *C. elegans* mutants lacking synaptotagmin. *Cell* 73(7):1291-1305.
33. Wilson KJ, Qadota H, & Benian GM (2012) Immunofluorescent localization of proteins in *Caenorhabditis elegans* muscle. *Methods in molecular biology (Clifton, N.J.)* 798:171-181.
34. Miller DM, 3rd, Ortiz I, Berliner GC, & Epstein HF (1983) Differential localization of two myosins within nematode thick filaments. *Cell* 34(2):477-490.
35. Schmittgen TD & Livak KJ (2008) Analyzing real-time PCR data by the comparative C(T) method. *Nature protocols* 3(6):1101-1108.

36. Hannak E, *et al.* (2002) The kinetically dominant assembly pathway for centrosomal asters in *Caenorhabditis elegans* is gamma-tubulin dependent. *The Journal of cell biology* 157(4):591-602.
37. Miller RK, *et al.* (2009) CSN-5, a component of the COP9 signalosome complex, regulates the levels of UNC-96 and UNC-98, two components of M-lines in *Caenorhabditis elegans* muscle. *Molecular biology of the cell* 20(15):3608-3616.

## Chapter 5: Conclusions and future directions

### Overview of Findings and Significance:

#### Conserved regions of the UCS domain of UNC-45 are essential for thick filament assembly and organization:

Through collaboration with the Oberhauser lab at the University of Texas Medical Branch (UTMB), we have used a combination of biophysical and biological experimental tools to analyze conserved residues/regions of UNC-45 and obtain a better understanding of the molecular mechanisms by which the UCS domain of UNC-45 chaperones myosin. We engineered mutations in the chaperoning domain of the human UNC-45B designed to test 1) if the putative client-binding groove in the UCS domain of human UNC-45B is functional by mutating highly conserved residues (the Groove, Y737W, and 2xW mutants); and 2) whether our homology-modeled loop is important for binding and holding myosin (the DEL and PRO mutants). We also introduced the R805W mutation to test the hypothesis that the stability of the salt bridge between R805-E767 plays a role in UCS-client interactions(1). We also analyzed six, two of which are new, temperature sensitive *unc-45* mutants that all have mutations at conserved residues within highly conserved regions of UNC-45 (primarily the UCS domain)(2).

Overall, our data strongly support our hypotheses regarding the putative client-binding groove and the loop region of the UCS domain. The in vivo data show that the R805W mutation, which segregates with human congenital and infantile cataracts, had the most drastic disorganizing effect on the structure and organization of the worm sarcomeres. This mutation is predicted to disrupt a salt bridge, but it does not affect UCS secondary structure or its structural stability but significantly impairs its chaperoning

activity on protecting S1 or CS from thermal aggregation (53 and 24% lower activity than WT, respectively).

My results indicate that the ts mutations in UNC-45 lead to reduced and abnormal thick filament assembly by a combination of reduced UNC-45 protein stability and reduced UNC-45 chaperoning function. One potential reason for a difference in in vivo versus in vitro mutant protein stability is that the mutations result in a change of posttranslational modifications that ultimately lead to increased degradation. Both in wild type and the *unc-45* mutants, there are two protein bands detected by western blot, one of which is of lower mobility than the predicted molecular weight. In fact, this larger species increases in the mutants when grown at the restrictive temperature, which could be interpreted as temperature induced unfolding of the mutant proteins lead to further post translational modification. One of the likely PTMs is ubiquitination, which has been reported to occur on UNC-45 and is involved in its degradation(3). The unfolding may alter UNC-45's interaction with another protein that normally covers a PTM site or causes residues to be slightly more or less exposed for modification. This may provide evidence that these conserved residues not only play a role in chaperoning activity, but also in vivo UNC-45 stability and/or regulation.

UNC-45 has a crucial role in maintaining muscle sarcomeres during aging in *C.*

*elegans*:

We find that perturbation of UNC-45 during adulthood is enough to cause an early onset of sarcopenia-like pathology. Thus, our results demonstrate that UNC-45 is crucial to maintaining muscle health specifically during adulthood. We found that *hsp-90* transcript declines at day 2 of adulthood, directly before the decline in HSP-90 protein.

The loss of HSP-90 at day 3 directly precedes a loss of UNC-45 protein at day 4 of adulthood. Then, there is a major decline in MHC B, the main client of UNC-45 and more abundant body wall muscle myosin isoform, at day 8 of adulthood. We theorize that the decline in UNC-45 protein is due primarily to protein degradation.

We observe what appears to be an increase in post-translational modification of UNC-45 with age and have identified that one of these modifications is phosphorylation at serine 111. A caveat is that although this was the only phosphorylation site identified from ~94% coverage of the UNC-45 sequence, it was identified from a population of worms of mixed developmental stages and adult ages. We do not yet know if this is the main site phosphorylated during adult aging. Phosphorylation may be related to the already known ubiquitylation of UNC-45 and its degradation by the proteasome (4). Intriguingly, serine 111, though in a highly conserved region, is not a conserved residue. In fact, in *Drosophila* it is an aspartic acid and in humans and zebrafish it is a glutamic acid – both negatively charged residues. Perhaps the negative charge here is important to the protein's regulation and the residue evolved to have an inherent negative charge.

The *age-1(hx546)* longevity mutant shows a delay in the loss of assembled thick filaments but not spontaneous crawling motility (Figure 6). A major characteristic of aging muscle and sarcopenia pathology is the loss of muscle mass, which does not begin to occur in these animals until day 16 of adulthood (day 8 in wildtype). The amount of UNC-45, HSP-90, and MHC B protein continues to increase in these animals well past day 0 of adulthood. *hsp-90* and *unc-54* transcripts remain above wildtype levels while *unc-45* transcript has the same trend as in the wildtype animals. Since one theory behind the improved stress resistance of this strain is an increase in

heat shock proteins and chaperones(5, 6), it is not surprising that the *hsp-90* mRNA is upregulated. However, we do still observe a decline in HSP-90 protein back to wildtype levels by day 8 of adulthood, which precedes a decline in UNC-45 protein back to wildtype levels by day 12 of adulthood. This delay in the loss of UNC-45 protein may be one of the mechanisms that allow this long-lived mutant to have an extended health span as well as lifespan.

We find that in a loss of function *hsp-90* mutant there is significantly reduced UNC-45 protein, but not transcript. This suggests that interaction with HSP-90 is important for the protein stability of UNC-45 and that in the absence of HSP-90, UNC-45 is left more susceptible to degradation. This leads us to theorize that during aging there is a loss of HSP-90, which leaves regions of UNC-45 more open to post translational modifications, like phosphorylation, and leads to increased degradation of UNC-45.

Therefore, our model is that during adult aging, the loss of HSP-90, followed by the loss of the myosin head chaperone UNC-45, leads to fewer myosin heads being re-folded, and these myosin molecules and even thick filaments are removed from the sarcomere, forming aggregates and/or being degraded. Because of the low level of myosin transcripts and translation, there is not enough new myosin protein available to replenish the myosin within existing thick filaments, or to form new thick filaments. This results in an overall decline in thick filament number, sarcomere size and number, and muscle function. The results presented here suggest that increased expression and/or increased activity of UNC45B might be a strategy for prevention and treatment of sarcopenia, and even age-associated heart failure. (Matheny et al., under revision)

Indole improves aging muscle mass and function and increases Myosin in aged nematodes in an AHR-1, HSP-90, and UNC-45 dependent manner:

Previously, our lab has found that wildtype crawling motility declines by day 4 of adulthood when grown under standard conditions. Worms grown on NGM containing indole and fed K12 *E. coli* maintained their crawling motility up to at least day 8 of adulthood. Worms grown on NGM containing vehicle (methanol) and fed a  $\Delta$ tnaA mutant *E. coli* experienced a decline in motility by day 4 of adulthood, similar to wildtype conditions. Wildtype animals grown under standard conditions start to experience a decline in assembled thick filaments by day 8 of adulthood. Indole treated worms maintained their total number of assembled thick filaments until at least day 12 of adulthood, while vehicle (methanol) treated worms did experience a decline in assembled thick filaments by day 8 of adulthood. This provides more definitive evidence of indole's ability to maintain muscle health during aging.

When worms are treated with indole, they not only maintain young protein levels of UNC-45 and myosin, but they have a 2.8-fold increase in UNC-45 and a 4-fold increase in myosin at day 8 of adulthood. The vehicle (methanol) treated control experiences a decline in UNC-45 and myosin protein similar to wildtype conditions. As expected, the increases in UNC-45 and myosin protein appear to not be correlated with increased transcription. Interestingly, indole treatment does not seem to affect the total protein level of HSP-90. However, we speculate that without available HSP-90 to bind to the TPR domain, UNC-45 is likely degraded. Thus, we postulate that indole is increasing the amount of freely available HSP-90 without increasing the total protein level of HSP-90. We found that, like with the *ahr-1* mutant, indole has no protective effects on the muscle

health of the *hsp-90* or *unc-45* mutants. We also found that the UNC-45 from animals grown with indole did in fact have an increase in associated HSP-90. This supports our hypothesis that one of the ways in which indole is acting at a molecular level is by causing more HSP-90 to be released from the complex with AHR-1 and, thus, available to stabilize UNC-45. With more UNC-45, more myosin, and thus sarcomeres, are maintained during aging.

#### Additional data – UNC-45 is increased during stress

In addition to data in chapters 3 and 4 that support the idea that UNC-45 is important for maintaining adult muscle sarcomeres, I have also found that UNC-45 protein levels increase during both heat and oxidative stress. When worms were heat shocked at 30°C and 37°C for 2 hours, I saw an approximate 50% and 25%, respectively, increase in UNC-45 compared to worms that remained at 20°C (Figure 5.1A). This is not surprising since I also find an increase in *unc-45* transcript when worms are grown at 25°C (Chapter 3, Figure S3.7). This suggests that like HSP-90, and many other chaperones, UNC-45 increases in response to stress. This supports the hypothesis that UNC-45 is responsible for re-folding myosin heads during times of stress that would otherwise cause protein unfolding, aggregation, and degradation. I also see an increase of about 10-20% and 25-50% in UNC-45 protein when worms are treated with either 5mM or 160mM paraquat in M9 buffer for 2 hours (compared to worms in M9 buffer alone, Figure 5.1B). Paraquat causes oxidative stress and is widely used as a herbicide, making it a chemical that nematodes in the wild would have to contend with. As mentioned in previous chapters, it has already been shown that UNC-45 moves from the Z-discs of zebrafish muscle to the thick filaments after exposure to thermal, oxidative, or physical stress(7). Our data and

the data from other labs strongly suggest that the UNC-45 chaperone is part of the cellular stress response, at least in muscle cells.

### **Pitfalls and technical difficulties:**

We sought to conditionally increase UNC-45 during adulthood by using tagged extrachromosomal UNC-45 under the control of a heat shock promoter. We initially tagged UNC-45 with three HA repeats at the N' terminus. However, putting any tag, even a small HA tag, at the N' terminal of UNC-45 (by the TPR domain) might cause the transgenic protein to be quickly degraded. This was surprising to us since Gazda et al. placed a FLAG tag at the N' terminus with success(8). This could be due to their use of a constitutive muscle specific promoter (*unc-54* or *myo-3*), while we used a heat shock inducible promoter. I was only able to see expression of the HA-tagged UNC-45 via Western Blot analysis after an overnight heat shock, whereas normally a 2-hour heat shock is sufficient. For this reason, we decided to re-make the construct with an eGFP tag at the C' terminus of UNC-45 (still under the control of a heat shock promoter).

As the worms age, we see an increase in a modified version of UNC-45. Since it has already been demonstrated that UNC-45 is degraded via multi-ubiquitination, we wanted to determine if this modified band on our Western Blots was simply due to an increase in ubiquitinated UNC-45 with age. We wanted to determine if there is an increase in UNC-45 ubiquitination with age by pulling down endogenous UNC-45::mNeonGreen from our CRISPR *unc-45::mNeonGreen* worms using an mNeonGreen magnetic bead trap and reacting the elution with a ubiquitin antibody on a Western Blot. Unfortunately, we were unable to detect any ubiquitin from the UNC-45::mNeonGreen immunoprecipitation elution. Alternatives we have considered are: 1) growing larger

quantities of worms for our immunoprecipitation experiment, 2) pulling down all ubiquitinated proteins using an anti-ubiquitin immunoprecipitation and reacting the elution with anti-UNC-45 on a Western Blot. There is of course the possibility that ubiquitinated UNC-45 is being degraded too quickly to detect and the experiment could be repeated by inhibiting the proteasome with MG132 or by RNAi. If this were the case, then the modified UNC-45 we see on our Western Blots is caused by one or more other post translational modifications.

**Future directions:**Identification of new clients of UNC-45, as well as new PTMs of UNC-45:

We can use the CRISPR generated UNC-45::mNeonGreen strain to immunoprecipitate UNC-45 using magnetic beads conjugated to mNeonGreen nanobodies and analyze via mass spectrometry any interacting proteins being pulled down with UNC-45. We can then take any new client candidates identified and analyze them via Western Blot and/or immunostaining in an *unc-45* ts mutant background. We can also use this method to attempt to identify new post translational modifications. Through this exact method, we now know that UNC-45 is phosphorylated at serine 111. Some PTMs may only exist/ some proteins may only be clients of UNC-45 during certain developmental stages or under certain conditions, like stress. We can perform the immunoprecipitations at different nematode ages (L1, L2, L3, L4, young adult, adult, aged adult) and under different conditions (heat shock at 30°C, starvation, oxidative stress, etc.).

### Increasing UNC-45 in older animals to alleviate sarcopenia:

We have created a transgenic animal that expresses extrachromosomal UNC-45::eGFP under the control of a heat shock promoter (*hsf-1*). We wanted to use an inducible promoter so that we could only induce increased *unc-45* expression during adulthood after the endogenous levels have declined (day 4). We chose a heat shock promoter because heat shock should also increase the endogenous HSP-90, which, based on our hypothesis, would be necessary to stabilize the increased UNC-45. Currently, I am working on integrating the transgene into the chromosome so that it can be expressed in every cell equally and eliminate any mosaic effects. We integrate our transgenes by using UV exposure to create random double strand breaks in the endogenous DNA sequence. Some of these double strand breaks should be repaired by ligating with the extrachromosomal array containing our transgene. We allow the worms to produce progeny and starve for approximately two to three weeks after irradiating. Once we have an integrated line, we should be able to induce UNC-45::eGFP expression with heat shock and evaluate the effects on sarcopenia using motility assays, A-band immunostaining, and Western Blot quantitation of myosin protein levels. My preliminary data using the non-integrated worms shows an improvement in crawling motility of day 8 animals that had been heat shocked overnight on day 4 (Figure 5.2B). Through Western Blot analysis, I can still see an increase in the eGFP tagged UNC-45 at day 8 – 4 days after the heat shock and 4 days after the normal decline in the endogenous protein. However, based on the Western Blot, it does appear as if the heat shock promoter is slightly “leaky” at 20°C (Figure 5.2A).

#### Knocking down HSP-90 or UNC-45 in young adults:

In order to validate the results of the *unc-45(e286)* mutant and the *hsp-90(p673)* mutant, we want to use double stranded RNA interference feeding to knock down either *unc-45* or *hsp-90* and see if they result in an early onset of sarcopenic phenotypes. We are also using the *hsp-90* RNAi to determine if UNC-45 protein is quickly degraded after a significant loss of HSP-90. This experiment could provide crucial support for our hypothesis that HSP-90 stabilizes UNC-45, and that during aging a loss of HSP-90 leads to a loss of UNC-45, which in turn leads to a loss of myosin and assembled thick filaments. These experiments are relatively quick and easy to perform with *C. elegans*. We will clone the first ~1kb of the cDNA sequence into a double T7 promoter plasmid, which is IPTG inducible. The T7 promoters on either side of the insert will create a double stranded RNA. We can seed our nematode growing plates with the induced culture, and they will eat the bacteria containing the ds RNA. Once eaten, the ds RNA is highly penetrant to multiple tissues, including the muscle cells. We will begin our RNAi feeding experiments at the L4 stage (to avoid dauer larvae formation or even lethality if exposed earlier) and we will need to transfer our worms to fresh RNAi plates daily (for approximately 2-4 days).

#### Analysis of TPR domain *unc-45* mutants from the million-mutation project:

The TPR domain of UNC-45 is responsible for binding to HSP-90, and, as such, we believe that it may play a very important role in UNC-45 stabilization/regulation. Additionally, we have identified one site of post translational modification within this domain – phosphorylation at serine 111. Before attempting a complete deletion of this domain, we wanted to obtain the four TPR domain mutants from the million-mutation project (Figure 5.3) and analyze the stability of the UNC-45 protein, its ability to bind to

HSP-90, and whether any of these strains experience an early onset of sarcopenia. We are particularly interested in the R46Q and the A104T mutants since they are the biggest amino acid changes within highly conserved regions. These residues are not strictly conserved, but they are functionally conserved – i.e. amino acids of the same charge and similar size (see figure below). When we receive these strains, I will first determine if they are temperature sensitive and display a phenotype when grown at 25°C. I will then quantify the amount of steady state UNC-45 when grown at different temperatures (15°C, 20°C, 25°C) via Western Blot. I expect there to be less UNC-45 protein and for the worms to develop at least a mild Unc phenotype. I will also see if less HSP-90 is associated with the mutant UNC-45 via co-immunoprecipitation experiments. Additionally, I would like to determine if indole treatment no longer has its protective effects on the TPR domain mutants.

#### High throughput drug screening:

We have verified that UNC-45-mNeonGreen from our CRISPR/Cas9 generated strain is expressed in the same muscle cells as endogenous UNC-45 and is localized in the sarcomere in the same way as endogenous UNC-45 (same pattern of A-band localization as native untagged UNC-45 when detected with anti-UNC-45 antibodies). With the help of Nic Vega (Dept. of Biology, Emory), we were able to use a “worm sorter” to measure fluorescence above background levels and to dispense them into wells of a 96 well plate (Figure 5.4). We planned to perform a drug screen to identify compounds that increase the fluorescence from UNC-45- mNeonGreen, suggesting increased expression or stability. One potential problem of using *C. elegans* is that they are protected by a thick cuticle made of complex layers of cross-linked collagens that acts as a physical barrier

against the uptake of chemical compounds. A screen of 5 genes with defects in cuticular structure showed that one mutant, *bus-5(br19)*, showed the greatest increase in permeability as compared to wild type animals and this mutant is commonly used for *C. elegans* drug screens(9). Thus, to increase the sensitivity of our drug screen and increase the probability of positive hits, we have crossed in UNC-45-mNeonGreen into *bus-5(br19)*, thus making the strain, *unc-45::mNeonGreen; bus-5(br19)*. We worked with Yuhong Du of the Biological Discovery Through Chemical Innovation (BDCl) group at Emory and she showed that we could use her HCS system to image green fluorescent worms in a 384 well tray. Unfortunately, our initial experiments showed that the fluorescence signal increased rather than decreased with age, first noticeable at day 2 adults. (We expected a decrease in signal given our quantitative western results). When we examined these worms under higher resolution, we noticed that the increased fluorescence signal arose from gut granules. These autofluorescent granules are lysosome-like organelles and are known to increase with age. On the other hand, when we focused on the pharyngeal muscle which is anterior to the intestine (and does not have autofluorescent granules), we observed that the UNC-45-mNeonGreen signal from pharyngeal muscle does indeed decrease as the adult ages, including the critical day 4 when UNC-45, by western blotting shows its largest decline (Figure 5.5). To avoid the problem of the gut granules, we crossed in the mutant, *glo-1*, which has greatly reduced gut granules. (*glo-1* encodes a Rab family GTPase required for gut granule biogenesis). Using *unc-45::mNeonGreen; bus-5(br19); glo-1(zu391)* animals, we observe a decline in pharyngeal and body wall muscle fluorescence at day 4, suitable for use in Yuhong's device. If we can optimize the conditions for the 384 well plate, then we can begin a drug

screen utilizing a ~4000 compound collection from the Emory Chemical Biology Discovery Center (ECBDC). We expect to observe at least several “hits”, and then with the expert advice of ECBDC staff, we will test compounds that are structurally similar or are even derivatives of the hit compounds obtainable from the vast indexed collection of >500,000 compounds available at the ECBDC. Positives will be followed up by performing a dose response experiment using a range of drug concentrations: 10 nM, 100 nM, 1  $\mu$ M, 10  $\mu$ M, 50  $\mu$ M, 100  $\mu$ M. We will next address the mechanism: (1) Positives will be tested on *bus-5(br19); glo-1(zu391)* animals (i.e. no expression of the fusion protein), for drug induced increased expression of UNC-45 protein (by western blot using our well-established antibodies to UNC-45), and *unc-45* mRNA by qRT-PCR. (We are “agnostic” regarding whether a drug works at the RNA or protein level, as long as UNC-45 protein is increased.) (2) We will also determine if the drug effect depends on hsp-90; this will be assessed by examining the levels of HSP-90 protein (by western blot using our well-established antibodies to nematode HSP-90), and mRNA at day 3 of adulthood, when there is normally a decline in HSP-90 protein levels. Again, we don’t care if the drug increases the level of HSP-90, as long as the level of UNC-45 is increased. (3) We will determine the time-course of the increase in UNC-45 expression; i.e. does the drug only increase expression at day 4, and then quickly decline, or sustain the increase for a longer period (more desirable); to do this, we will determine the UNC-45 protein levels at days 8 and 12, even after the drug is withdrawn at day 4. (4) Most importantly, we will determine if the drug can reduce sarcopenia by determining if drug exposure from L4 through day 4, can improve crawling motility and increase the number (and organization) of thick filaments in aged worms.

### Analysis of UNC-45 Phosphorylation:

Through phospho-tag gels, phosphatase treatment, anti-phospho antibodies, and mass spectrometry, we know that UNC-45 is phosphorylated at serine 111. We also see an increase in the overall phosphorylation of UNC-45 with age. We have multiple ways to continue to analyze and understand the significance of UNC-45 phosphorylation: 1) Create transgenic animals that express either wildtype, S111D (phosphomimetic), or S111A (non-phosphorylatable) eGFP tagged UNC-45 under the control of a body wall muscle specific promoter and determine if S111D UNC-45 declines faster and the S111A UNC-45 declines slower than wildtype, 2) Have a CRISPR strain made in which the serine was made non-phosphorylatable – S→A – and compare the levels of UNC-45 and myosin and analyze motility and the number of assembled thick filaments during aging, 3) Order production of a phospho-specific antibody to S111 and use it to prove this site becomes more phosphorylated with age, and 4) Have our collaborator Dr. Andres Oberhauser approach this biochemically – make WT and phosphomimetic recombinant worm UNC-45 and conduct a binding assay with HSP-90 to determine if phosphorylation reduces binding. Additionally, we could begin a screen to identify the kinase or kinases responsible for phosphorylating UNC-45 by obtaining strains from the million-mutation project that have mutations in muscle specific kinases. There are several hundred kinases expressed within *C. elegans* body wall muscle, so this could be an exhaustive task.

Figures:

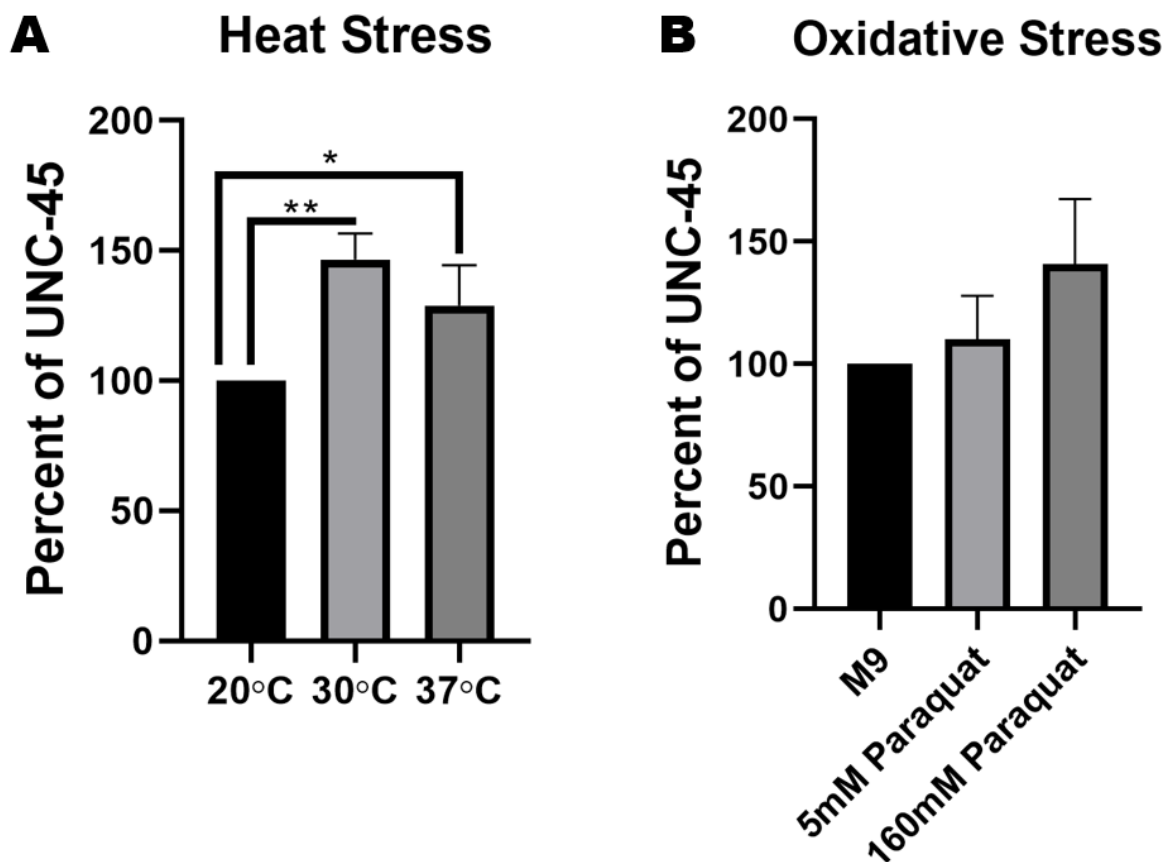


**Figure 5.1. UNC-45 protein increases after exposure to heat and oxidative stress.** A) Graphical quantification of UNC-45 protein level after exposure to 30°C or 37°C for 2 hours. UNC-45 levels from worms left at 20°C were set to 100% and used for comparison (n=3). B) Graphical quantification of UNC-45 protein level after exposure to 5mM or 160mM paraquat in M9 for 2 hours with constant agitation. UNC-45 levels from worms incubated in M9 buffer alone were set to 100% and used for comparison (n=2). A students t-test was used for statistical analysis of significance. \*\*p-value < 0.005, \*\*\*p-value < 0.0005\*\*\*\* p-value < 0.0001.

## A heat shocked 1 time, overnight on day 4

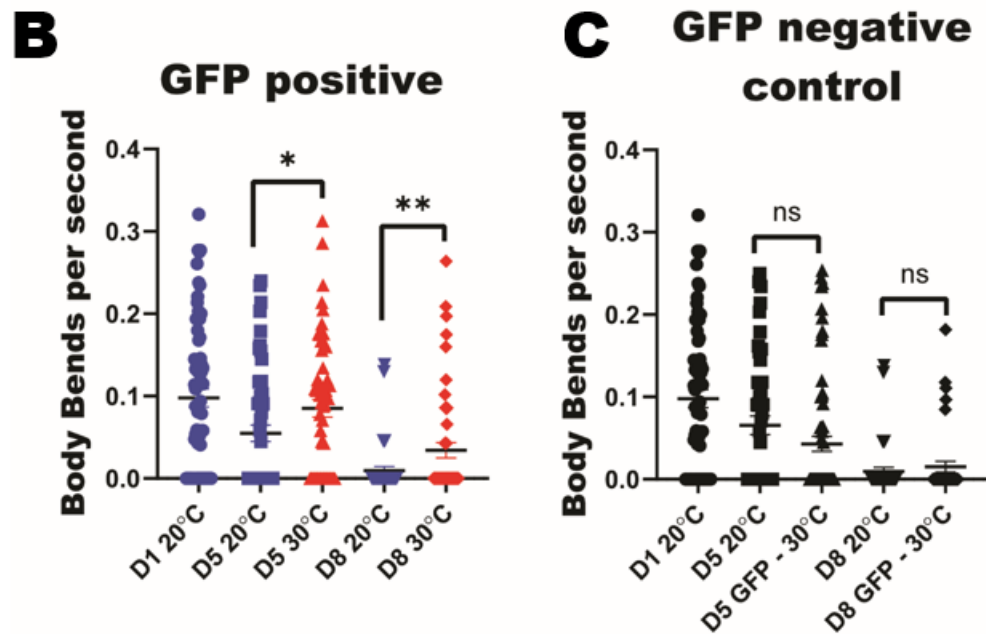
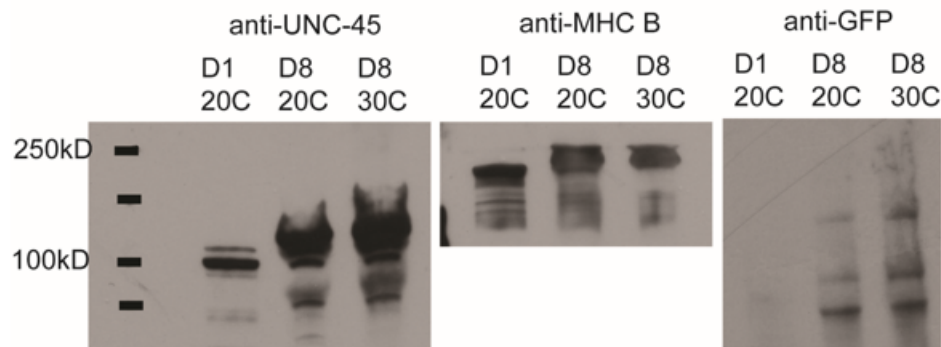


**Figure 5.2. Increasing UNC-45 during adulthood may improve motility in aged animals.** A) *hsp::UNC-45::eGFP* transgenic animals collected at day 1 and 8 either left at 20°C or heat shocked at 30°C overnight at day 4 were lysed and run on a 4-20% SDS-PAGE and blotted with antibodies to UNC-45, MHC B, and GFP. The three blot panels are from the same blot, but at different exposure times. B) graphical quantification of crawling motility assays from GFP positive transgenic worms on day 1, 5, and 8 either left at 20°C or heat shocked at 30°C overnight at day 4. Worms that were heat shocked to express extrachromosomal UNC-45::eGFP displayed a slight, but significant, improvement in crawling motility. C) graphical quantification of crawling motility assays from GFP negative transgenic worms on day 1, 5, and 8 either left at 20°C or heat shocked at 30°C overnight at day 4. There is no significant difference in crawling motility between GFP negative worms left at 20°C or heat shocked at 30°C. \* p-value < 0.05, \*\*p-value < 0.005

Strain	Allele	Mutation	Effect
VC40785	<i>gk810743</i>	G→A	R46Q
VC20065	<i>gk164733</i>	G→A	R91H
VC40980	<i>gk910614</i>	G→A	V97I
VC40132	<i>gk477468</i>	G→A	A104T

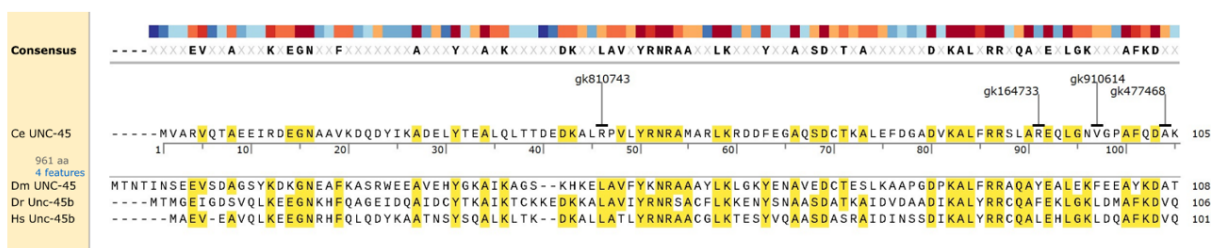


**Figure 5.3. TPR domain mutations from million-mutation project strains.** The table shows the strain identification, allele name, DNA sequence mutation, and amino acid change from the four TPR domain mutants available from the million-mutation project. Below the table is the sequence alignment of *C. elegans*, *Drosophila*, zebrafish, and human UNC-45/Unc-45b TPR domain where the mutations are located.

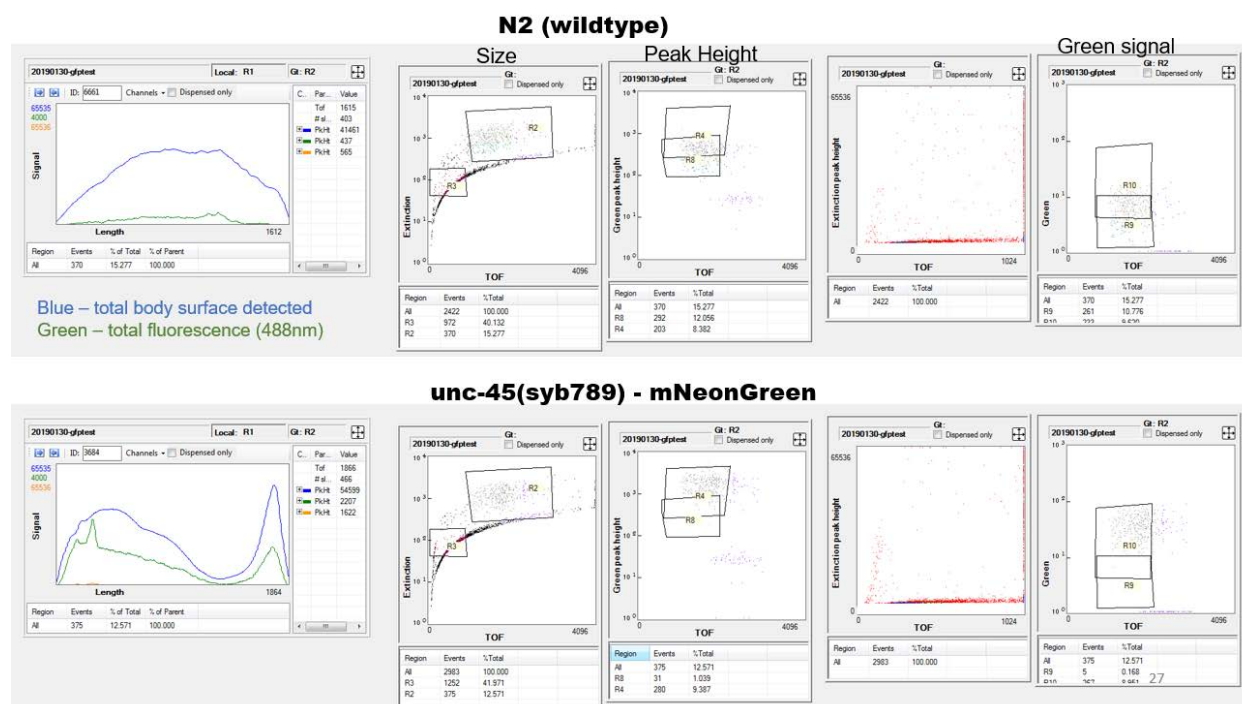


**Figure 5.4. Fluorescence detection using the BioSorter.** The top readout shows the total fluorescence at 488nm and the total body surface detected from young adult wildtype worms. The bottom readout shows the same thing but from young adult UNC-

45::mNeonGreen worms. The BioSorter can sort the worms by size, thus excluding larvae, and by fluorescence. The UNC-45::mNeonGreen worms had the largest fluorescent peaks around the pharynx and the vulva.

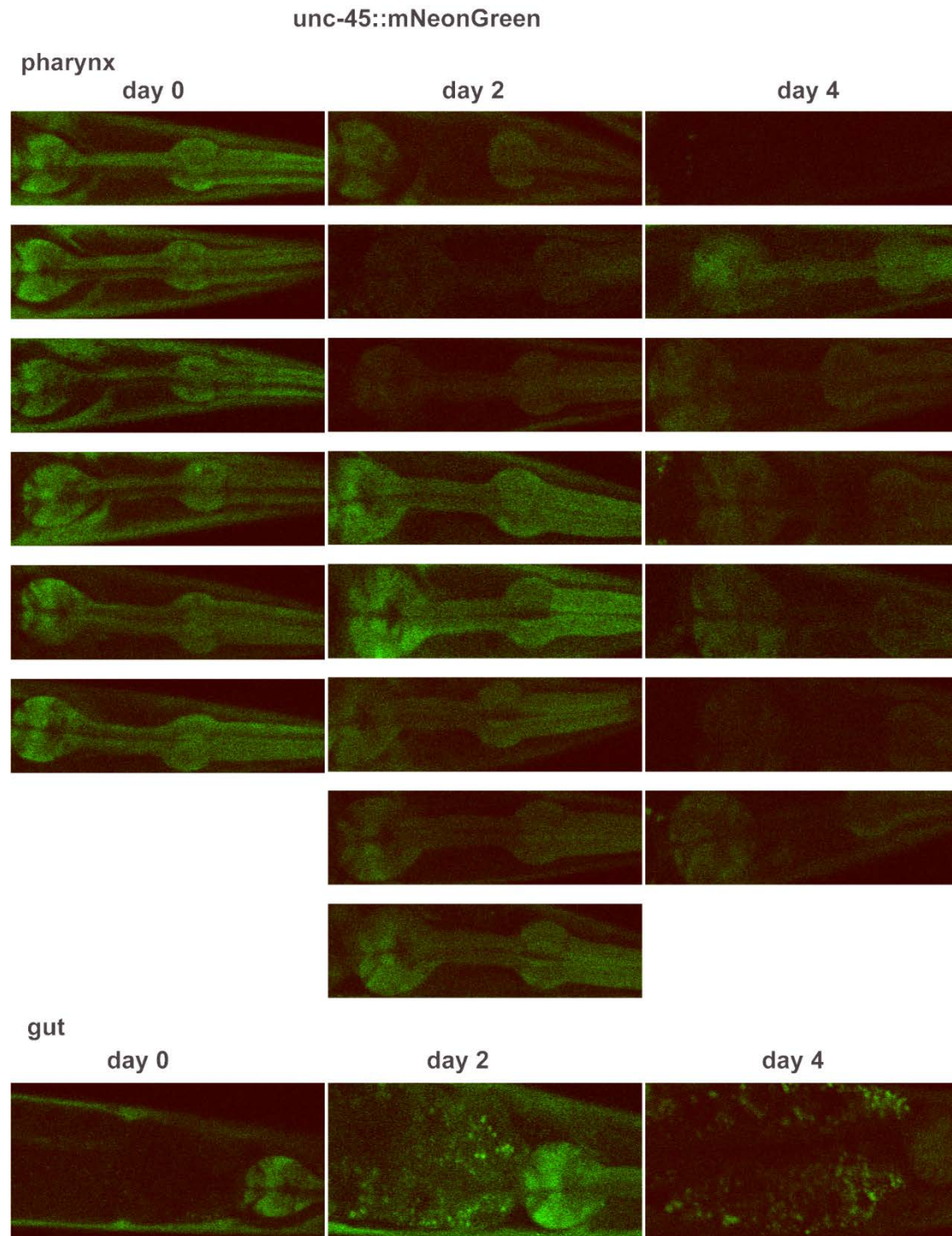


**Figure 5.5.** Live imaging of the pharynx and the gut from *unc-45::mNeonGreen;bus-5(br19); glo-1(zu391)* animals at day 0, 2, and 4 of adulthood. Live imaging confirms

that UNC-45 is reduced within the pharynx by day 4 of adulthood and that this region will be ideal to monitor for an increase in fluorescence.

## Acknowledgments

This project was funded in-part by National Institutes of Health grant R01GM118534 to G.M.B. and A.F.O., and in-part by the Emory Initiative Biological Discovery Through Chemical Innovation (BDCI) to G.M.B. The BCDB training grant T32 5T32GM008367-27 supported C.J.M. for one year during this project. Many of the nematode strains used in this work were provided by the Caenorhabditis Genetics Center, which is funded by the NIH Office of Research Infrastructure Programs (P40 OD010440). Monoclonal culture supernatants for 5-6 and 5-8 antibodies were obtained from the University of Iowa Hybridoma Bank, and the 5-6 ascites fluid was kindly provided by Henry F. Epstein (deceased).

I would like to thank Guy Benian for being a wonderful adviser, Hiroshi Qadota for being like a second adviser, and Jasmine Moody for being the best lab mate! They have supported me, taught me how to work with *C. elegans*, provided invaluable expertise when designing experiments and writing papers/grants, and made me laugh innumerable times. I could not have done this without them.

I would also like to thank my committee members – Dr.'s Mike Koval, Sho Ono, Jennifer Kwong, and Hyojung Choo – for their insight, suggestions, tough questions, and support when I needed it the most.

I would also be remiss if I didn't thank Dr. Dan Kalman for unwittingly giving me the hypothesis for how UNC-45 may be involved in the mechanism by which indole protects muscle thick filaments. I would also like to thank Dr. Robert Sonowal from his lab for providing me with indole and bacterial strains.

## Literature Cited

1. Gaziova I, *et al.* (2020) Mutational Analysis of the Structure and Function of the Chaperoning Domain of UNC-45B. *Biophysical journal* 119(4):780-791.
2. Moncrief T, *et al.* (2021) Mutations in conserved residues of the myosin chaperone UNC-45 result in both reduced stability and chaperoning activity. *Protein science : a publication of the Protein Society* 30(11):2221-2232.
3. Hoppe T, *et al.* (2004) Regulation of the myosin-directed chaperone UNC-45 by a novel E3/E4-multiubiquitylation complex in *C. elegans*. *Cell* 118(3):337-349.
4. Janiesch PC, *et al.* (2007) The ubiquitin-selective chaperone CDC-48/p97 links myosin assembly to human myopathy. *Nature cell biology* 9(4):379-390.

5. Walker GA, *et al.* (2001) Heat shock protein accumulation is upregulated in a long-lived mutant of *Caenorhabditis elegans*. *The journals of gerontology. Series A, Biological sciences and medical sciences* 56(7):B281-287.
6. Shmookler Reis RJ, Ayyadevara S, Crow WA, Lee T, & Delongchamp RR (2012) Gene categories differentially expressed in *C. elegans* age-1 mutants of extraordinary longevity: new insights from novel data-mining procedures. *The journals of gerontology. Series A, Biological sciences and medical sciences* 67(4):366-375.
7. Etard C, Roostalu U, & Strahle U (2008) Shuttling of the chaperones Unc45b and Hsp90a between the A band and the Z line of the myofibril. *The Journal of cell biology* 180(6):1163-1175.
8. Gazda L, *et al.* (2013) The myosin chaperone UNC-45 is organized in tandem modules to support myofilament formation in *C. elegans*. *Cell* 152(1-2):183-195.
9. Xiong H, Pears C, & Woollard A (2017) An enhanced *C. elegans* based platform for toxicity assessment. *Scientific reports* 7(1):9839.

**Abbreviations:**

CS – citrate synthase

CD – circular dichroism spectroscopy

Daf – dauer forming mutant

DSF – differential scanning fluorimetry spectroscopy

KD – dissociation constant

kDa – kilo Dalton

MDa – mega Dalton

Pat – paralyzed and arrested at the two-fold embryonic stage

S1 – skeletal muscle myosin head

SAXS – small angle X-ray scattering

TPR – tetratricopeptide repeat

ts – temperature sensitive

UCS – Unc – Cro – She

Unc – uncoordinated

WT – wildtype